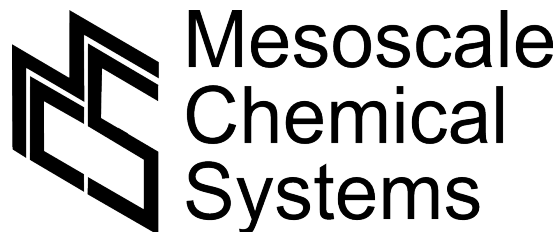

Low Voltage High Performance Silicon Nitride EOF Pump

Master Thesis by:

Lucas J. Kooijman

Research group:

Mesoscale Chemical Systems



UNIVERSITY OF TWENTE.

University: University of Twente

Programme: Electrical Engineering

Master defence at: 13-2-2019

Supervising committee:

Dr. ir. Niels R. Tas

Prof. dr. Jan C. T. Eijkel

Ing. Erwin W. Berenschot

Dr. ir. Remco J. Wiegerink

ABSTRACT

This is the master thesis of a project in which a high flow and high pressure SiO₂ covered SiN nanopore membrane EOF pump and its production process flow have been designed and created. The pump consists of a 1 cm square chip with 37 100 µm square membranes which have been created by sacrificial moulding. The moulds are created using a novel technique for creating high density high aspect ratio nanopillars in Si. The current pump-design has a measured maximum pressure strength of 180 kPa. Based on the flow measurements it shows that this pressure can be reached at a calculated potential of just 1.36 V over the membrane with a calculated maximum flow rate of 40.7 ml/min or 686 µl/s for a 0.2M K₂HPO₄-KH₂PO₄ solution at a pH between 7 and 8.

CONTENTS

Abstract	1
Contents	3
1	Introduction 6
1.1	Outline 6
1.2	Pumps 6
1.3	Electro-osmotic Flow - EOF 7
2	Theory..... 9
2.1	Nanopore Membrane..... 9
2.1.1	Existing Design 9
2.2	Mechanical 9
2.2.1	Notch Effect 10
2.2.2	Elasticity and Ultimate Tensile Strength 10
2.2.3	Maximum Pressure..... 11
2.3	Electrohydrodynamics 12
2.3.1	Fluidic Properties..... 12
2.3.2	Wall Charging Effect 15
2.3.3	EOF..... 16
2.3.4	EOF Pump Characteristics..... 16
2.3.5	Heating 19
2.3.6	Efficiency 24
3	Experimental and Measurement Setup Development - Proof of Concept..... 25
3.1	Chips Batch 1 25
3.1.1	Pore Geometry 25
3.1.2	Mask Design Description 25
3.2	Measurement Setup Design 26
3.2.1	Chipholder 27
3.2.2	Voltage Control..... 28
3.2.3	Current Control..... 29
3.2.4	Hydraulic..... 29

3.3	pH Buffer	29
3.4	Measurement Protocol	30
3.4.1	Preparing Chemicals	30
3.4.2	Voltage and Current Controlled Measurement Protocol	31
3.4.3	Hydraulic Resistance and Maximum Pressure Measurement Protocol	32
3.5	Initial Production, Experiments and Results	33
3.5.1	Chip Production	33
3.5.2	Measurement Setup - Found Details and Issues	36
3.5.3	EOF	39
4	Design Batch 2	42
4.1	Pore Geometry	42
4.2	Process Flow	43
4.2.1	Complete Overview	44
4.2.2	Critical and Notable Steps	49
4.3	Masks	51
5	Result and Discussion	53
5.1	Fabrication Batch 2	53
5.2	Mechanical	56
5.2.1	Hydraulic Resistance	56
5.2.2	Maximum Pressure	57
5.3	EOF	57
5.3.1	Voltage Controlled	57
5.3.2	Current Controlled	58
5.3.3	Flow and Pressure Characteristics	61
5.3.4	Power and Efficiency	61
6	Summary, Conclusion and Recommendations	63
6.1	Fabrication	63
6.2	Mechanical	63
6.3	EOF	64
6.3.1	Chipholder	64
6.3.2	Voltage Controlled Measurements	64
6.3.3	Current Controlled Measurements	64
6.3.4	Buffered Solution and Power and Efficiency	65
7	List of abbreviations	67

8	References.....	68
Appendix A	Curve Fittings for Temperature Dependent Density, Viscosity and Conductivity	71
Appendix B	Calculations - Plug Flow Heating.....	72
Appendix C	Calculations - Membrane Blow-Out Current	73
Appendix D	Masks	74
Appendix E	Chipholder Design	76
Appendix F	Detailed Process Flow: From Wafer to Pillars	77
Appendix G	Detailed Process Flow: from Pillars to Membrane.....	87
Appendix H	Measurement Results Batch 1	119
Appendix I	Measurement Results Batch 2	122

1 INTRODUCTION

This document is the master thesis of Lucas J. Kooijman about the design, construction and characterisation of an EOF (electro-osmotic flow) pump that has been developed within the group of MCS at the University of Twente. The pump consists of a silicon oxide covered silicon nitride membrane with nanopores with a length of several hundreds of nanometres and a width in the range of several tens of nanometres up to 100 nm. The chips are created by means of thermal oxidation of silicon, low pressure chemical vapour deposition (LPCVD) of SiN and sacrificial moulding of silicon.

1.1 OUTLINE

Due to the course of the project, this thesis contains several subjects which might make the outline a bit less evident. Two different batches of pumping chips have been created. The first batch based on a mould that was already present and was used for initial testing for a proof of concept and the developing of the measurement setup for testing. The results were on its term used to redesign the membrane geometry to create a second batch of chips that were used to perform test for the characterisation of the pump.

The introduction is the first part of the thesis, and will give some background information on EOF pumps and a short explanation of how EOF actually works. In chapter 2, the theory section, at first the theory of the mechanics and strength of the membrane will be dealt with after which the properties of the used measurement solutions will be mentioned. This is followed by a more extensive explanation of how EOF works and the expected characteristics of both chip designs.

In chapter 3 the first set of experiments is mentioned, including part of the designing and processing of the chips of batch 1, the development of the measurement setup, the used measurement protocols and the results of the first set of measurements, performed with the first batch of chips. This is followed by chapter 4 that deals with the design and production process flow of the chips for batch 2.

In chapter 5 the results are discussed, starting with the results of the fabrication of the second batch of chips, followed by the realised mechanical properties of the membrane after which all the pump and EOF related results are dealt with. In chapter 6 the conclusion and recommendations can be found for the issues that has been brought to attention in chapter 5. In chapter 7 there is a list of all used abbreviations throughout the thesis. This includes chemical notation of substances. The cited references can be found in chapter 8 which is then followed by the appendices.

1.2 PUMPS

The microfluidic pump find its use in many fields including healthcare, science (in micro reactors and lab-on-a-chip-devices [1]), measurement equipment (chromatography devices [1]) and future chip cooling [1] [2]. However these days this is all still largely done by mechanical pumps [3]. The main disadvantages of a mechanical pump is that they contain moving parts which wear out over time, causing the pump to break and that most of them create pulsed flows [1][3]. This due to the use of chambers or propellers, a lot of pumps work with minimum steps at which the fluid gets in or pressure/flow wave effects due to the movement of the mechanical parts.

A solution to this could be the electro-osmotic flow (EOF, see chapter 1.3 for a more detailed explanation) pump which is based on porous material and electrical fields. It contains no moving

parts, so as long as there is no interaction with the pumped fluids or degradation due to the electrical fields, it can theoretically not break or stop functioning. Also the pump is voltage (or current) controlled and its flow rate has a linear relationship with the electrical actuation [1][3]. There is direct control and no minimum step size at which volume can be moved or flow can be applied (due to e.g. the use of chambers of a pump or minimal speed at which a propeller starts spinning).

However over the last years a lot of EOF pumps have been developed [3] where most of them show a trade off between either a high flow or a high pressure, but in general with a high actuation voltage in the range of several hundreds of volts to several kilovolts for generating an output flow in the range of several millilitres/minute or a pressure in the range of several kPa and up to MPa [1]. The most promising results found in literature are a high flow porous membrane fritted glass EOF pump that produces a flow of 33 ml/min and a maximum pressure of 132 kPa at 100 V or $26 \mu\text{l}/(\text{min V cm}^2)$ and 1.32 kPa/V [4], a high pressure packed capillaries pump with a flow of 4.5 nl/min and a pressure of 40 MPa at 1.5 kV or $75 \text{ nl}/(\text{min V cm}^2)$ and 27 kPa/V [2] and a relatively low voltage packed capillary pump of 5 ml/min and 1 MPa at 15 V or $7 \text{ ml}/(\text{min V cm}^2)$ 69 kPa/V [1].

The trade offs are generally caused by the fabrication technique. A lot of higher flow pumps are created by using fritted glass, naturally porous material or packed silica beads [1][3][4]. This however creates non-uniform passages or pores for the water and EOF, meaning that also passages with a larger diameter than desired are present, which will cause a higher leakage when backpressure is applied. This results in the low pressures these systems can generate which can only be (partially) be compensated by using high actuation potentials.

For generating higher pressures, a higher hydraulic resistance is needed, which is generally achieved by using long thin etched parallel capillaries of several tens to hundreds of micrometres in diameter, or long capillaries that are packed with silica beads, both with lengths in the order of several millimetres up to tens of centimetres [1][2][3][5]. However this way of increasing the hydraulic resistance to compensate for large the radii of the channels or the non-uniformity of fritted or packed beads membranes, means higher actuation potentials will be needed to create EOF with significant flows.

The system described in this thesis, makes use of a novel developed technique [6] that enables the formation of wafer scale uniform closely spaced nanopillars with a square pitch of just 250nm and diameter that is tuneable from 10 nm up to around 100 nm with currently a maximum height up to 1 μm . By means of sacrificial moulding a silica coated silicon nitride membrane can be created with closely packed nanometre capillaries of the same dimensions as the nanopillars. Resulting in a closely packed uniform nanometre capillary membrane.

The uniformity removes undesired leakages that are described for the other systems and enables the possibility to finely adjust the hydraulic and electrical resistance for optimal maximum backpressure and EOF per pore, while the small pitch allows for larger flows (by means of parallel EOF flows from every pore). It also enables the realisation of a desired high hydraulic resistance with micrometre thick membranes which allows for actuation at very low potentials while generating a high output performance.

1.3 ELECTRO-OSMOTIC FLOW - EOF

When a surface of silica, also known as silicon dioxide (SiO_2), comes in contact with air or water, in general silanol (SiOH) will form at the surface. When this silanol-rich silica on its turns comes into contact with water, protons (H^+ ions), will dissociate and dissolve into the water. This

1 - Introduction

process is called deprotonation and due to the loss of positive protons, will result in a negatively charged silica surface.

On its turn, if the water contains traces of salts or other ionic solutes, the positive ions of these salt will be drawn to the charged silica surface and be collected as a layer on it, as is illustrated in Figure 1. By applying a voltage gradient parallel to the silica surface, these ions will move accordingly while also moving the nearby water by means of drag. This is called electro-osmotic flow or EOF. When applying this to for instance a tubular structure, this can be used to create a flow for pumping water which is what is demonstrated in the research described in this thesis.

More detailed information about EOF can be found in chapter 2.3.

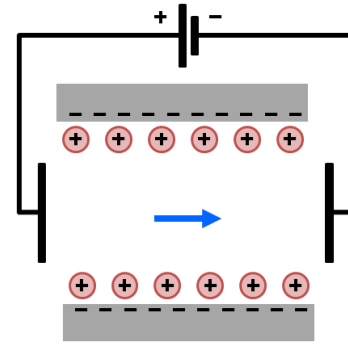


Figure 1: EOF model of a cross section of a silica tube with negative charged walls and positive ions creating a flow under influence of an applied voltage.

2 THEORY

2.1 NANOPORE MEMBRANE

2.1.1 EXISTING DESIGN

For creating the EOF pump, a within the group already designed and partially realised structure and production process will be utilised [7]. The process is based on sacrificial moulding. High aspect ratio nanopillars are created in silicon (Si) <100> wafers with a square pattern pitch of 250 nm. With the currently developed techniques, they have a tuneable diameter in the order of 100 nm that can be adjusted to 10 nm (due to minimum dimensions in wet etching [8]) and a maximum height around 1 μm for cylindrical shapes and 455 nm for conical shapes, where these maxima are determined by the technical development so far.

The Si nanopillars are then coated with a 10 nm layer of silicon dioxide (SiO_2) by means of oxidation after which they are fully covered by conformal deposition of silicon nitride (SiN). Then the Si is anisotropically etched away from the bottom at the desired place to create membranes also etching the away the pillars, creating nanopores.

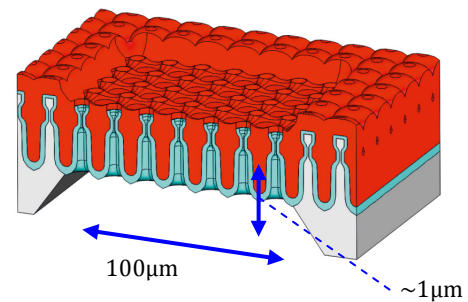


Figure 2: Sketch of a nanopore membrane. Grey: Silicon. Red: Silicon nitride. Light blue: Silicon dioxide.

Hereafter the wafers are etched from the top side at the areas where the membranes will be formed. The etching removes the part of the SiN that extends beyond the ends of the nanopores and the SiO_2 that closes the end of the nanopores. The result is a nanopore membrane as is illustrated in Figure 2.

The advantage of using this sacrificial moulding technique over directional etching of holes in SiN, is that a high aspect ratio can be achieved with below 100 nm diameters, but also the profile of the pillar can be tuned (narrowed and widened) as desired. At the same time a really low pitch of just 250 nm is realised, giving a porosity of 13 % for 100 nm diameter pores.

The full process flow for producing the structure will be discussed in detail in chapter 4.2.

2.2 MECHANICAL

The membrane mainly consist of a SiN membrane with a thickness of several hundreds of nanometres. Because of the relatively small thickness of the silica coating, its influence will be neglected when dealing with the strength of the membrane. Also for the convenience of calculating, the silicon wafer will be assumed infinitely strong compared to the membranes. This can be justified by the fact that the readily available silicon wafers have a thickness of 350 μm and 525 μm which are in the order of a 1000 times thicker than the membrane thickness while both materials have an elastic strength that lies in the same order.

Thus for further calculations only SiN will be taken into account.

2 - Theory

2.2.1 NOTCH EFFECT

The diameter of the pores (and also possibly small inclusions in the SiN resulting from the production process) are small to such a degree that that strictly speaking to the material, they are not just geometrical shapes anymore. They fall under the notching effect where every pore can be considered to be a notch, so a beginning tear/crack that might lead the SiN to fully crack.

For ceramic materials such as SiN it is unfortunately not possible to just calculate, based on geometry, to see if and when a material would crack or not. For this Weibull strength distributions are used to determine the probability of a certain material to rupture at a certain force with a certain size of notches. However, these distributions are created by performing statistical tests during which enough substrates are put under stress until breaking, to create a probability distribution at which they will break [9].

Up to date there seems to have been no relevant publications about notching effects or Weibull distributions for low pressure chemical vapour deposited (LPCVD) or SiN in general. Therefore the notching effect will be disregarded while calculating the strength of the membrane, but kept into account as an explanation for when the actual strength would turn out to be much lower than expected.

2.2.2 ELASTICITY AND ULTIMATE TENSILE STRENGTH

2.2.2.1 SILICON NITRIDE

As long as a ceramic material does not belong to the tough ceramics, there will be virtually no plastic deformation, meaning that the yield strength is (almost) equal to the ultimate tensile strength or fracture strength at which it will break [9]. The ultimate tensile strength of SiN is largely dependent on the manner in which it is created or grown, the exact proportions of silicon and nitride and the structure of the crystal lattice. Even though the exact growing mechanism as used in the cleanroom, has been investigated and characterised by Gardeniers et al. [10], the exact Young's modulus and strength for the SiN used for the membranes are not exactly known.

In literature a Young's modulus of 290 GPa and a fracture strength of 4 GPa for silicon rich and nitride poor $\text{Si}_{\text{rich}}\text{N}_{\text{poor}}$ [11] is mentioned and a fracture strength of 6.9 GPa and a Young's modulus of 260.5 GPa is mentioned for LPCVD grown SiN at 298 K or 25 °C [12]. These last mentioned values will be used from hereon. However, the same literature does note that previous research showed values ranging of 6.4 GPa up to 12.1 GPa fracture strength with this difference caused by differences in fabrication and testing techniques [12].

2.2.2.2 PERFORATION CORRECTION

For calculating the actual deflection, the Young's modulus will need to be adjusted for the perforation which will result in a effective Young's modulus with a lower value than the original Young's modulus. The new Young's modulus is dependent on the distribution of the pores and the size of the pores my means of the ligament efficiency [13]. The ligament efficiency is given by the distance between the edges of the pores and the centres or the pores [14]. Where d_{pitch} is the pitch distance or distance between the centres of the pores, d_{pore} is the diameter of the pore and η_{lig} is the ligament efficiency:

$$\eta_{\text{lig}} = \frac{d_{\text{pitch}} - d_{\text{pore}}}{d_{\text{pitch}}} = \frac{250\text{nm} - 100\text{nm}}{250\text{nm}} = 0.60 \quad \text{F. 1}$$

For the in-plane Young's modulus for a squarely perforated plane this leads to a correction factor of roughly 0.72 [13] leading to a corrected Young's modulus of 187.6 GPa.

For the deflection of the membrane, it will be assumed only that only small deflections will take place of less than about one half of the thickness of the membrane. The membrane itself has a thickness to minimal span ratio of 1/100 which is below 1/4, which means it can be regarded as a thin flat plate, which approximation and its corresponding mathematics can thus be used [15].

Due to the small deflection, the lumped element model can be used for a single cell of 250 nm by 250 nm with a single pore in the middle. This will be regarded as a plane with only in-plane tensile stress. ;For round holes it is the case that locally at the edge of the hole perpendicular to the applied stress, the stress will be 3 times as high as the stress applied at the ends of the plane [16]. This means that due to the geometry of the pores, the material will fracture at a 3 times lower strength than the actual expected ultimate tensile strength of SiN.

2.2.3 MAXIMUM PRESSURE

For calculating the maximum pressure before fracture of a membrane that is fixed on all the edges, the membrane is assumed to be a thin flat plate with the assumptions as mentioned in section 2.2.2. Under these assumptions the following formulae can be used and derived, where σ_{max} is the maximum internal stress of SiN, the factor 3 is added for correcting for the perforated geometry, q_{max} is the maximum pressure, b is the smallest span of a rectangular plane, t is the thickness of the plane and β_1 is a factor depending on the ratio between the width and height of the membrane [15]:

$$\sigma_{max} = \frac{-3 \beta_1 q_{max} b^2}{t^2} \quad \text{F. 2}$$

$$q_{max} = \frac{-\sigma_{max} t^2}{3 \beta_1 b^2} \quad \text{F. 3}$$

To give an idea; for a membrane with a thickness of 1 μm and 455 nm and a span of 1 cm by 1 cm, this would give a maximum pressure of 75 Pa and 15 Pa which corresponds to 7.6 mm and 1.5 mm height of water column, before the membrane would break. This is of course not enough by far to be of any use for a pump, but this can be compensated by supporting the membranes with silicon beams, dividing the membrane in several smaller membranes.

The silicon structures that can be considered as clamping the edges of the membrane and theoretically speaking, the smallest span of the membrane is dominant for the strength of the membrane [15]. With the addition of beams, b and β_1 would scale, however the influence of β_1 is very little and does not change more than by a factor of 1.8 when the ratio between the longest and shortest span becomes larger than 2. This means that for every downscaling the width by a factor 10, the strength goes up by a factor 100.

See Figure 3 for a plot of the membrane strength versus silicon beam spacing. Therefore at a beam distance spacing of 100 μm , the maximum pressure has already increased to 750 kPa or 76 m height of water column, which is more than sufficient for testing while leaving enough pumping surface area with respect to the beam surface area, for measuring the flow. Therefore this dimension is chosen as the value for testing.

2 - Theory

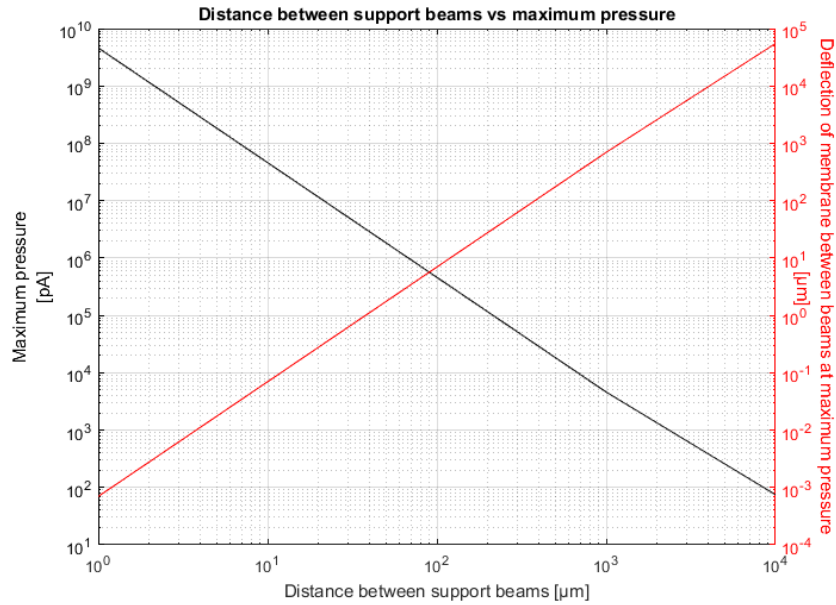


Figure 3: Distance between silicon support beams versus the maximum pressure before breaking and deflection of the membrane with a membrane thickness of 1 μm .

2.3 ELECTROHYDRODYNAMICS

Considering the electrochemical side, the pores are covered with an 10nm layer of silica with silanol groups. See 2.3.2 for more details about this.

2.3.1 FLUIDIC PROPERTIES

For performing the tests, potassium nitrate (KNO_3) solution will be used instead of the more commonly used NaCl and KCl solution. This is because at the expected high powers and potentials for testing, chloride salts pose the risk of chlorine gas formation. Based on preliminary tests, the concentrations of 0.1 M and 1 mM KNO_3 solutions are chosen and will be used. Furthermore also a 0.1 M $\text{K}_2\text{HPO}_4/\text{KH}_2\text{PO}_4$ phosphate pH buffer solution will be used. Of the first two solutions all the values are given in this section. For the phosphate solution the pH and conductivity will be measured and all other values will be assumed the same as for the 0.1 M KNO_3 solution.

Other properties, constants and values relevant to calculations about fluidics are as described below.

Symbol	Value	Description
A	$45 \cdot (10^{-4})^2$ $= 4.5 \cdot 10^{-7} \text{ [m]}$ $37 \cdot (10^{-4})^2$ $= 3.7 \cdot 10^{-7} \text{ [m]}$	Total membrane area per chip batch 1: 45 membranes of 100 μm by 100 μm Batch 2: 37 membranes of 100 μm by 100 μm
A_0	$3.14 \cdot 10^{-8} \text{ [m}^2\text{]}$	Area of cross section of a single 100 nm nanopore
c_0	0.1 [mM] 1 [mM]	KNO_3 solution concentrations used for performing the experiments

C_p	4181.8 [J/kg l·K]	Heath capacity of water at 20 °C [17]
e	$1.60217653 \cdot 10^{-19}$ [C]	Elementary charge [17]
F	96485.309 [C/mol]	Faraday constant [18].
K_w	$10^{13.91}$	Water ionisation equilibrium constant [19].
K_a	$10^{-pK_a} = 10^{-6.82}$	Acid dissociation constant as specified by the chemical supplier Sigma Aldrich.
n	$7.2 \cdot 10^7$ $5.92 \cdot 10^7$	Total amount of pores per chip Batch1 Batch2
r	$50 \cdot 10^{-9}$ [m]	Radius of a single 100 nm nanopore
R	8.31451 [J/mol·K]	Molar gas constant [18].
T	293.15 [K] or 20 [°C]	The used temperature when not otherwise specified.
ϵ	78 [F/m]	General relative permittivity of water [20] that also holds for low concentration salt solutions.
Z_{val}	1	The amount of bonds an atom or ion can make with other atoms and/or ions. For the KNO_3 -ion this is 1.
ϵ_0	$8.854187817 \cdot 10^{-12}$ [F/m]	Vacuum permittivity [21]
ζ	-110 [mV] at 1 mM -36 [mV] at 0.1 M	Zeta potential is the potential at the slipping plane between a solid and a solution. For more info, read 2.3.2. The zeta potential for a KNO_3 solution on SiO_2 at 1 mM at room temperature is found in [22] [23] and at 0.1 M at 30 °C in [24] [23] The temperature dependence will be dealt with in section 2.3.1.1.
η	$1.6 \cdot 10^{13}$ [m ⁻²]	Channel density with a square pattern and a pitch of 250 nm.
κ_{cond}	$14.5 \cdot 10^{-3}$ [S/m] at 1 mM 1.45 [S/m] at 0.1 M	The conductivity is determined by using equation F. 4 and values below [25] [26] where λ_+ and λ_- are the molar ionic conductivities of sodium and nitride ions. The formula is known to deviate for low salt concentrations [27] (2 % for KCl at 1 mM), but for 1 mM KNO_3 solutions there are no measured conductivity values found in literature.
$\kappa_{cond} = c_0 \cdot (\lambda_+ + \lambda_-) = c_0 \cdot \frac{73.52 + 71.44}{10}$ F. 4		
λ_D	$9.508 \cdot 10^{-9}$ [m] at 1 mM $0.9508 \cdot 10^{-9}$ [m] at 0.1 M	Debye length at 20 °C as calculated by using F. 5. The temperature dependence will be dealt with in section 2.3.1.1 and the definition of the Debye length will be dealt with in chapter 2.3.2.
μ	$1.002 \cdot 10^{-3}$ [Pa s]	Viscosity of water at 20 °C [18].

2 - Theory

2.3.1.1 TEMPERATURE DEPENDENCE

The measurement setup that will be used, as is described in chapter 3.2, has a distance between the electrodes of 3.5 cm. For measurements at the 0.1 M concentration the desired current and voltages used for the measurements will lead to several watts of joule heating dissipated into the water which are expected to cause a rise in temperature of several degrees to several 10 s of degrees Kelvin over the time of one measurement series. Because of this significant rise a lot of the previously mentioned values in section 2.3.1, which are generally taken to be constant, cannot be seen as constants anymore and the temperature change will need to be taken into account.

Debye Length

The formulae for calculating the Debye length is given by F. 5 [25] and shows a temperature dependence of the Debye length by \sqrt{T} .

$$\lambda_D = \sqrt{\frac{\varepsilon \varepsilon_0 R_{gas} T}{2 F^2 z_{val}^2 c_0}} \quad \text{F. 5}$$

Zeta Potential

Though there are still a lot of uncertainties and inconsistencies in literature about the exact expected zeta potential values, it is clear they are influenced by temperature. Based on the results of [23] the zeta potential of KNO₃ solutions and silica increases 1.56 %/°K for 1 mM and 1.96 %/°K for 10 mM compared to their taken reference value at 25 °C or 298.15 K. For 0.1 M More information about the definition of the zeta potential can be found in 2.3.2.

Permittivity

For higher temperature-dependent accuracy the following formula is used with T in °K and where the deviation in ε is roughly 0.5 % per K [28]:

$$\varepsilon = 5321T^{-1} + 233.76 - 0.9297T + 0.1417 \cdot 10^{-2}T^2 - 0.8292 \cdot 10^{-6} \cdot T^3 \quad \text{F. 6}$$

Density, Viscosity and Conductivity

For the density, viscosity and conductivity of the 0.1 M KNO₃ solution, the data of Isono [29] has been used to plot and calculate the temperature dependence by means of a second order polynomial approximation in Matlab with a certainty of 95 %. The resulting plots and formulae of the temperature dependence of these properties can be found in Appendix A and are also plotted in Figure 4.

For 1 mM KNO₃ solutions this data were not available and constant values have been used. This can also be supported by the fact that preliminary testing showed that at the low currents used for these measurements, the solution had a relatively stable temperature around 30 °C, as can be seen in Appendix H.

For the 0.1 M potassium phosphate buffer, such data were also not available and constant values have been assumed. Because the zeta potential (see section 2.3.4) depends on the ionic strength and thus the concentration and valence of ions, it is assumed that for the zeta potential the same value can be taken since the same concentration of potassium ions is dissolved. Its exact conductance and pH will be measured, but the pH is desired to be around 8.

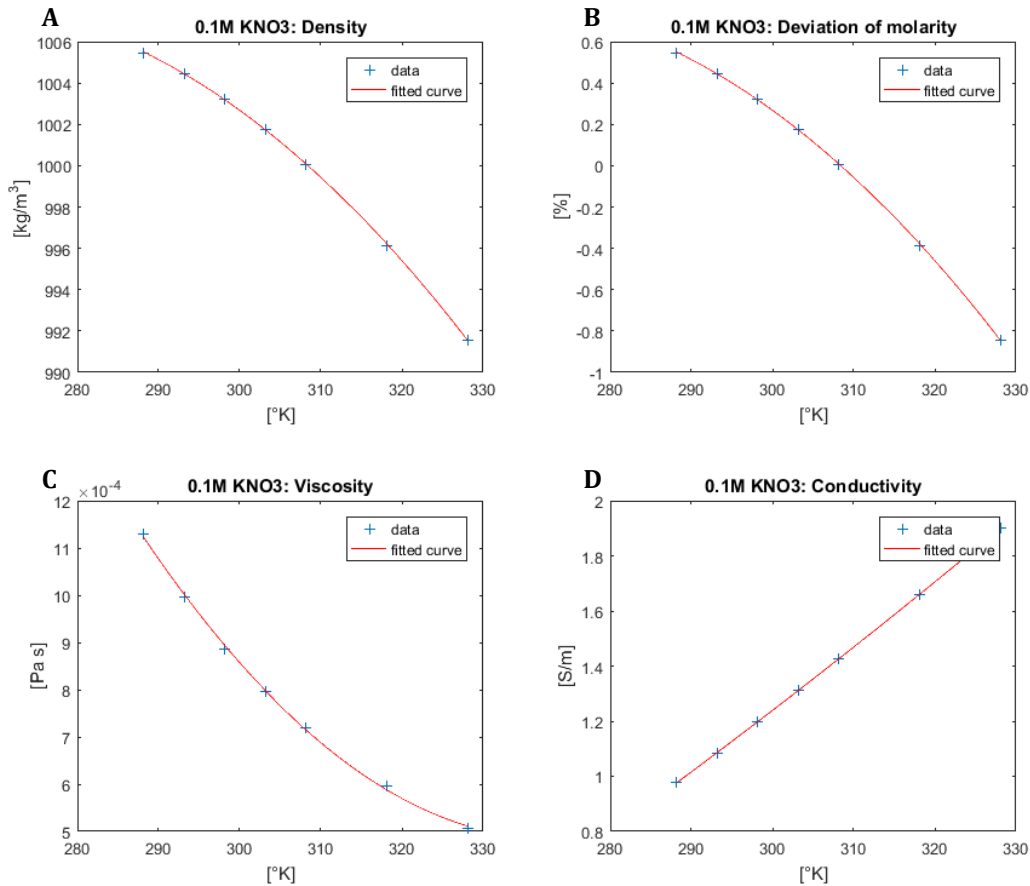


Figure 4: Density, viscosity and conductivity of 0.1 M KNO₃ solutions vs. temperature [K]. A: Density [kg/m³]. B: Deviation of molarity due to change in density in [%] to check whether the molarity had to be compensated due to the change in density. C: Viscosity [Pa s]. D: Conductivity [S/m].

2.3.2 WALL CHARGING EFFECT

Whenever silicon comes into contact with air, it will start to oxidise and a native oxide will start to form. In general this will be a layer of SiO₂ (silicon dioxide), also known as silica. Both the native silica and most deposited and artificially grown silica layers have an imperfect crystalline lattice with unbounded positions in the crystal lattice. Under normal conditions, these open positions are partially filled with hydroxyl groups (-OH) creating silanol (Si-O-H) groups [30].

When silica comes into contact with water at a pH larger than 3, the present silanol groups at the interface with the water will partially deprotonate with its positive hydrogen ions dissolving in the water leaving negatively charged oxygen groups and thus a negative

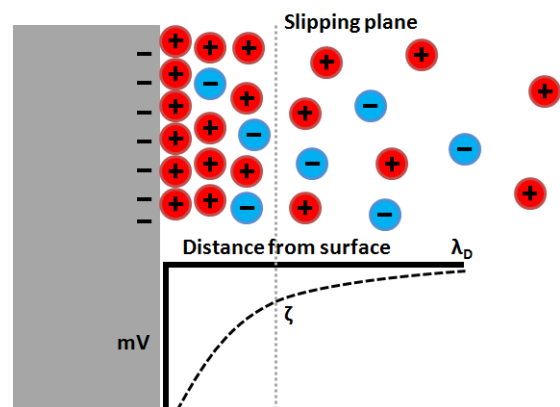


Figure 5: Simplified presentation of the Stern EDL model of silica and a saline solution showing the Helmholtz plane on the surface of the Silica, the slipping plate at which the zeta potential is defined and the potential in the solution over the length of the Debye layer.

2 - Theory

charge on the surface of the silica [30][31][32]. To compensate for this negative surface, positive ions from the water solution will settle on the silica surface, as is modelled in Figure 5, and an electrical double layer (EDL) will form [33][34]. Close to the surface positive ions will assemble at the Helmholtz plane and at larger distance there will be a positively charged mix that gradually will converge to the bulk potential and concentrations, over the distance perpendicular to the wall. In most cases this means converging to 0 V with an equal concentration of positive and negative ion charges. The length over which this positive charging is present is called the Debye length λ_D [24][32].

2.3.3 EOF

The layer of settled ions closest to the wall, will be immobile due to the high attractive forces. At the distance where ions experience an attraction force low enough that they can move, the slipping plane is defined. This is the plane at which a fluidic no slip boundary is present and the voltage present at this boundary is known as the zeta potential ζ [24][35].

The ions beyond this slipping plane are mobile and can be moved by applying a potential perpendicular to this plane. Due to the friction or no-slip condition at the slipping interface, the flow will be zero at the interface and increase with the distance from the wall. In the middle of the channel there will be a neutral charge distribution of ions and thus no electro-osmotic forces are present, but due to drag from the moving sides, the liquid there will move as a flat flow front, resulting in a plug flow [33] [34].

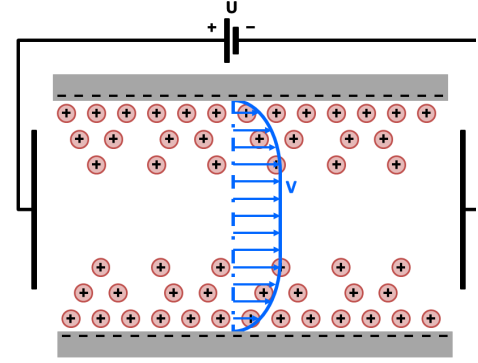


Figure 6: Simplified model of EOF in a silica capillary filled with a saline solution. A potential U is applied, resulting in a flow V (in blue) over the width of the channel.

2.3.4 EOF PUMP CHARACTERISTICS

2.3.4.1 FLOW

Assuming cylindrical nanopores and no counter pressure, the following holds for the maximum flow Q_{max} for a potential U_{eff} applied over the membrane at a channel length/membrane thickness l of $1\mu\text{m}$ and a diameter of 100 nm [33]:

$$Q_{max} = \frac{\eta A A_0 \varepsilon \varepsilon_0 \zeta}{\mu l} U_{eff} \quad \text{F. 7}$$

Which leads to the flows as listed in Table 1.

	$[m^3/s]$	$[\mu l/s]$	$[ml/min]$
$c_0=1 \text{ mM}$ Square 1cm membrane*	$9.5 U_{eff} \cdot 10^{-7}$	$9.5 U_{eff} \cdot 10^2$	$57 U_{eff}$
$c_0=1 \text{ mM}$ Batch 1 chip	$8.6 U_{eff} \cdot 10^{-9}$	$8.6 U_{eff}$	$0.52 U_{eff}$
$c_0=1 \text{ mM}$ Batch 2 chip	$5.3 U_{eff} \cdot 10^{-9}$	$5.3 U_{eff}$	$0.32 U_{eff}$
$c_0=0.1 \text{ M}$ Square 1cm membrane*	$2.8 U_{eff} \cdot 10^{-7}$	$2.8 U_{eff} \cdot 10^2$	$17 U_{eff}$
$c_0=0.1 \text{ M}$ Batch 1 chip	$2.8 U_{eff} \cdot 10^{-9}$	$2.8 U_{eff}$	$0.17 U_{eff}$
$c_0=0.1 \text{ M}$ Batch 2 chip	$1.7 U_{eff} \cdot 10^{-9}$	$1.7 U_{eff}$	$0.10 U_{eff}$

Table 1: Expected flows. *The square 1 cm membrane has 1 μm long 100 nm diameter channels.

2.3.4.2 PRESSURE

The maximum pressure that can be generated by the pump is determined by the amount of flow that it can generate. A backwards pressure over the membrane will cause a backflow and at the point where the backflow and generated flow are equal, the maximum generated pressure or backpressure $P_{max.back}$ is achieved. For calculating this value, the hydraulic resistance of the membrane is used in combination with the generated flow using the Hagen-Poiseuille equation for all pores in parallel [24] resulting in formula F. 8 which relates the pressure to the flow via the hydraulic resistance.

$$P_{max.back} = \frac{1}{\eta} \frac{8 \mu l}{A \pi r^4} Q_{max} \quad \text{F. 8}$$

When combining F. 7 and F. 8, one can see that this maximum pressure only depends on the cross section of the channel and no other geometries as can be seen in F. 9. A plot of the flow and maximum (back-)pressure versus the diameter of the channel can be seen in Figure 8.

$$P_{max.back} = \frac{1}{\eta} \frac{8 \mu l}{A \pi r^4} \cdot \frac{\eta A A_0 \varepsilon \varepsilon_0 \zeta}{\mu l} U_{eff} = \frac{8 \varepsilon \varepsilon_0 \zeta}{r^2} U_{eff} \quad \text{F. 9}$$

For a KNO_3 concentration of 1mM this results in a maximum backpressure of $240 U_{eff} \text{ kPa}$. Assuming the pump would respond as ideal fluidic power source with a hydraulic resistance, a flow-pressure diagram can be drawn as can be seen in Figure 7.

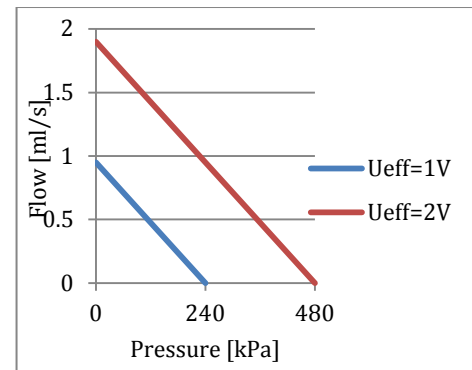


Figure 7: Flow pressure characteristics of a 1 cm² and 1 μm thick membrane with a 1mM KNO_3 solution, under the assumption it will respond as an ideal source with a hydraulic resistance.

2 - Theory

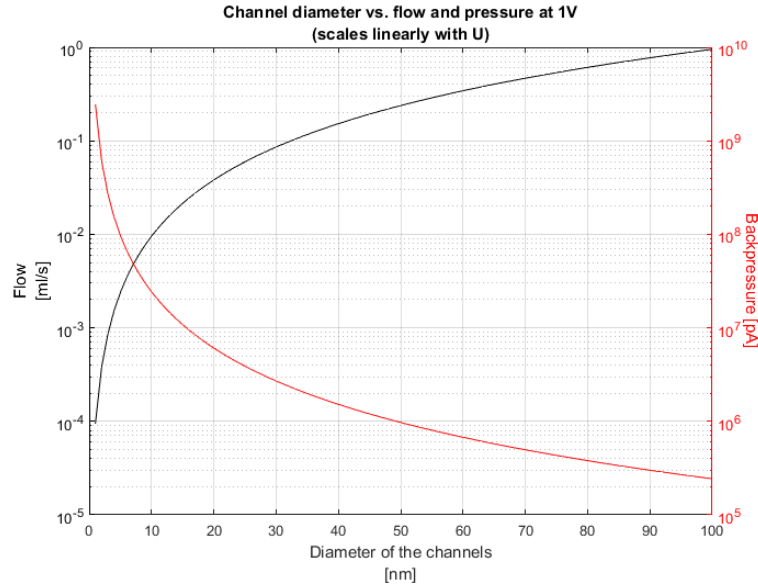


Figure 8: Channel diameter vs. flow and maximum (back-)pressure of a 1 mM KNO₃ solution at 1 V.

2.3.4.3 PORE GEOMETRIES

As described in chapter 1, two different batches of chips will be produced. The first batch will be based on mould wafers that were previously produced by Oxford Instruments. The second batch will be self produced and has a chosen geometry based on the results of the first batch..

Batch 1

The batch from Oxford will have pores with a total length and a membrane thickness of 276 nm with 3 sections of different widths and lengths as is sketched in Figure 9.

For the EOF this can be seen as three individual EOF pumps in series. The effective potential over each of the individual sections depends on the ratio between the individual electrical resistances of the sections. This leads to $U_{eff,x} \propto U_{eff} \cdot l/A_0$, where x denotes the section, while the flow scales with $Q_{max,x} \propto U_{eff,x} \cdot A_0/l \propto U_{eff}$. This means that the produced flow will be the same in every section and only one section needs to be calculated for calculating the total flow, but also that there will be no loss or section restricting the in-series flow of the other sections.

However from F. 9 it follows that the hydraulic resistance and thus the maximum backpressure scales with $P_{max,back,x} \propto U_{eff,x}/r^4 \propto U_{eff} \cdot A_0/r^2$. This means that the maximum backpressure per section is different. For the total maximum backpressure that can be provided by these pores, the individual backpressure of every section needs to be summed.

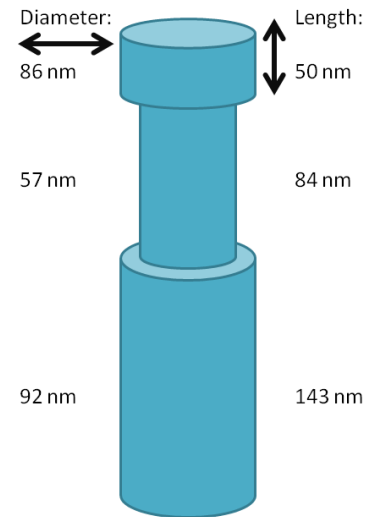


Figure 9: Pores of the membrane as produced by Oxford Instruments.

For 1 cm by 1 cm membrane and the 1 mM KNO_3 solution this gives a flow of $1.9 U_{eff} \cdot 10^{-6} \text{ m}^3/\text{s} = 1.9 U_{eff} \text{ ml}/\text{s}$ or $0.12 U_{eff} \text{ l}/\text{min}$ and a maximum backpressure of $543 U_{eff} \text{ kPa}$. At 0.1 M this would be 67 % less, or about 1/3 of this value.

When looking at the voltage versus the hydraulic power, this looks promising, but it needs to be taken into account that a membrane of this thickness, also with lower surface area, has very limited strength. At a span of only 100 μm , the membrane would already break at 57 kPa. From this it must be concluded that the U_{eff} should not be higher than 105 mV to prevent breaking of the membrane when the pump is pressure loaded.

It must be noted that the chosen 1 mM KNO_3 solution is chosen with a pore diameter around 100 nm in mind. The thinned section of the pore has a diameter of only 57 nm whereas the Debye length at 1 mM is 9.5 nm, meaning that the effective bulk area has a diameter of only 38 nm which means only 44 % of the area. This means that the influence of the double layer is significantly large in most of the channel, while the used mathematics for the EOF and plug flow profile approximation are based on the assumption that the radius to Debye length follows $r/\lambda_D \gg 1$. When this is not the case a whole different set of approximations is needed to calculate the EOF and plug profile, meaning a possibly partially lower EOF might be measured then here predicted [25] [32][33][34].

Batch 2

The second batch will be produced by means of a process that is developed in the group. As can be read in chapter 4, the pores will have a total length and a membrane thickness of 455 nm and be slightly conical with an angle of 1.7 °. For calculations, the pore will be assumed cylindrical with a fixed diameter. Since the flow and electrical resistance depend on the cross sectional area, the average cross sectional area will be taken for determining the corrected average diameter for the calculations and not simply the average diameter. The chosen process flow will result in pores with an corrected average inner diameter of 83 nm.

For 1 cm by 1 cm membrane and the 1 mM KNO_3 solution this gives a flow of $1.4 U_{eff} \cdot 10^{-6} \text{ m}^3/\text{s} = 1.4 U_{eff} \text{ ml}/\text{s} = 87 U_{eff} \text{ l}/\text{min}$ and a maximum backpressure of $353 U_{eff} \text{ kPa}$. At 0.1 M this would be 67 % less, or about 1/3 of this value.

Again when looking at the voltage versus the hydraulic power, this looks promising, but it needs to be taken into account that a membrane of this thickness, at a span of only 100 μm , the membrane would already break at 155 kPa. From this it must be concluded that the U_{eff} should not be higher than 552 mV to prevent breaking of the membrane when the pump is pressure loaded.

2.3.5 HEATING

It is interesting to know the heating to make an estimate of feasibility of the design. If the water in the membrane gets near the boiling point, gas can be formed, resulting in clogging of the membrane, losing efficiency due to less water being moved in the membrane and pressure build-up, which might locally lead to damaging the membrane.

The heating by the bulk solution in the membrane, is caused by 2 mechanisms. Viscous heating by means of friction between the particles which can also be modelled as the shear forces between adjacent flow layers, which is both caused by the flow caused by the pump, and the backflow caused by any backpressure, and joule heating caused by the electrical currents and potentials involved [25].

2 - Theory

2.3.5.1 VISCOUS HEATING

The electro-osmotic flow behaves as a flat front plug flow [34], but due to the backpressure, an inverse parabolic flow profile can be superimposed on this plug flow profile [25] with the largest shear forces near the walls. The only shear forces of the plug flow are also found near the wall, but in opposite direction. Therefore in practice there will be a partial cancellation.

The exact models for the plug flow profile near the edges are highly complex and there is not yet a unanimous consensus on which model is the most accurate while the individual models are not agreeing with each other. Because of this the heat production for both flows will be considered individually and added to see if they are within desired limits. Since the total heat produced in practice, should always be below the sum of these two heat sources, they should prove no problem if the sum is still within limits.

Plug Flow

For viscous dissipation at steady-state laminar flows in circular pores F. 10 holds for heating power $W_{plug.vis.unit}$ per unit of volume, under the assumption that no compression will take place. Here U stands for the dissipated energy per time t , ρ is the density and Φ is the three-dimensional dissipation function that with the present flow, can be simplified to the last term in F. 10. [36][37] This last simplification follows from since F. 11 holds for the flow velocity V_z and thus the profile of the plug flow.

$$W_{plug.vis.unit} = \frac{DU}{Dt} = -\frac{\mu}{\rho}\Phi = -\frac{\mu}{1000}\left(\frac{\delta v_z}{\delta r}\right)^2 \quad \text{F. 10}$$

The plug flow will be simplified and modelled as the flow profile that can be seen in Figure 10. $V_z = 1$ is the normalised value for the maximum flow velocity R_{max} that decreases linearly to 0 over the Debye length λ_D at $r = R_\lambda = R_c - \lambda_D$ to R_c . Leading to:

$$V_z(r) = \begin{cases} V_{max} & 0 \leq r \leq R_\lambda \\ \frac{V_{max}}{\lambda_D}(R_c - r) & R_\lambda \leq r \leq R_c \end{cases} \quad \text{F. 11}$$

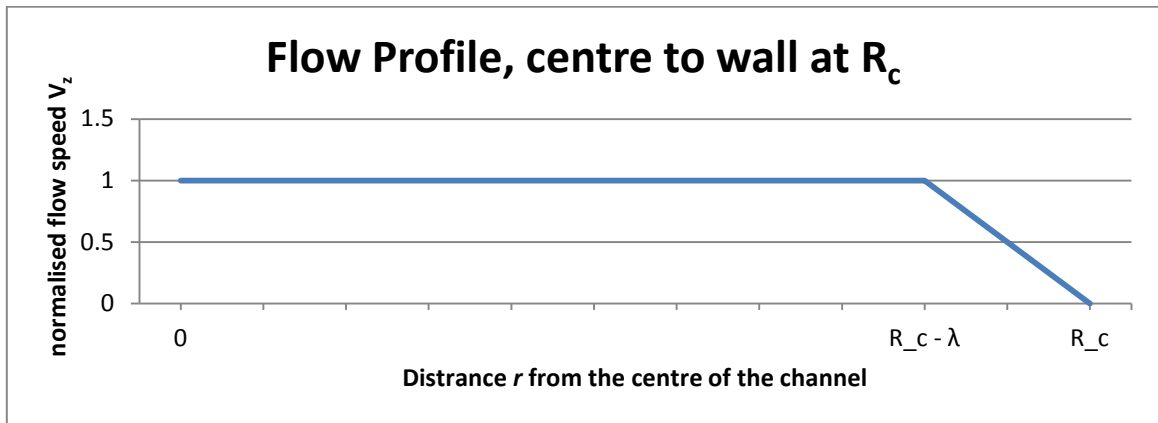


Figure 10: Simplified plug flow model showing the normalised flow speed V_z in the channel where R_c is the location of the channel wall and λ is the Debye length.

From F. 11 F. 12 can be deduced. The full calculations can be found in Appendix B. Since the direction of energy is not relevant here, the absolute value will be taken.

$$W_{plug.vis.unit} = -\frac{\mu}{\rho} \left(\frac{\delta v_z}{\delta r} \right)^2 = -\frac{\mu}{\rho} \left(\frac{V_{max}}{\lambda_D} \right)^2 \quad \text{F. 12}$$

Taken into account that the heating only takes place in the outer ring of the filled channel and is equal for every section due to its linearity with r , it gives a total viscous plug heating power as can be found in F. 12 and Table 2:

$$W_{plug.vis.total} = W_{plug.vis.unit} n l \pi (R_c^2 - (R_c - \lambda_D)^2) \quad \text{F. 13}$$

	[W], $c_0=1$ mM	[W], $c_0=0.1$ M
Batch 1 Square 1 cm membrane	$1.4 U_{eff}^2 \cdot 10^{-3}$	$1.0 U_{eff}^2 \cdot 10^{-3}$
Batch 1 Realised chip	$6.4 U_{eff}^2 \cdot 10^{-6}$	$4.5 U_{eff}^2 \cdot 10^{-6}$
Batch 2 Square 1 cm membrane	$7.9 U_{eff}^2 \cdot 10^{-4}$	$6.2 U_{eff}^2 \cdot 10^{-4}$
Batch 2 Realised chip	$2.9 U_{eff}^2 \cdot 10^{-6}$	$2.3 U_{eff}^2 \cdot 10^{-6}$

Table 2: Viscous heating plug flow powers.

Back Flow

For the maximum heating power of the backflow, it is assumed that the maximum backpressure is achieved, meaning that all the flow caused by EOF, is flowing back again as a backflow due to the backpressure. Thus for calculating the generated heat energy, the product of the backpressure $P_{max.back}$ and backflow Q_{max} can be used.

$$W_{back.viscous} = P_{max.back} \cdot Q_{max} \quad \text{F. 14}$$

	[W], $c_0=1$ mM	[W], $c_0=0.1$ M
Batch 1 Square 1 cm membrane	$1.0 U_{eff}$	$0.11 U_{eff}$
Batch 1 Realised chip	$4.7 U_{eff} \cdot 10^{-3}$	$5.0 U_{eff} \cdot 10^{-4}$
Batch 2 Square 1 cm membrane	$0.51 U_{eff}$	$5.5 U_{eff} \cdot 10^{-2}$
Batch 2 Realised chip	$1.9 U_{eff} \cdot 10^{-3}$	$2.0 U_{eff} \cdot 10^{-4}$

Table 3: Viscous heating backflow powers.

2.3.5.2 JOULE HEATING

The conductivity of the channels depends on two mechanisms. The first one is the ohmic conductivity of the pore determined by its dimensions and the ion conductivity of the bulk solution by means of the ions valence and mobility following formula F. 4 in section 2.3.1. The second form of conductivity is caused by the accumulation of ions at the channel walls causing the so-called surface conduction.

The ohmic conductance of a pore G_{pore} is described by F. 15.

$$G_{pore} = \frac{l}{\pi r^2} \kappa_{cond} \quad \text{F. 15}$$

2 - Theory

Where for κ_{cond} it holds that it scales with the molar conductivity Λ according to F. 18 [25].

$$\kappa_{cond} = \Lambda_+ c_+ + \Lambda_- c_- = 2\Lambda_0 c_0 \quad \text{F. 16}$$

In general the molar conductivity is approximated by $\Lambda_m = \kappa_{cond}/c$ under the assumption that the ions can move completely independently. However, strong electrolytes at low concentrations, that fully dissolve, such as KCL and KNO_3 , behave more accordingly to Kohlrausch law shown seen in F. 17. Here Λ_m^0 is the molar conductivity at infinite dilution, at which the ions can truly move independently and K is an empirical positive constant [27].

$$\Lambda_m = \Lambda_m^0 - K \sqrt{c} \quad \text{F. 17}$$

This means that at very low concentrations the molar conductivity nears an asymptote. At the same time the influence of the H^+ and OH^- of the water will become more dominant, determining the final conductivity limit when the salt concentration goes to 0 M. This can also explain where the 2 % of deviation of κ_{cond} of F. 4 for KCL at very low concentration comes from. This also means that lower conductances could still be partially achieved by choosing a different salt type with a lower value of Λ_m^0 , but that the joule heating cannot be decreased unlimited by lowering the concentration.

Surface Conductivity

When a voltage is applied over a system where there is a surface conduction in the form of an accumulation of ions on the surface, this will cause a current, which adds to the conductivity of the pore. One of the measures for determining the surface conductance versus the bulk conductance, is the Duhkin number Du with the following definition and with a as a characteristic length, generally the radius of a particle or capillary [35] [38]:

$$Du \equiv \frac{\kappa_{surface}}{a \kappa_{cond}} \quad \text{F. 18}$$

However not all the needed data for calculating this number is known for KNO_3 solutions and also at which exact value of Du the crossover point lies for the one or the other type of conductance to become dominant. It also is not clearly defined in literature, other than mentioning the cases of $Du \ll 1$ and $Du \gg 1$, where in the first case the surface conductivity can be neglected. However, it can be found that when the EDLs have a significant overlap in nano-capillaries, the surface conductance becomes more important and adjusted formulae need to be used [39].

For KCL solutions it is shown in literature, that the turning point between the dominance of bulk conductance to surface conductance for 50 μm wide and 70 nm high silica nano-capillaries lies at a concentration around . The bulk conductance becomes dominant at higher concentrations and the surface conductance at lower concentrations. Increasing the height to 1015 nm, lowered this turning point to just below 1 mM [40]. Since in both cases the ionic strength is the same, it is assumed these data are similar for KNO_3 solutions.

Since later during the tests it will turn out, the tests at 1 mM were not performed, but the ones at 0.1 M were, it is decided not to invest more time into determining the exact influence of the surface conduction on the total conduction at 1 mM.

Heating

Neglecting surface conductance, for the joule heating F. 19 holds per unit of volume [25] and thus F. 20 holds for the whole chip with the numerical results in Table 4:

$$W_{joule.unit} = \kappa_{cond} \left(\frac{U_{eff}}{l_{chan}} \right)^2 \quad \text{F. 19}$$

$$W_{joule.total} = n A_0 l_{chan} W_{joule.unit} = n A_0 l_{chan} \kappa_{cond} \left(\frac{U_{eff}}{l_{chan}} \right)^2 = \frac{n A_0 \kappa_{cond} U_{eff}^2}{l_{chan}} \quad \text{F. 20}$$

	[W], $c_0=1$ mM	[W], $c_0=0.1$ M
Batch 1 Square 1cm membrane	$0.37 U_{eff}^2$	$37 U_{eff}^2$
Batch 1 Realised chip	$1.7 U_{eff}^2 \cdot 10^{-3}$	$0.17 U_{eff}^2$
Batch 2 Square 1cm membrane	$0.28 U_{eff}^2$	$28 U_{eff}^2$
Batch 2 Realised chip	$1.0 U_{eff}^2 \cdot 10^{-3}$	$0.10 U_{eff}^2$

Table 4: Joule heating powers.

2.3.5.3 TOTAL HEATING

The total heating is then given by adding F. 13, F. 14 and F. 20 which results in the values that can be found in Table 5:

$$W_{heating} = W_{plug.vis.total} + W_{back.viscous} + W_{joule.total} \quad \text{F. 21}$$

	[W], $c_0=1$ mM	[W], $c_0=0.1$ M
Batch 1 Square 1cm membrane	$0.36 U_{eff}^2 + 1.0 U_{eff}$	$37 U_{eff}^2 + 0.11 U_{eff}$
Batch 1 Realised chip	$1.7 U_{eff}^2 \cdot 10^{-3} + 4.7 U_{eff} \cdot 10^{-3}$	$0.17 U_{eff}^2 + 5.0 U_{eff} \cdot 10^{-4}$
Batch 2 Square 1cm membrane	$0.28 U_{eff}^2 + 0.51 U_{eff}$	$28 U_{eff}^2 + 5.5 U_{eff} \cdot 10^{-2}$
Batch 2 Realised chip	$1.0 U_{eff}^2 \cdot 10^{-3} + 1.9 U_{eff} \cdot 10^{-3}$	$0.10 U_{eff}^2 + 2.0 U_{eff} \cdot 10^{-4}$

Table 5: Total heating powers.

For the heating rate of the water in the pores per second (assuming no flow), formula F. 22 holds where m is the mass of the water.

$$E_{heating} = C_p m \Delta T$$

$$\Delta T = \frac{E_{heating}}{C_p m} = \frac{W_{heating}}{C_p m} \quad \text{F. 22}$$

It is assumed that the thermal conductance of the membrane does not play a role. Also all the water will be refreshed with the rate of the maximum flow and it will be assumed that the water flowing back due to the backflow, will be colder buffer water from the output reservoir and that no water is circulating within the pore itself due to the two flows. The resulting heating of the water for $U_{eff} = 1$ V is then given by Table 6

2 - Theory

	[°C], $c_0=1$ mM	[°C], $c_0=0.1$ M
Batch 1	0.18	14
Batch 2	0.13	14

Table 6: Heating of transported water.

At 0.1 M this seems like quite a lot, but this is only the heating of the volume that is inside the membrane for one second, which is equal to the flow. For the created chips with the 0.1 M KNO_3 solution, this is mere microliters (per second) that in this case will be cooled down in a reservoir of tens of millilitres. Thus under normal conditions, the heating in the membrane should not provide any problems for the system.

There is also heating taking place in the rest of the system, but since this will depend wholly on the system geometry and electrode orientation and is not chip dependent, it will not be dealt with in detail. For the used measurement setup the heating would be 0.009 °C/s or 0.9 °C/s for 1 mM or 0.1 M KNO_3 solutions respectively when achieving 1 V over the membrane. Only taking into the account the joule heating and not the simultaneous heat loss of the system.

2.3.6 EFFICIENCY

The efficiency of the system is given by $P_{\text{out}}/P_{\text{in}}$, where P_{in} is the electrical power going into the system and P_{out} is the hydraulic power generated by the EOF.

Only batch 2 of the produced chips was used to do any type of efficiency measurements, so the efficiency will be estimated for that batch. As can be found in section 2.3.4.3, for a 0.1 M KNO_3 solution at $U_{\text{eff}} = 1$ V the chip has a flow of $1.4 \cdot 10^{-6} \text{ m}^3/\text{s}$ for a square 1 cm chip. For the realised chip this would be $5.2 \cdot 10^{-9} \text{ m}^3/\text{s}$. The output pressure is effectively surface independent and is 235 kPa, which gives an output power of 0.33 W/cm², so 1.2 mW for one chip.

At 1 V this gives a total input power for on chip of $0.1 + 2 \cdot 10^{-4} + 1.2 \cdot 10^{-3} = 0.1$ W (as follows from Table 5). Thus the total efficiency is equal to 0.012 or 1.2 %. Combining this output power with the input power, F. 23 can be acquired for expressing the expected efficiency.

$$\text{efficiency} = \frac{0.329 U_{\text{eff}}^2}{0.10 U_{\text{eff}}^2 + 2.0 U_{\text{eff}} \cdot 10^{-4} + 1.2 U_{\text{eff}}^2 \cdot 10^{-3}} \quad \text{F. 23}$$

It is worth noting that the EOF is caused by the surface conduction, but that the surface conduction was found insignificant for a 0.1 M KNO_3 solution compared to the joule heating (as discussed in section 2.3.5.2). Thus this is not included for the total input power and the total input power is given by the total heating power. The surface conduction might be relevant however for a 1 mM concentration, but as also mentioned, this was in the end not thoroughly tested and thus no further time was spent on determining its exact value. Therefore the efficiency for a 1 mM KNO_3 solution will also not be taken into account.

The relevance of knowing the total output power does however depend a lot on the intended purpose. For some applications only a high flow is desired without any pressure, whereas for other purposes a high pressure might be desired without any flow. Having a pressure of 0 Pa or a flow of 0 m³/s, would result an output power of 0 W.

3 EXPERIMENTAL AND MEASUREMENT SETUP DEVELOPMENT - PROOF OF CONCEPT

The first batch of chips was produced and the first EOF tests were performed as a proof of concept to determine if the project was feasible or not. These tests were also used to develop the measurement setup and measurement protocols. The test results were used for designing the second batch of chips. The measurement setup and protocols, and the tests and its results will be shortly discussed in this chapter

3.1 CHIPS BATCH 1

3.1.1 PORE GEOMETRY

The design of the sacrificial pillars for batch 1 as produced by Oxford Instruments, has already been largely described in section 2.3.4.3. The used sacrificial mould pillars can be seen in Figure 11 and a sketch of the resulting dimensions of the pores can be seen in Figure 9. The wafers with the pillars were already available and because of this, the design was not optimised for this project, but used to perform preliminary test and as a proof of concept of the idea. The resulting membrane has a total thickness of 176 nm with 3 sections of 50 nm, 84 nm and 143 nm in length and a diameter 82 nm, 57 nm and 92 nm respectively.

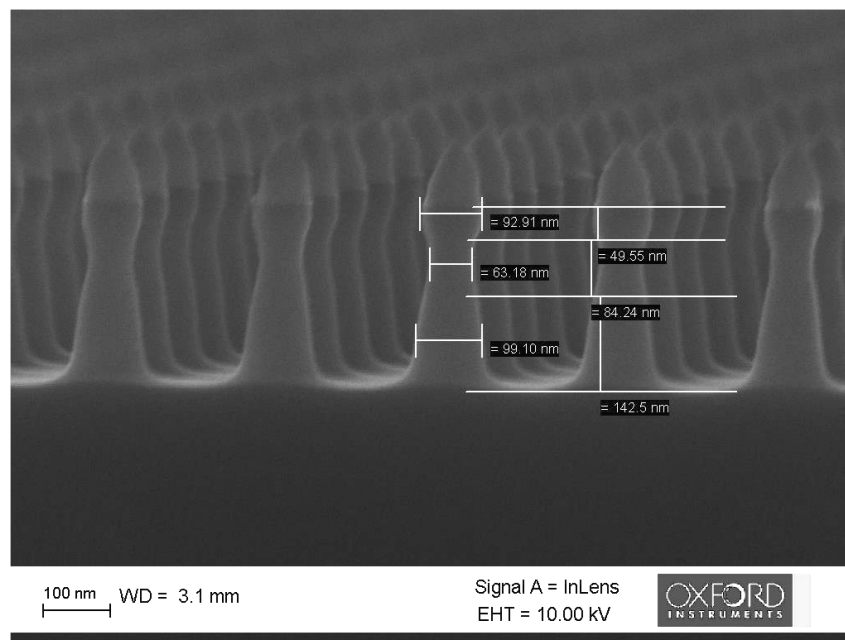


Figure 11: SEM (scanning electron microscope) image made by Oxford Instruments that are also produced by Oxford Instruments. These wafers with a single thinning geometry are the basis of the production of the first batch of membranes.

3.1.2 MASK DESIGN DESCRIPTION

The produced wafers only have the centre area of 3 cm by 3 cm filled with pillars since it was not yet possible to produce the pillars on full wafer scale. Most of the wafers have been split in half for previous imaging, but not totally symmetrical. Due to it being (semi) half wafers, aligning the top and bottom side could become quite difficult. Because of this it is decided to only make a mask for the bottom side for etching the windows into the silicon wafer and make a cardboard

3 - Experimental and Measurement Setup Development - Proof of Concept

mask for the topside to expose the full 3 cm by 3 cm area and not the exact windows, so it would not be possible to have misaligned blocked windows. For clarification see Figure 12.

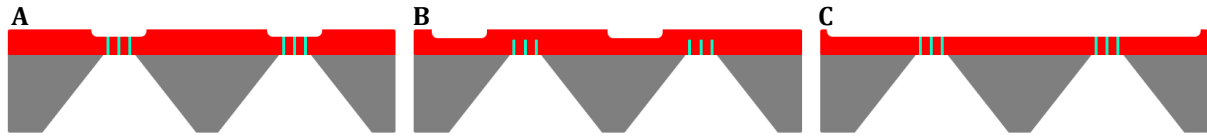


Figure 12: Alignment situations for top and bottom. A: Ideal situation with aligned top and bottom window. B: Possible misalignment with blocked pores. C: Open full top area as a solution against misalignment. Grey: Silicon. Red: SiN. Green: SiO₂ coated nanopores.

Most of the effective membrane space is lost due to the etching profile in the silicon. Since mathematically only the smallest span/dimension dominates for the strength, it should theoretically not matter if the membrane is square or rectangular for the functionality of the pump. Thus a rectangular shape is preferable for more membrane area per chip area, but might be more prone to breaking during the actual production process e.g. due to build-up of tension over the length of the membrane due to different thermal expansion rates during heating and cooling during production steps.

Because of this it is decided to make different 1 cm by 1 cm chips with square and rectangular membranes. All the membranes have to be within a circle with a diameter of 9 mm to fit and being tested in the measurement setup that is described in 3.2. The full resulting bottom mask for etching, can be found in Appendix C. In Figure 13 a cut out of the mask for the chip with the rectangular and square membranes can be seen.

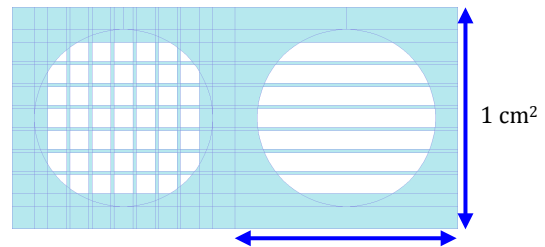


Figure 13: Cut out of the batch 1 bottom-side mask for the two models of 1 cm by 1 cm chips. In total this model is 1 cm high and 2 cm wide.

For the full process flow of the production, please take a look at the process flow for the production of the second batch in Chapter 4.2.

3.2 MEASUREMENT SETUP DESIGN

Since very small flows were expected to be needed to measure (in the order of several $\mu\text{l/s}$) while the system would most likely generate relatively large volumes of gas (at least 10 times the volume that is displaced by the EOF at maximum flow), it was decided not to use a regular flow meter in a closed system. Instead two water columns will be used and the height increase, representing integrated flow over time, will be measured. Dividing this by the time will give the flow. The advantage of the water columns is that it is an open system with direct contact to the air, where the bubbles can escape to the surface, so they will not stay part of the measured volume nor create undesired pressures, influencing the measurement.

For a flow pressure characteristic, the output tube could then be closed off and fitted with a pressure sensor. The compressed air in the tube will then provide the counter pressure and such the pressure versus flow can be measured. Since there is no direct flow measurement, but an integration of the flow, a longer time is needed to measure the flow than with a direct flow sensor.

It might happen that the pressure build-up is too fast to accurately measure the flow. (Meaning the produced gas caused the maximum pressure to be reached before enough height increase has taken place to accurately determine the flow over time.) In this case a larger volume or air reservoir can be fitted to the output. Due to the larger volume of air to compress, it will take

more time for reaching the same pressure, meaning there is more time for the EOF to create a height difference for determining the flow.

3.2.1 CHIPHOLDER

For testing a custom plexiglass (polymethyl methacrylate) chip holder has been designed and fabricated. The full design can be seen in Appendix E and the realisation in Figure 15. In the middle of the chipholder, the chip will be clamped in between two Viton rubber O-rings of 9.25 mm to keep the chip in place and create an watertight seal. Both halves of the chipholder are kept together at the rectangular flanges by 4 $\varnothing 3$ mm stainless steel hexagonal socket screws with washers that are also responsible for clamping the chip.

The chip is accessible by the buffer solution via a 7.5 mm wide circular channel from both sides. These are connected to a the cylindrical main reservoirs that have the same orientation as the access channels and a width of 10.5 mm. The floor of the reservoir is at the same height as the floor of the channel, meaning that the roof or the reservoir is oriented higher than that of the channel. This is done in order to make sure that any bubbles generated by the electrodes, will not get near the chip and block the membranes.

The other end of the reservoirs has been fitted with a Viton rubber 10.82 mm O-ring and a rectangular flange for allowing easy exchange of electrodes for experimenting with suitable electrodes. Ultimately a platinum electrode was chosen since the expected needed powers where too high for sacrificial electrodes (such as silver chloride) to not dissolve quite rapidly. Platinum wire of 0.5 mm is formed into an elongated spiral to fit the reservoir as is illustrated in Figure 14.

The distance between the windings is about 3 mm to prevent big bubbles by bubble combination at the electrode. The end is clamped with another rectangular plate of plexiglass with an 10.82 mm O-ring by which the platinum electrode is squeezed between the two O-rings to both keep it in place and form a watertight seal. The spacing between the closest points of the electrodes is 3.5 cm.

For the inlet and outlet of the reservoirs, the chipholder is on both sides fitted with 10x1 metric thread. At first it was fitted with tube fittings holding two 6 mm with 4 mm inner diameter, polyurethane tubes. However it turned out that the formation of bubbles due to the electrolysis in the channel created too many bubbles, which on its turn resulted into agglomeration, sometimes forming bubbles that blocked the entire inlet and outlet, making it impossible to measure the actual height of the buffer solution.

Because of this, two plexiglass tubes are custom made with an inner diameter of 6 mm and threaded to fit the chipholder. For better sealing, they are fitted with an O-ring and a thing layer of hot-glue as it turned out there was a slight leakage at higher pressures. The inner diameter of the tubes are drilled at 6 mm and the outside end of the thread is made conical to prevent accumulation of bubbles.

For reading the heights of the buffer solution, two rulers have been fitted on a holder, just behind the inlet and outlet of the chipholder. For measuring, roughly 5 ml of solution is present at both sides at the start of the measurement.



Figure 14: Sketch of the elongated spiral platinum electrodes. The left side is connected to the power source and measurement equipment.

3 - Experimental and Measurement Setup Development - Proof of Concept

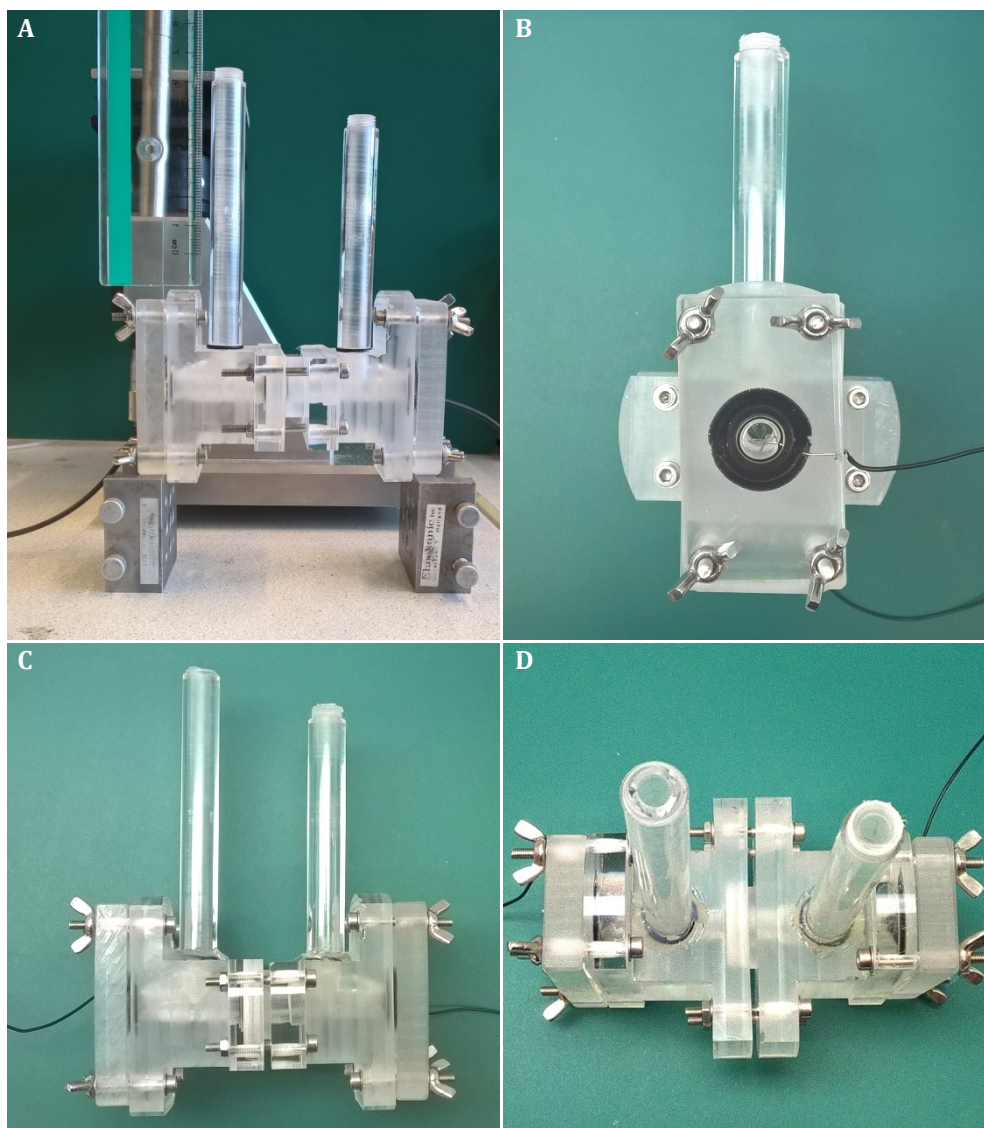


Figure 15: Several views of the build chipholder. A: Chipholder containing a plexiglass bushing with another O-ring to make the chip-holder suited to contain half wafers instead of square 1 cm chips.

3.2.2 VOLTAGE CONTROL

For the first set of measurements, the measurements are voltage controlled. The expected resistance between the two electrodes is estimated to be above $700\ \Omega$ with a $0.1\ \text{M KNO}_3$ solution and $70\ \text{k}\Omega$ for a $1\ \text{mM KNO}_3$ solution. For calculating this value, the assumption was made that the electrodes are flat plates as big as the reservoir at the positions of the closest points of the electrodes. The resistances of the batch 1 and batch 2 membranes at $0.1\ \text{M}$ are $6.06\ \Omega$ and $7.80\ \Omega$ respectively and at $1\ \text{mM}$ $606\ \Omega$ and $780\ \Omega$ respectively, so in the order of $1\ \%$ of the total resistance between the electrodes. For this also the redox potential of H_2O should be taken into account at $1.23\ \text{V}$.

For taking measurements, the chipholder is connected to a series of two dual power sources (Votcraft Labornetzgerät TNG 245, dual $30\ \text{V}$ $2.5\ \text{A}$ and Topward Electric Instruments Co., LTD. Dual-Tracking Power Supply Model: TPS-4000, dual $60\ \text{V}$ $2\ \text{A}$) to be able to reach higher potentials for higher currents. For any potential below $60\ \text{V}$, the second power supply was removed from the chain.

For measuring potential and current, two multimeters (Tenma 72-7732A Multimeter) are connected, one in parallel with the outputs of the power source for voltage measurements and one in series between the positive output of the power source and the positive input of the chipholder. For measuring the temperature a thermocouple was used in combination with a thermometer (Tenma 72-7715 Thermometer). The thermocouple is inserted via the tube into the reservoir at the positive electrode. To prevent any chemical interaction between the thermocouple and the buffer solution, the thermocouple was covered in epoxy.

For acquiring the data, all three multimeters have been connected to a computer, via their USB-connections. These are build-in for the Thermometer and an optical add-on for the multimeters. A custom LabVIEW script has been used for reading and saving the data.

3.2.3 CURRENT CONTROL

After the first measurements it was decided that current control was a better solution (due to breaking membranes, as can be read in 5.3.1). For this, a current source (Keithley 6221 DC and AC Current Source) was used, with its voltage compliance set to 105 V (maximum).

For acquiring all the data, the same setup is used as with the voltage controlled setup as can be seen in 3.2.2. Only the power sources have been exchanged.

3.2.4 HYDRAULIC

For the hydraulic and maximum pressure measurements, the inlet of the chipholder is fitted with 6mm polyurethane tubing (774-7030 RS Components Polyurethane Tubing) which leads to the outlet of an inversely connected gas washing bottle with screw cap for high pressures. The lower inlet is submerged in water and used as an outlet, while the original above-water outlet, is used as the inlet for gas under pressure, in order to have water under pressure at the output.

The inlet was connected via the same tubing to an adjustable pressure regulator (SMC IR1020-F01) with digital sensor (ifm Electronic PU5404) and readout (Lascar PanelPilot SGD 24-M) which was on its turn connected to the central high pressure nitrogen gas outlet in the laboratory.

3.3 PH BUFFER

Due to acidification problems that were discovered in the initial measurements of batch 2 (see section 5.3.2) use of a buffer is desired. In the experiments, at the positive side a low pH was unintentionally created while a high pH was created at the negative side. Since the acidic solution is pumped through the pores, they get acidified, while EOF can only take place at a pH above 3 (see section 2.3.2). Thus a slightly basic buffer pH is needed to keep the pores liquid at $\text{pH} > 7$ for as long as possible.

For this purpose a KH_2PO_4 - K_2HPO_4 buffer is chosen with an intentioned pH around 8 and a realised pH of 7.907. Ideally another buffer would have been used since the pK_a of the phosphate reaction involved (negative $10\log$ of the acid dissociation constant) lies at 6.86 and not around 8, however this was the only potassium based buffer that was readily available. Also since the pK_a lies below the desired pH and the reaction causes the pH to lower, the buffering capacity gets stronger the closer the pH gets to 6.86.

Because of the lack of time within the planning, as a rule of thumb it is taken that the buffer solution could take about 1/3 of its molarity in acid change before the pH would change

3 - Experimental and Measurement Setup Development - Proof of Concept

significantly. Since for the first 5 to 10 minutes the bubbles dominate the readout of the measurement, the solution should be able to buffer longer than this time. The buffering time is given by the buffer concentration c_0 and buffer volume V_{res} and the current passed and faraday constant F . For a 0.1 M buffer in the 5 ml reservoir at the current I of 20 mA that will be used during these measurements, this gives:

$$\text{capacity time} = \frac{\text{capacity}}{\text{current}} = \frac{c_0 V_{res} F}{I} = 804 \text{ s or } 13 \text{ min } 24 \text{ s} \quad \text{F. 24}$$

This however only gives only about 3 minutes of measurement time after the settling of the bubbles. Thus it is decided to work with a buffer concentration of 0.2 M, giving a total time of 26 min 48 s on which basis is then decided to measure for 26 min.

Later the calculation was looked at more carefully. The buffer capacity β is given by F. 25 [41]. It gives the amount of moles $[H^+]$ that can be added of an acid or base to cause a pH change of 1.

$$\beta = \frac{d[H^+]}{d\text{pH}} = \ln(10) \left(\frac{K_w}{[H^+]} + [H^+] + \frac{c_0 [H^+]}{(K_a + [H^+])^2} \right) \quad \text{F. 25}$$

Plotted against pH, the buffer capacity can be found in Figure 16. At a pH of 7.907 the capacity is only 0.0348 mol, which at a rate of 20 mA in a volume of 5 ml is reached in 12 min 57 s. However when the pH lowers towards 6.82, the buffer capacity increases, as can be seen in the plot. When it reaches the pH of 7, the capacity reaches 0.1103 mol, which relates to 44 min 21 s, meaning that for the measurements of 26 minutes, the pH in the reservoir at the positive electrode should still most likely be above 7.

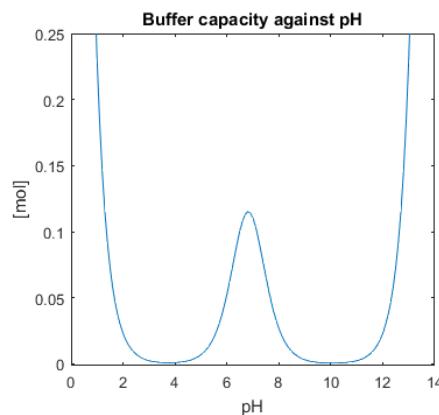


Figure 16: Plotted KH_2PO_4 buffer capacity at 0.2M.

3.4 MEASUREMENT PROTOCOL

3.4.1 PREPARING CHEMICALS

All used H_2O was prepared by either the Milipore Mili-Q or the Elga Purelab Flex 2 water purification system with a resistance of 18.2Ω and a total organic carbon (TOC) of 3-4 ppb.

The piranha solution prior to testing was prepared using 95.0-98.0 % sulphuric acid and 31 % hydrogen peroxide both acquired from Sigma-Aldrich and mixed at a 3:1 ratio.

For the KNO_3 solutions, solid potassium nitrate from ReagentPlus® was acquired from Sigma-Aldrich.

pH Buffer

For preparing the pH buffer for the last tests of batch 2, potassium phosphate monobasic (KH₂PO₄) and potassium phosphate dibasic (K₂HPO₄) from Sigma-Aldrich were used to create a solution with a pH around 8 and a potassium concentration of 0.2 M. The exact pH and conductivity were measured after preparation and were a pH of 7.907 and 2.44 S/m with an S47 SevenMulti™ dual pH conductivity meter.

All other pH values were measured using Hydrion® Brilliant Dip Sticks pH range 1-14.

All solutions used for measuring were filtered after production by means of a 0.22 µm filter after it turned out the chips clogged up significantly fast.

3.4.2 VOLTAGE AND CURRENT CONTROLLED MEASUREMENT PROTOCOL

Step	Description
1. Inspection	Quickly inspect the selected chip under the microscope for damaged membranes.
2. Cleaning and activation	2.1 Make at least 50ml of piranha by adding 15 mL H ₂ O ₂ to 45 mL H ₂ SO ₄ , 1:3 ratio for cleaning and activating the silanol groups [42]. 2.2 Add the chip on its side directly after preparing the solution for at least 10 min. When placed under an angle, make sure the bottom side is up for bubbles to be able to escape. 2.3 Remove the piranha from the pores by placing the chip in DI water for at least 10 min. 2.4 Dry the surfaces of the chip by use of an N ₂ blower parallel to the surface. (The drying for better sealing in the chipholder preventing a water bridge to remain. Keeping it parallel to prevent damaging the membranes.)
3. Chip placing and preparation	3.1 Place the chip in the chipholder and tighten the screws until adequate pressure to prevent leakage. 3.2 Add the desired buffer solution to an adequate amount that a significant height difference (raising of buffer in one tube and lowering of buffer in the other tube) can still be measured by using both rulers. Make sure the positive side, is a bit lower to compensate for the thermocouple. 3.3 Put the thermocouple in reservoir at the side of the positive pole.
4. Equipment preparation	4.1 Turn on the two multimeters and the thermometer and enable the data-send. 4.2 Connect them to the computer via USB. 4.3 Turn on the power supplies and double check that all multimeters devices are reading the correct data.
5. Software preparation	5.1 Run 3 instances of the Tenma ddm.exe program. Select the right USB interface and select two times model vc-960 for the multimeters and ut325 for the thermometer and check if the data corresponds with the changes on the multimeters devices. 5.2 Open the dd1V1.vi in LabVIEW and fill in the corresponding models and USB interfaces in the right fields in the VI (virtual instrument). Also fill in the path for the data to be saved to.
6. Start of measurement	6.1 Set the power supply to the adequate voltage or current depending whether the setup is voltage or current controlled. (See section 3.2.) 6.2 Note the column water height. 6.3 Start the Labview VI. 6.4 For the voltage controlled setup: Connect the negative connector of the chipholder to the connector pole of the voltage meter and start the clock

3 - Experimental and Measurement Setup Development - Proof of Concept

	at the same time. 6.5 For the current controlled setup: Make sure the power source is connected to the chipholder. Turn on the output and start the clock at the same time.
7. Measuring	Make sure the software keeps running and the values keep corresponding with that of the multimeters devices, to see if the communication crashes. At chosen time intervals, pick up the chip holder and hold it under an angle and then note down the column water height: First the left side up, then the right side up for 1 to 2 seconds to let the big bubbles flow out of the holder. Then write down the height of the ellipsoidal front of the buffer-air interface.
8. End of measurement	8.1 Disconnect the negative pole of the setup together with the one of the voltmeter. 8.2 Stop the running VI
9. Chip extraction and cleaning	9.1 Drain the chipholder with the custom syringe with tube nozzle. 9.2 Fill the chipholder with filtered H ₂ O. 9.3 Drain the chipholder with the custom syringe with tube nozzle. 9.4 Open the chipholder and remove the chip, put it in H ₂ O for at least an hour and dry in vacuum for at least an hour. 9.5 Flush both sides of the chipholder with H ₂ O.

3.4.3 HYDRAULIC RESISTANCE AND MAXIMUM PRESSURE MEASUREMENT PROTOCOL

Step	Description
1. Inspection	Quickly inspect the selected chip under the microscope for damaged membranes.
2. Cleaning	2.1 Make at least 50ml of piranha by adding 15 mL H ₂ O ₂ to 45 mL H ₂ SO ₄ , 1:3 ratio for cleaning and activating the silanol groups [42]. 2.2 Add the chip on its side directly after preparing the solution for at least 10min. When placed under an angle, make sure the bottom side is up for bubbles to be able to escape. 2.3 Remove the piranha from the pores by placing the chip in DI water for at least 10min. 2.4 Dry the surfaces of the chip by use of an N ₂ blower parallel to the surface. (The drying for better sealing in the chipholder preventing a water bridge to remain. Keeping it parallel to prevent damaging the membranes.)
3. Chip placing and preparation	3.1 Place the chip in the chipholder and tighten the screws until adequate pressure to prevent leakage. 3.2 Add the H ₂ O to an adequate amount at the outlet tube, for the height differences to be measured by using the ruler. 3.3 Add the H ₂ O to the inlet tube until the brim.
4. Connecting the chipholder	4.1 Make sure the water dispensing pressure reservoir is filled with enough water. 4.2 Make sure the outlet tube of the water dispensing pressure reservoir is fully filled with water. 4.3 Insert the tube into the inlet of the chipholder, making sure no major airpockets are trapped. 4.4 For better sealing at higher pressures, apply hot glue to the edge of the chipholder inlet to seal the tubing to the inlet.
5. Prepare the gas pressure flow	5.1 Connect the pressure regulator to the N ₂ outlet. Make sure the outlet is closed. 5.2 Fully open the pressure regulator vent valve to make sure the initial

	<p>pressure applied to the system will be 0bar.</p> <p>5.3 Open the N₂ outlet far enough that the desired pressure can be reached with adequate flow. (Read the value at the indicator of the N₂ outlet.)</p> <p>5.4 Make sure the digital readout of the pressure regulator powered and turned on.</p>
6a Measuring resistance/flow	<p>6.1 Adjust the pressure regulator valve rapidly until the desired height is reached and then note the water height and start the timer.</p> <p>6.2 At chosen time intervals, note down the column water height.</p> <p>6.3 When measuring at non-constant pressure: Change the pressure to the next desired step and note the time and column water height.</p>
6b Measuring maximum pressure	<p>6.1 Adjust the pressure regulator at the desired starting pressure and look at the flow. Since the system will not break before being in the 1bar region, the expected flow when breaking is expected to be high and should easily be distinguishable from the flow before breaking.</p> <p>6.2 Increase the pressure stepwise and look at the flow while waiting about 1 minute between the steps.</p> <p>6.3 When the flow suddenly becomes really high, possibly spouting from the outlet of the chipholder.</p>
7 End of measurement	<p>7.1 When finished, bring the pressure back to 0bar using the pressure regulator.</p> <p>7.2 Close the N₂ valve and disconnect it from the pressure regulator.</p>
8. Chip extraction and cleaning	<p>8.1 Wiggle free the tubing from the inlet of the chipholder.</p> <p>8.2 Drain the chipholder with the custom syringe with tube nozzle.</p> <p>8.3 Fill the chipholder with H₂O.</p> <p>8.4 Drain the chipholder with the custom syringe with tube nozzle.</p> <p>8.5 Open the chipholder and remove the chip, put it in H₂O for at least an hour and dry in vacuum for at least an hour.</p> <p>8.6 Flush both sides of the chipholder with H₂O.</p> <p>8.7 Peel away the hot glue from the chipholder inlet.</p>

3.5 INITIAL PRODUCTION, EXPERIMENTS AND RESULTS

3.5.1 CHIP PRODUCTION

The first 5 steps of production process, as can be found in chapter 4.2, for creating the sacrificial pillars of the first batch, were already performed previously by Oxford Instruments with the result visible in Figure 11 in chapter 3.1.1. The other steps were performed and partially developed within the scope of this project as can be found in 4.2.

Etched Extra holes

The processed wafers were examined by use of a scanning electron microscope (SEM) directly after step 26. This is the last SiN etching step, freeing up the pillar tops, as can be seen for clarification in Figure 19 A. Images from wafer 3, the one used for the actual experiments, can be seen in Figure 19 C-D. It shows the edge of the membrane and thus the transition from the still filled oxidised pillar tops from the pillars filled with crystalline silicon, in white, and the pillars refilled with poly-Si in grey.

The tops of the pillars are looking as expected, however between the pillars there are large holes. These are possibly caused by inclusions, formed during conformal deposition of SiN. These inclusions are caused by the symmetry of the pillars and should not prove problematic as long as they are being sealed at the top by SiN.

3 - Experimental and Measurement Setup Development - Proof of Concept

However clearly the isotropic etchant got in and etched the holes, making them larger. The access for the etchant is most likely caused by the top part of the pillars being not fully cylindrical with possibly a negative tapering or a small broadening at the very top due to some under etching during the start-up of the etching process. This caused a very thin covering layer at the top with an access tube to the pocket below as is illustrated in Figure 17.

This theory is supported further by the images from wafer 7 that underwent the same processing, that are shown in Figure 20. This wafer has similar geometry with the main difference that the thinned area in the middle is elongated with respect to the ones are described before. When looking at the images taken under a tilt, one can see that some of the adjacent holes have been etched away far enough to connect again and one can clearly see the holes are shaped in similar fashion as the shape of the original pillars.

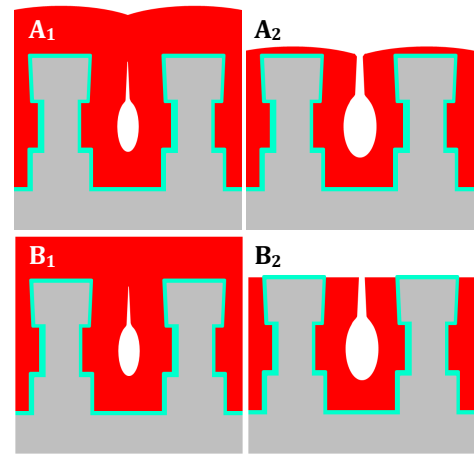


Figure 17: Two sketches from left to right for the two mechanisms for causing the etched holes in the membrane. The cross section is taken through two diagonally oriented pillars.

There are two hypotheses of how the etching of the holes starts. The first one is that the top layer of the deposited SiN was not yet fully levelled due to the added layer being too thin, which left minor pits at the location of the already thin SiN above the pockets, enabling the etchant to reach them before the tops of the pillars were fully etched free, as is shown in Figure 17 A. The second one is that the SiN above the pockets was so thin, that with the first uncovering of the tops of the pillars, the access channel also got opened up and that the holes got etched wider during the little overetching that took place to be sure that all tops would be free for when the SiN layer thickness would be slightly inhomogeneous, as is shown in Figure 17 B.

These extra holes should not prove any difficulties for the EOF flow, since they do not fully penetrate the membrane. However they might prove problematic for the structural integrity, preventing it to withstand higher pressures. However for the mechanical strength of the membrane, the most important are the sturdiness of the topside and bottom side of the membrane. The bottom side is still intact and at the top side, the adjacent pillars are still connected as squares by the SiN. Meaning it should still be able to withstand significant pressures.

At the end of all the processing steps, before the dicing into individual chips, the wafers were inspected. It turned out that all the chips containing the 100 μm wide rectangular membranes had at least one or more of the membranes shattered and were thus unusable. The rectangular membranes that were not shattered, showed signs of bending patterns across the length of the membrane. Possibly the use of different materials and deposition at different temperatures, caused too much internal stress for them to be strong enough to survive the production process.

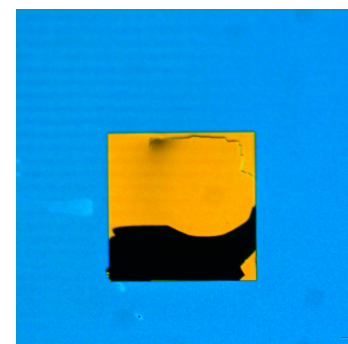


Figure 18: Example of a broken 100 μm membrane.

Of the four half wafers, only three made it to through the full processing steps. Of the 9 chips in total, the 3 chips with rectangular membranes were all not usable and 4 most of the 6 chips with square membranes had the membranes partially ripped or entirely broken out. An example of this can be seen in Figure 18. Because only 2 chips remained, it was decided not to dice the chips,

lest the dicing forces causing the last membranes to break, and use the full half wafers for testing.

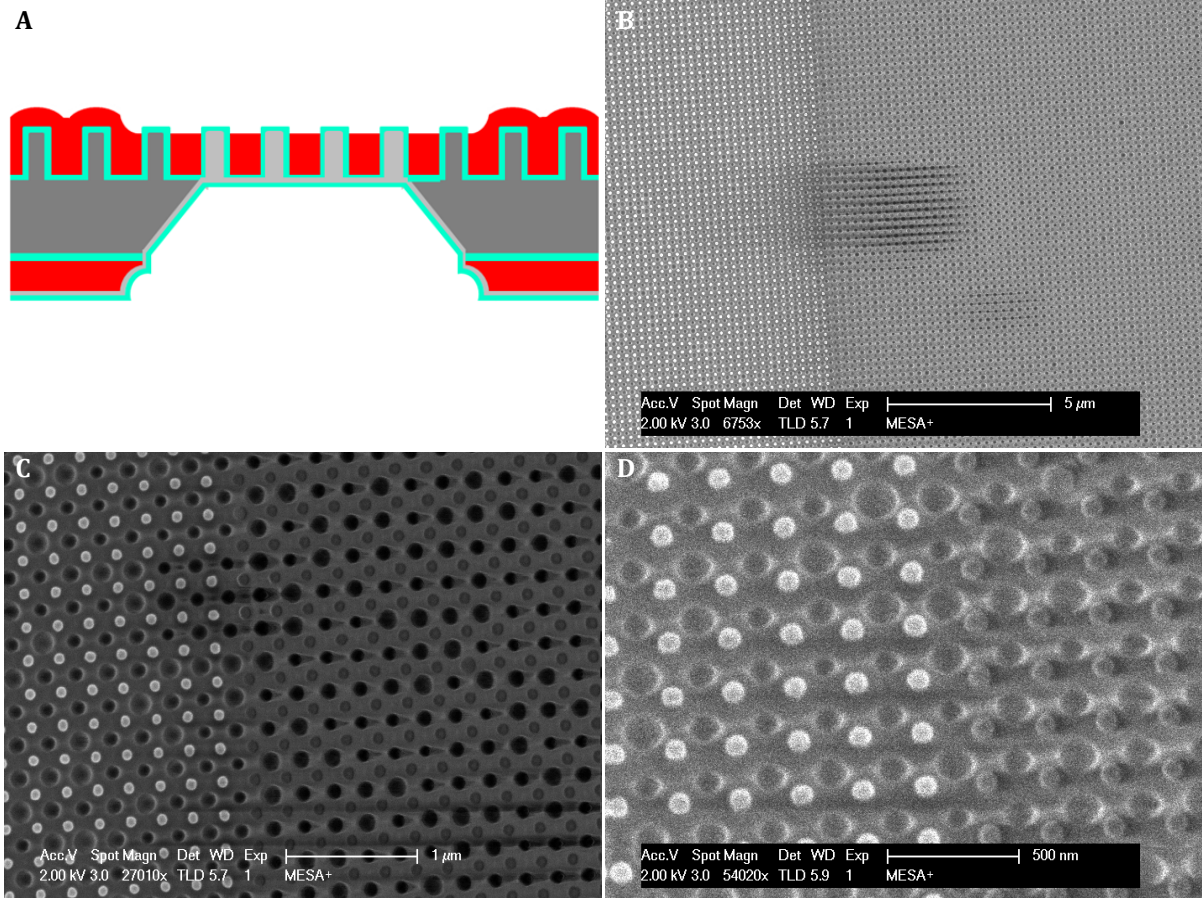


Figure 19: A: Step 26 of the process flow as found in chapter 4.2. The last SiN (red) etching step has been performed and the tops of the oxidised (green) and poly-Si (light grey) filled pillars are exposed. Also some original silicon (dark grey) pillars made from the wafer, are exposed at the edges. Note that here only part of the SiN has been etched at the top, while for batch 1, the whole SiN layer has been etched. B-D: SEM images of wafer 3 right after processing step 26. It shows three times an image from the same chip with a different magnification and/or contrast and D under an tilt of 15 °. The smaller dots are the tops of the pillars with the white ones on the left the ones from the wafer, that are still filled with crystalline Si while the ones on the right are filled with poly-Si. The bigger holes are holes etched into the SiN. The tails of the holes that are found on the right and the black horizontal lines, are artefacts from taking the SEM image and not there in reality.

3 - Experimental and Measurement Setup Development - Proof of Concept

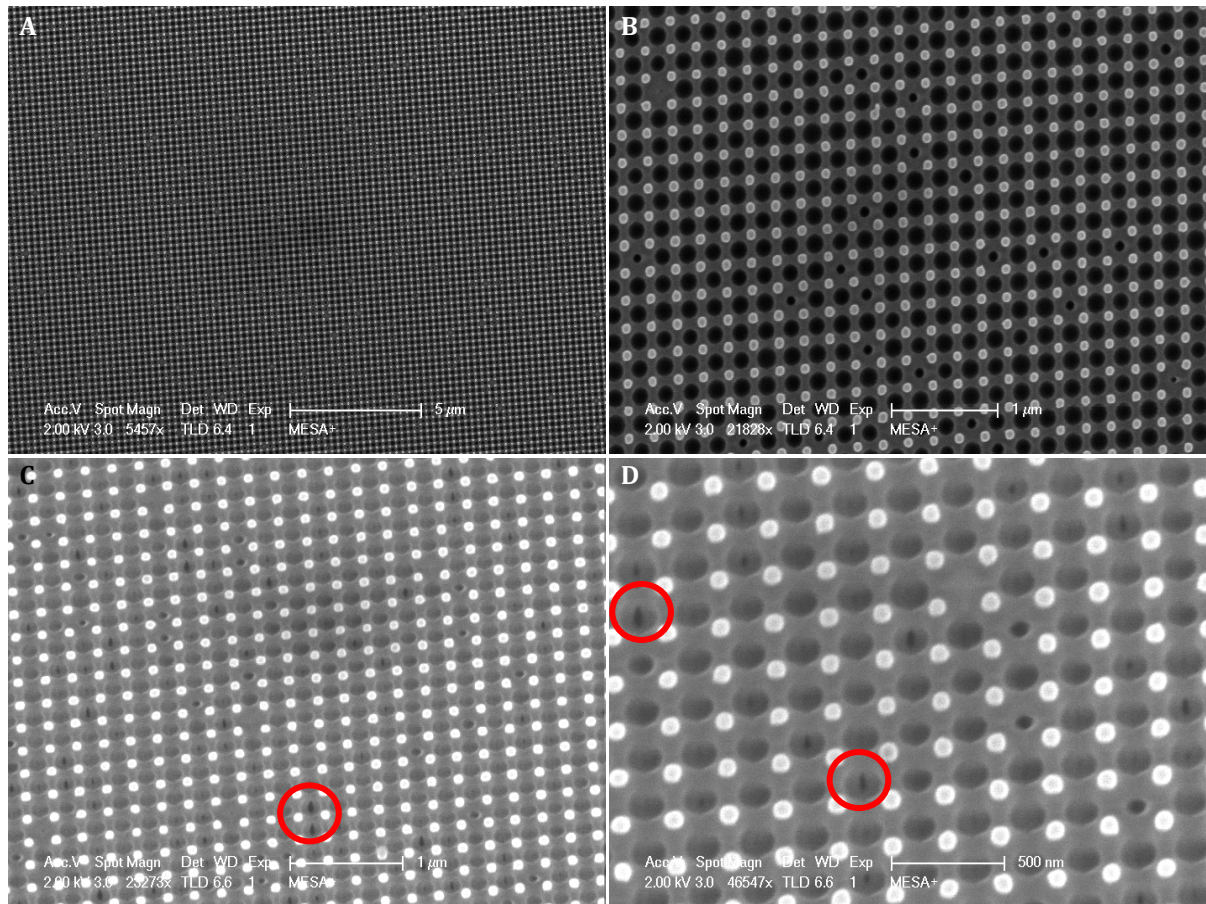


Figure 20: SEM images of wafer 7 right after processing step 26. It shows four times an image from the same chip with a different magnification and/or contrast with C with a tilt of 15 ° and D with a tilt of 35 °. Within the red circles are examples of the connected under etching of adjacent holes within the SiN membrane.

3.5.2 MEASUREMENT SETUP - FOUND DETAILS AND ISSUES

The original design of the chipholder was made such, that square 1cm chips are housed within the chipholder. However since it was feared the two remaining chips from the first batch would not withstand the dicing process, a plexiglass 5 mm thick bushing with a 7.5 mm inner diameter, was made to fit the holder space within the chip-holder for containing the square 1 cm chips. Making it possible to fit flat objects larger than the square 1 cm chips.

Electrodes

The original set-up contained brass tube fittings, holding 6 mm polyurethane tubes with a 4 mm inner diameter for measuring the height. However after extensive testing, it kept happening that the positive oxygen side, created bubbles that agglomerated, resulting in airpockets in the tubing, making it impossible to measure the actual buffer height.

Initially also two platinum coated pieces of wafer were mounted at the end of the chipholder as the electrodes, covering the full electrode inlet hole. However this meant the electric field had to cross a distance of about 11 cm, meaning about 3 times as high a potential was needed for the same actuation, which meant about 200 V for just 100 mA at 0.1 mA and about 20 kV for 1 mA. Both power supplies together could however not deliver more than 180 V and in the beginning it was thought to be interesting to go above 100 mA for higher flows which were easier to measure accurately.

All the gas bubbles were formed on the vertical flat plate electrode, with a slightly sloping roof over a horizontal distance of several centimetres from the electrode to the outlet. This made the small bubbles in general already accumulate into large bubbles before they reached the outlet, resulting plugs blocking the measurement tubes as is illustrated in Figure 21.

For decreasing the distance between the electrodes and thus lowering the needed voltage while also decreasing the distance for the bubbles to travel, a horizontal 0.5 mm platinum wire electrode was used. At first a tight spiral with 1 mm to 1.5 mm windings was made to fit right under the outlet, but the short distance between windings and thus the forming bubbles, made the bubbles form larger bubbles on the electrode already. This was solved using an elongated spiral with about 3 mm between the windings. Effectively the whole spiral consists of 1.5 horizontal windings as can be seen in Figure 14. The end of the electrode goes out of the reservoir between the O-rings at the mounting plate at the end of the chipholder for connecting to the power source and measurement equipment.

Height Columns

The change of electrodes largely improved the bubble problem and reduced the needed voltage. However incidentally there would still be too large bubbles at the positive oxygen side that could not be removed by removing unevenness and sharp edges. Also the tube fittings were made of metal and it seemed that debris was forming in the system while the surface of the fittings seemed corroded and sometimes the foam on top of the water front, turned slightly green, suggesting dissolved copper. This would be in accordance with the dissolving of the copper containing brass tube fittings. Even though the tube fitting were not in the direct path of the electrode and about 1 cm above the electrodes, the high voltages used by then (up to 120 V) probably created local electrical fields with large enough potentials over walls of the tube fittings to corrode the metal.

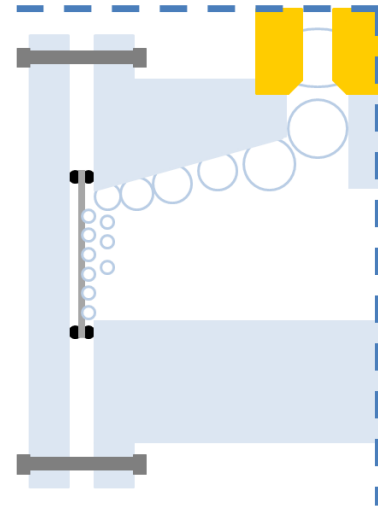


Figure 21: Sketch of a part of the chipholder showing the bubble formation. In the sketch the vertical flat plate electrode clamped in between O-rings on the left, the bubble clogged outlet with brass tube fitting connected to the measurement tubes on the top right and the channel to the chip on the right can be seen.

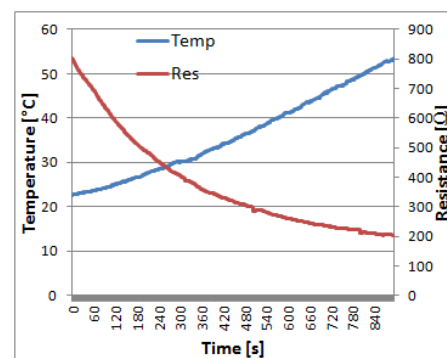


Figure 22: Temperature and resistance over time in the chipholder at 40V without a membrane.

3 - Experimental and Measurement Setup Development - Proof of Concept

To solve this and also the problem of still having too large bubbles, solid tubes were made from plexiglass with a thread for connecting and a larger inner diameter. The inner diameter of the new tubes was 6 mm, resolving the air plug problem.

Temperature

For calculating the effective voltage over the membrane, at first the voltage for the whole system was measured for 0.1 M solution by applying a stepwise increasing voltage from 15 V to 50 V and measuring the current. However over the duration of this measurement, the resistance decreased to about 30 %. Keeping the current around 100 mA for 5 min, decreased the resistance to 20 %. A measurement with the spiral electrodes at 40 V for 15 min can be seen in Figure 22. Repeating such experiments at 1 mM while keeping track of the temperature, showed no large increase in temperature, but because of this, no long term experiments were performed that also tracked the current/resistance since at first it was thought that the change of resistance was due to the change in temperature.

When looking at the numbers and also Figure 22, it was later realised however, that this was incorrect. Figure 22 shows a decrease in resistance of about 75 % and a temperature increase from 22.5 °C to 53.4 °C. When comparing this with the relationship between temperature and conductance shown in Figure 4 in section 2.3.1.1 and in Appendix B, it shows that only 39 % of the resistance decrease should be caused by the change in temperature of the 0.1 M KNO₃ solution.

Faradaic Concentration Polarisation

A linear relationship is expected between the decrease in resistance and increase in temperature, but when looking at Figure 22 it shows that the decreasing of the resistance is more rapid than expected in the beginning and gradually lessens over time. Due to the results found for the second batch, it is suspected that this more rapid decrease in the beginning, possibly accounting for the remaining total decrease of 26 % might be caused by a lowering of pH at one electrode and a increasing of pH at the other electrode.

Due to the production of O₂ at one side and H₂ at the other side, the one side will acidify and the other side will alkalify near the electrode. This local change in pH which from here on will be referred to as faradaic concentration polarisation, will cause a higher conductance near the electrodes, so a lower resistance while the pH in the middle of the chipholder will stay around neutral where the resistance is expected to follow earlier mentioned temperature depended relationship. This is however a chemical equilibration effect that should level out over time, possibly explaining the partially levelling of the curve in Figure 22 of the lowering resistance.

Resistance

With the new electrodes the resistance of the chipholder without a membrane at the start of a measurement is about 800 Ω at 0.1 M. This is lower than the 700 Ω mentioned in section 3.2.2, but this can be explained by the fact that in section 3.2.2 2 parallel facing flat plates were assumed for the electrodes while in practice these are two in-plane laying spirals with only the far ends as the closest points used for calculation, so a higher resistance is to be expected.

Determining the Effective Membrane Potential

It turned out that the electrodes could move around a bit while cleaning the measurement setup. Also due to different pressures on the 4 screws clamping the chips and holding the setup together, the setup length could vary by several millimetres due to the rubber O-rings. This made the percentagewise estimation of the resistance of the chip with respect to the whole

setup and thus the potential over the membrane, less reliable. Therefore it was decided to focus on the current and by means of calculating the resistance of the membrane based on geometry, ion concentration and temperature (as has been done in section 2.3.5.2), calculate the potential over the membrane and thus the expected EOF.

3.5.3 EOF

The first EOF tests with a 0.1 M KNO_3 solution showed to be quite promising for a proof of concept. It was shown that EOF took place by the increasing water height in the measurement column at the expected side of the measurement setup and also the decreasing water height at the other side under applying a voltage over the whole system, but as described in this section, there were some complications.

First of all these tests were made without measuring the temperature, so it cannot be evaluated with confidence if they fit the expected EOF. The change in conductance due to temperature and possibly due to a change in pH as mentioned in section 3.5.2 must have taken place with all the initial measurements with the 0.1 M KNO_3 solution and is supported by the fact that those measurements also showed a large increase in conduction. However the temperature was not yet measured rendering all these measurements quite useless with respect to calculating the exact EOF, since it was not possible to compensate for the temperature or the unknown change in pH.

Bubbles

During measuring at a constant voltage of 40 V the collection of both O_2 and H_2 bubbles on the walls of the reservoir were observed, at the positive and negative side respectively. In general the H_2 formed a relatively uniform coating of small bubbles of several tenths of millimetres in diameter, over the whole plexiglass while the O_2 created larger bubbles sometimes up to several millimetres that in general seemed to have less interaction with the plexiglass, since it did create a fully covering uniform coating.

The initial height increase in the water column was mainly caused by the bubbles forming. In general after about 2 to 5 minutes, this rapid accumulation of bubbles at the wall and resulting height increase largely stopped increasing and stabilised. However it must be noted that frequently larger bubbles did form and grow before finding their way to the surface, resulting in a large amount of noise on the measurements with its height increasing and decreasing.

0.1 M KNO_3 Solution Measurements

The measurement data of the 0.1 M KNO_3 solution that includes the temperature from the first batch of chips can be seen in Appendix H where also the expected height increase has been calculated. In Figure 23 an representative example can be seen for the calculated and measured height increase in the measurement column. For the 0.1 mM KNO_3 solution the measured values (where the slope is of importance) seemed in the range of the expected values for the 4 measurements made, ranging between 20 % to 58 % of the expected value after 10 minutes. A significant part of the total increase is however caused by bubbles settling on sides on the

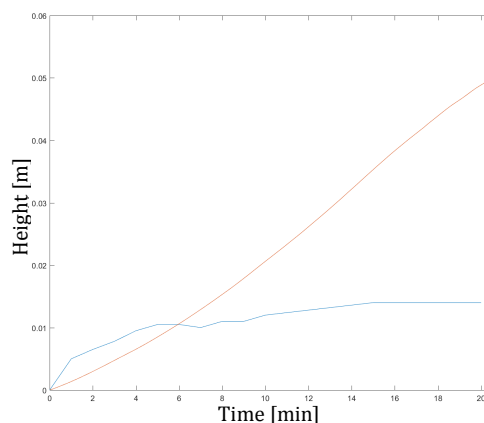


Figure 23: Representative example of the EOF measurements with the 0.1 M KNO_3 solution. Time in [min] in the X-axis, height in [m] on the Y-axis. Blue: Measured increase. Red: Calculated increase.

3 - Experimental and Measurement Setup Development - Proof of Concept

chipholder. To be able to draw more significant conclusions, more tests would need to be performed.

It should be noted that unlike the data from the second batch, where both the height of the increasing and decreasing water column have been measured, here only the height of the increasing water column has been measured. At the end of most measurements it was however checked if the height of the decreasing water column was either lower or at least at the same height. The latter case also showed signs of EOF since the bubbles that accumulated on the reservoir walls adding to the total volume, meant that the solution was pumped to the other side of the chip.

Faradaic Concentration Polarisation

With the second batch of chips, there was a clear faradaic concentration polarisation observed. Meaning that due to the production of O_2 at the positive electrode and H_2 at the negative electrode, locally at the positive electrode H^+ and at the negative electrode OH^- was formed. The membrane in the middle, largely kept the two reservoirs from chemical interaction, resulting in a pH in the reservoirs of about 1 at the positive electrode and a pH of over 13 at the negative electrode. This on its term seemed to initially acidify the channels due to which no EOF would take place. This process took about 1 hour before EOF started taking place, probably due to the high alkaline solution making enough OH^- getting into the channels, creating a neutral or at least more alkaline solution than at the start, as can be read in chapter 5.3.

Due to the fact that the decreasing water column has not been measured over time for the first measurements, it cannot with certainty be concluded if there was not a similar faradaic concentration polarisation taking place for these tests and that most of the increase at the other column was not mainly caused by more bubbles accumulating. Although it seems likely that a similar effect must have taken place with this batch of chips.

Most taken measurement where however well under an hour while still showing signs of EOF. This means that either this faradaic concentration polarisation effect for the chips of batch 1 happened much faster than with the chips of batch 2, or that significant EOF took place right at the start of the measurement to show up in the final heights at the ends of the measurements. If the EOF was present in the first few minutes, it cannot be seen due to the large influence and noise from the bubbles settling.

A possible faster faradaic concentration polarisation of batch 1 with respect to batch 2, might be explained by the difference in geometry with a thinner membrane, possibly making it easier for enough OH^- to neutralise enough H^+ in a significantly large section of the channel. The thinning in the middle might also have helped, creating a bottle-neck for the H^+ to diffuse to the other side and allowing the broader part at the alkaline for enough OH^- to diffuse into the channel to create EOF in that part of the channel. However, this would mean H^+ would get sucked into this section, meaning a balance between EOF and diffusion driven H^+ addition and diffusion driven OH^- addition would take place, which would be expected to cause a lower EOF.

Another explanation for the faster faradaic concentration polarisation, might be the fact that these measurements were performed at a constant voltage. This meant that during some test currents rose well over 50 mA whereas the second batch has mainly been measured at a constant current of 20 mA.

1mM KNO₃ Solution Measurements

When looking at the 4 datasets for 1 mM in Appendix H of which a representative example is shown in Figure 24., all height increases seem to have similar profiles as the expected height increase, but are all in the order of only 1 % of what was expected. This might be caused by the faradaic concentration polarisation and partially by the fact that the Debye layer is significantly large with respect to thinned part of the pore, as is described section 2.3.4.3.

Note also that after these tests it turned out one of the chips had a shattered membrane and the other one was significantly clogged. This would also explain a lower measured EOF due to parallel leakage and a lower effective pump area respectively.

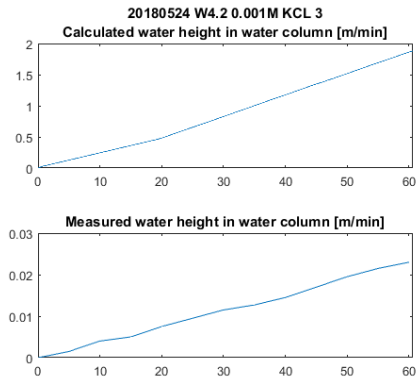


Figure 24: Representative example of the EOF measurements with the 1 mM KNO₃ solution. Time in [min] in the X-axis, height in [m] on the Y-axis.

4 DESIGN BATCH 2

Based on the results of batch 1, a design is created for the second batch of membranes.

4.1 PORE GEOMETRY

Strength

Since most of the membranes of batch 1 had already shattered during the production process, it is desired to create stronger membranes. Without changing the whole structure and process (for instance by adding extra beams of another material), this can be achieved by increasing the thickness of the membrane, reducing the span of the membrane and preventing the undesired extra etched holes that were found on batch 1 (described in section 3.5.1 and are visualised in Figure 17, Figure 19 and Figure 20), to be formed between the pores.

With the focus on the preventing the extra etched holes, it was decided that the pores and thus the sacrificial pillars should be slightly conical with a positive tapering to prevent the formation of inclusions. By the time the venerable Yasser Pordeli had developed a recipe for creating pillars with a positive tapering of 1.7 ° and a maximum height of 455 nm. This height is an increase of 65 % with respect to the previous design, giving the square 100 µm membranes a theoretical maximum loading pressure of 155 kPa. An image of the result of the sacrificial pillars of this recipe can be seen in Figure 25.

The SiN is conformally deposited, meaning it will coat the pillars in all directions with the same thickness. The bare minimum layer thickness of SiN needed to cover the space between the sacrificial pillars 263 nm, as is given by F. 26. Here d_{pitch} is 250 nm and d_{pillar} is the minimum diameter at the top of the pillar. The minimum diameter of the original is 80 nm, as can be seen in Figure 25, but the SiN is deposited after the oxidation which adds roughly 10 nm to the diameter, making it 90 nm.

$$\sqrt{2 d_{pitch}^2 - d_{pillar}^2} - d_{pillar} = \sqrt{2} d_{pitch} - d_{pillar} = 263.3 \text{ nm} \quad \text{F. 26}$$

In practice a thicker layer of 500 nm SiN is deposited since the layer evens out when growing thicker, creating a levelled flat surface for the etching. This should prevent a profile of pits to be left on the surface that will cause a non-flat surface after etching, or might still access inclusions during the etching before the tops of the pillars are etched free (see section 3.5.1 or Figure 17 A for clarification).

Flow

The flow was already relatively low to measure and no high actuation power could be used to increase the flow since the membranes were already shattered in at least one chip. Therefore it was decided to not decrease the span of the membranes and with that the effective pump-area per chip for higher pressures. Also for the geometry of the pores, this could be optimised to more easily create higher pressures, but since the flow is already hard to measure, the pores are kept as wide as possible to have a higher flow per volt over the membrane. The resulting sacrificial pillars have an average diameter of 93 nm.

After oxidation and further processing the pores will have an average diameter of 83 nm and a length of 455 nm as can be read in section 2.3.4. An excerpt of Table 1 with the expected flows is shown in Table 7 and as can be read in section 2.3.4.3 a theoretical maximum backpressure of $353 U_{eff} \text{ kPa}$ for a 1 mM KNO_3 solution and $118 U_{eff} \text{ kPa}$ for a 0.1 M KNO_3 solution can be achieved.

	$[m^3/s]$	$[\mu l/s]$	$[ml/min]$
$c_0=1 \text{ mM}$ Batch 2 chip	$5.3 U_{eff} \cdot 10^{-9}$	$5.3 U_{eff}$	$0.32 U_{eff}$
$c_0=0.1 \text{ M}$ Batch 2 chip	$1.7 U_{eff} \cdot 10^{-9}$	$1.7 U_{eff}$	$0.10 U_{eff}$

Table 7: Excerpt from Table 1 of expected flows for batch 2.

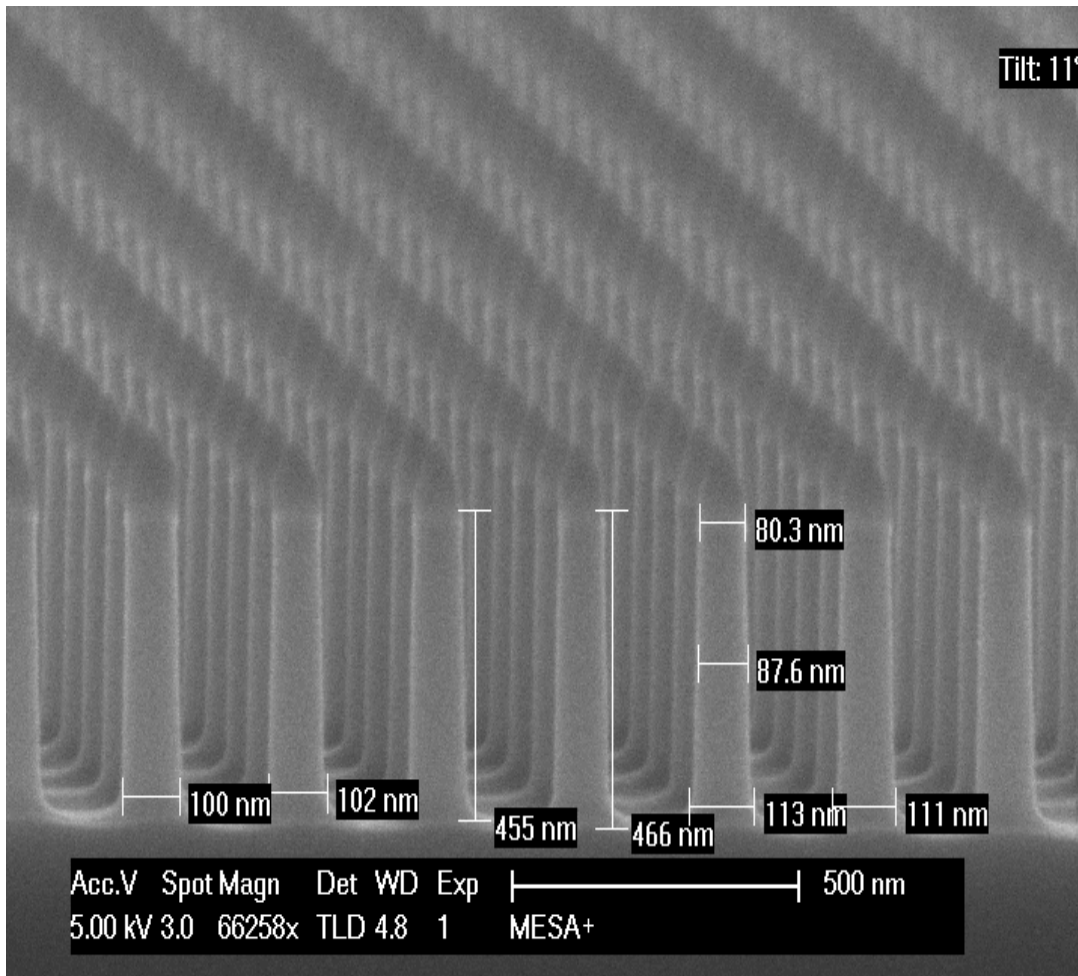


Figure 25: Example of the sacrificial pillars for creation of the membrane. The image was used with the courtesy of Yasser Pordeli.

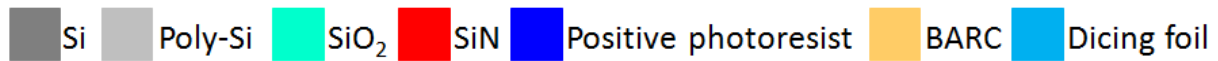
4.2 PROCESS FLOW

In the next section a complete illustrated overview of the process flow is shown followed by a section highlighting the more critical and noteworthy steps. All processes have been performed

4 - Design Batch 2

in the cleanroom of the MESA+ Institute and a detailed overview of all process steps including the used equipment and parameters can be found Appendix F and Appendix G.

4.2.1 COMPLETE OVERVIEW



0) For production a <100> single sided polished 4 inch wafer is used with a thickness of 350 μm or 525 μm .



1) A 180 nm BARC-resist (bottom anti reflective coating) is applied.



2) A 160nm thick layer of positive photoresist is applied and exposed by means of double displacement Talbot lithography (DTL) [43] at two times half the exposure time while changing the angle of the wafer in plane by 90°.



3) After exposure, the photoresist is developed and N₂ reactive ion etching (RIE) is applied to etch the BARC after which most of the photoresist is gone and the top of the BARC becomes cone-shaped.



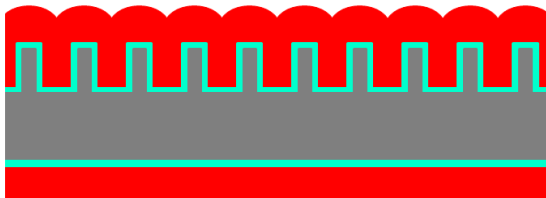
4) The wafer is etched by deep reactive ion etching (DRIE) with a mixture of SF₆ (sulphur hexafluoride) etchant and C₄F₈ (octafluorocyclobutane) passivation agent to create the pillars with the desired dimensions. By now all the leftover photoresist will be gone.



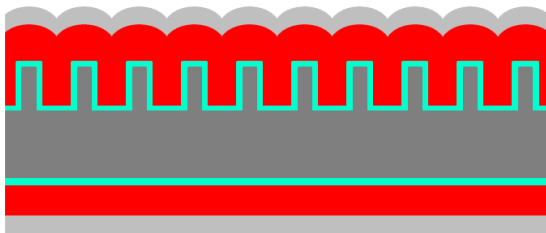
5) The BARC is stripped by means of oxygen plasma cleaning.



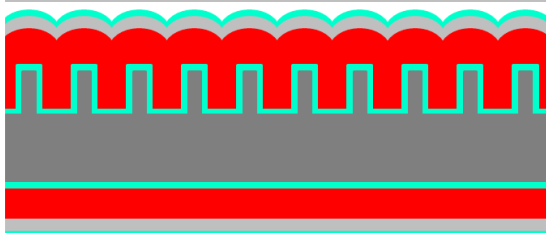
6) The silicon is thermally wet oxidised with a 10nm thick SiO₂ layer, sacrificing roughly 5 nm of Si. This is done to create SiO₂ coated pores in the final membrane.



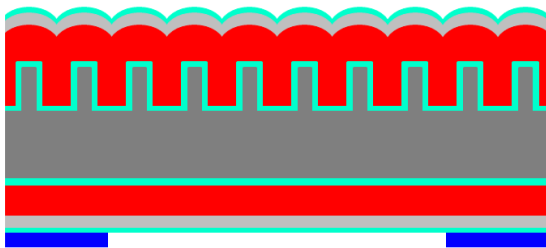
7) A layer of SiN is conformally deposited by means of LPCVD. For batch 1 the layer had a thickness of 250 nm, for batch 2 the layer had a thickness of 500 nm.



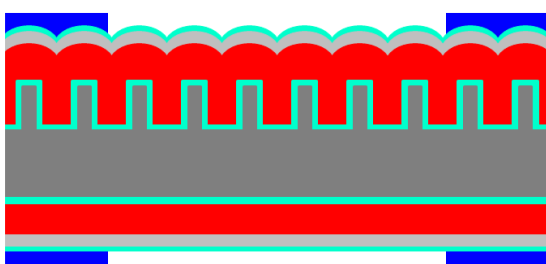
8) 50 nm of poly-Si is deposited for creating a hard mask.



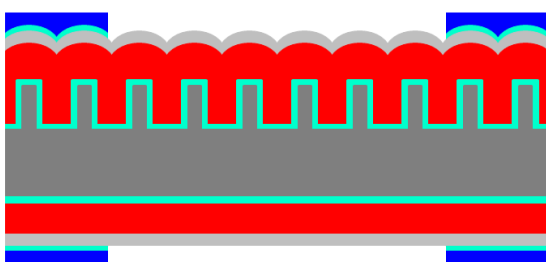
9) 10 nm of SiO₂ is thermally wet oxidised for creating a hard mask.



10) A layer of 3.5 μm positive photoresist is deposited on the bottom side, exposed and developed.

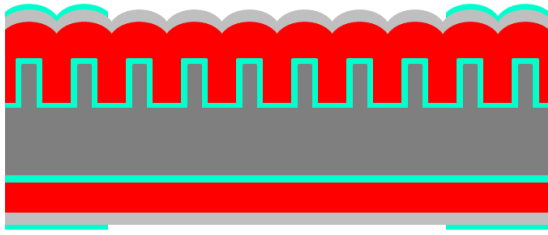


11) A layer of 1.7 μm positive photoresist is deposited on the top side, exposed and developed. Note that on this sketch the mask on top and bottom side, seem to have the same dimension, however in reality the bottom mask is wider to eventually create a square 100 μm window in the membrane. The top mask will create a square window of 150 μm to take care of possible misalignment.

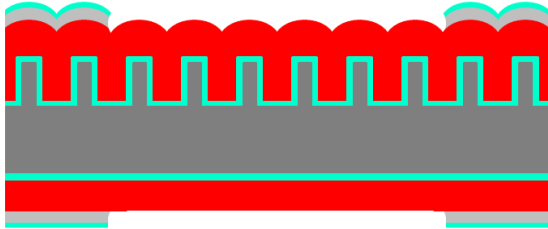


12) The SiO₂ is wet etched in BHF (buffered hydrofluoric acid).

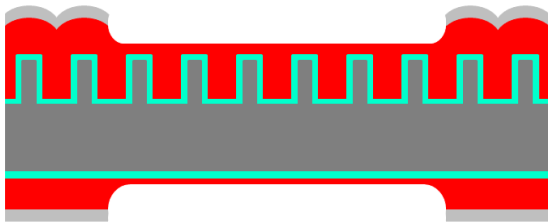
4 - Design Batch 2



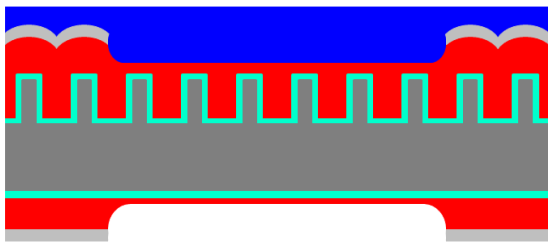
13) The photoresist is stripped in 99 % HNO₃ (nitric acid).



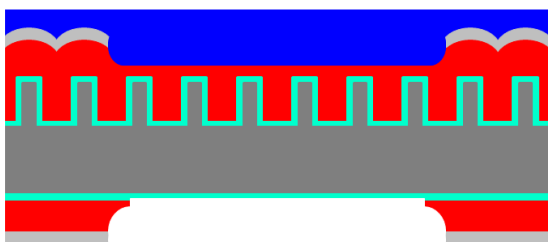
14) The poly-Si is wet etched in TMAH.



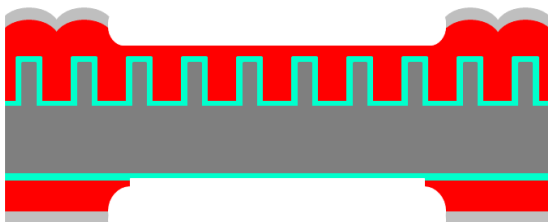
15) The SiN is wet etched in H₃PO₄ (phosphoric acid) until a layer of about 50nm is left.



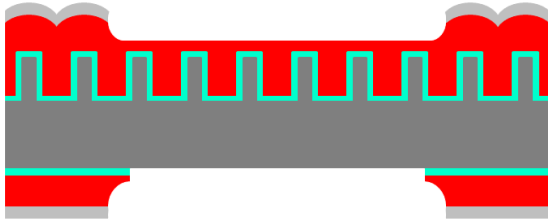
16) A layer of 1.7μm positive photoresist is deposited on the top side and cured as a protective layer.



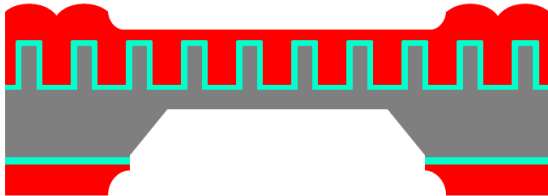
17) The SiN on the bottom side is etched by using RIE with a mixture of CHF₃ (fluoroform) and O₂ (oxygen) until the SiO₂ layer is reached.



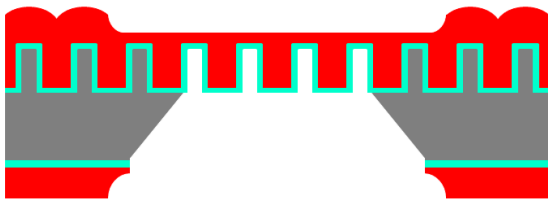
18) The photoresist is stripped by using O₂ plasma.



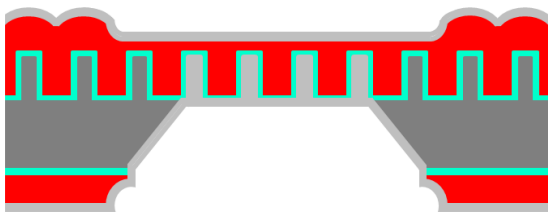
19) The SiO_2 is wet etched in BHF.



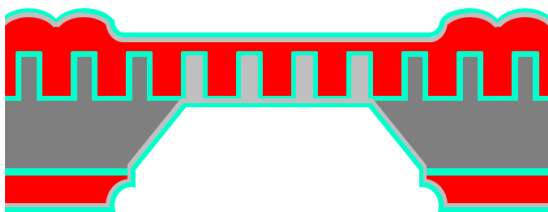
20) The Si is wet etched in KOH (potassium hydroxide) until a layer of about $80\text{ }\mu\text{m}$ is left.



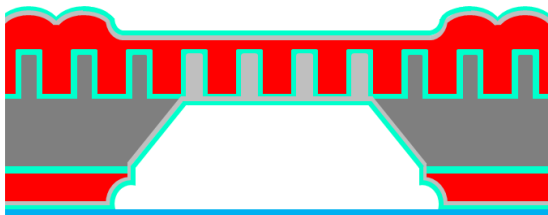
21) The remaining Si, including the pillars, is etched in TMAH because of its high selectivity for silicon versus SiO_2 , leaving the SiO_2 largely untouched.



22) 100 nm of poly-Si is deposited for creating a hard mask.

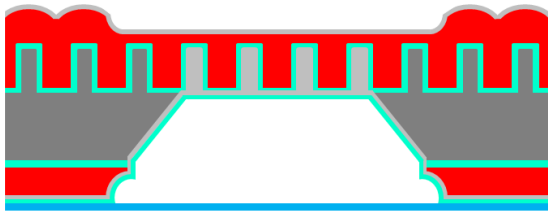


23) 5 nm of SiO_2 is thermally wet oxidised for creating a hard mask.

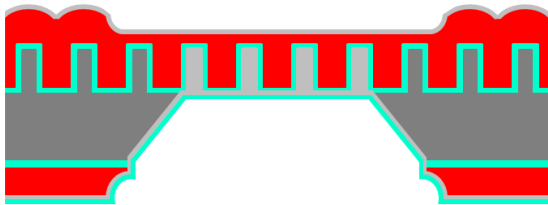


24) Dicing foil is placed on the bottom side for protection.

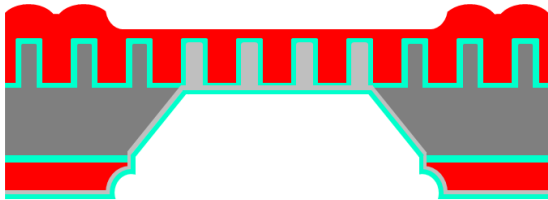
4 - Design Batch 2



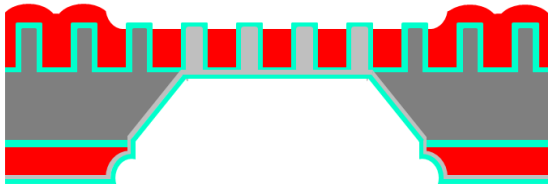
25) The SiO₂ on the top side is wet etched in BHF.



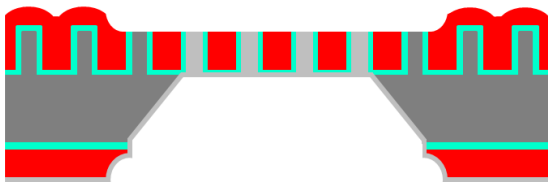
26) The dicing foil is removed.



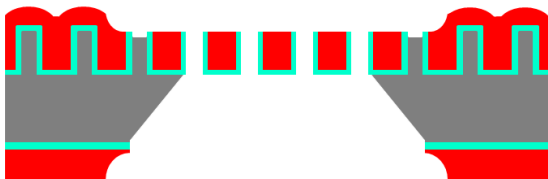
27) The poly-Si is wet etched in TMAH.



28) the remaining SiN is etched to free up the top of the pillars.



29) The SiO₂ on the top of the pillars and on the bottom side is wet etched in BHF.



30) The poly-Si is wet etched in TMAH with enough overetching to be sure that the pores are fully open, also when there would still be some Si left.

In the end the wafers are soaked in a piranha solution to clean and activate all possible silanol sites on the silica walls of the pores [42].

4.2.2 CRITICAL AND NOTABLE STEPS

Pillar Creation (Step 1-5)

At the core of the fabrication of the EOF pump membranes, lies the creation of the sacrificial pillar mould. This novel technique allows for both a very high density of pillars and full control on the profile of the pillars.

The high density is achieved by using double DTL [43] on a layer of resist that is on top of a layer of BARC-resist. DTL makes use of a grooved transparent mask that is illuminated with monochromatic collimated light. This creates Talbot sub-images at half the pitch of groove pitch of the original mask which allows for doubling the amount of exposed lines per area [43]. Here a grooved mask with a pitch of 500 nm is used, creating a striped pattern in the photoresist with a pitch of 250 nm while the wafer is moved up and down, ensuring the full dept of the photoresist gets the needed exposure energy.

For creating the nanodots, the exposure is done half time, meaning only half the needed energy for the lithography is transferred, after which the wafer is turned in plane by 90 ° and it is exposed again with the same settings, creating an 100 nm nanodot pattern with a 250 nm pitch that is fully exposed, as is illustrated in Figure 26.

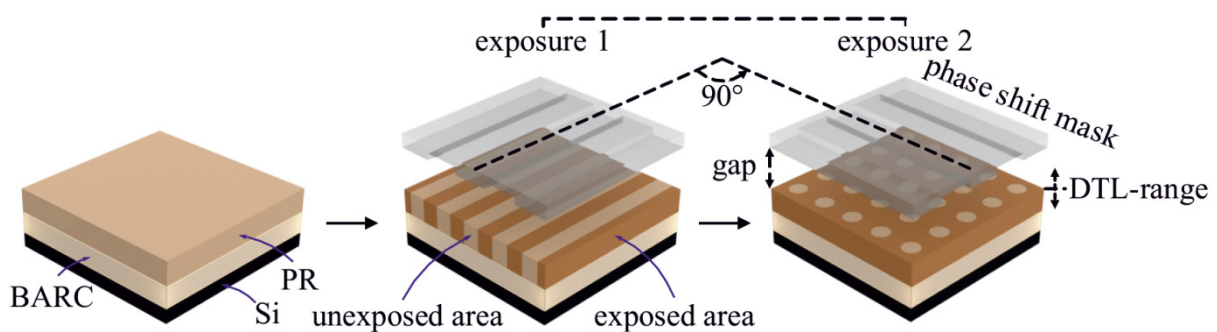


Figure 26: Illustration of double DTL for creating nanodots differing to the used process that here the mask is turned 90 ° and not the wafer [6]. PR stands for photoresist.

After development and etching of the photoresist and BARC-resist, the BARC-resists stays on the Si as a protective mask. Then Si is etched by means of DRIE with a mixture of SF_6 etchant and C_4F_8 passivation agent. By controlling the ratio of supply of these two gasses the pillars can be etched with a desired profile containing, cylindrical, positively tapered and negatively tapered sections. For the design of the second batch of chips, a slightly positively tapered cone will be etched with an angle of 1.7 °.

Conformal SiN deposition (Step 7)

For the strength of the resulting membrane, it is crucial that the layer thickness of the SiN is thick enough to provide a rigid structure. As described in chapter 4.1, it is important that all the gaps between the pillars are filled up with SiN. The minimum layer thickness for this is given by F. 26, which is 263 nm for batch 2. For batch 1 there is a thinned region halfway the sacrificial pillars. The wider top part of the sacrificial pillar during deposition, will close the gap before the distance between the pillars is covered at the height of the thinning, so the width of the cylindrical top section determines the minimum needed SiN layer. This top has a width of 92 nm (as can be seen in section 3.1.1), which will be 102 nm after the oxidation, leading to a minimal layer thickness of 251 nm.

4 - Design Batch 2

Masking for One-Sided Si Etching (Step 15-19)

Due to the thickness of the wafer, several hours of etching will be needed to create a window in the Si. For etching most of the wafer, 25 % KOH etching at 75 °C (standard processing bath in the cleanroom) is preferred due to its relative high etching speed, but it will still take several hours with an etchrate for 1 $\mu\text{m}/\text{min}$ for $\langle 100 \rangle$ Si and an etchrate of 180 nm/h for SiO_2 . This means that for 2-sided etching the SiO_2 covering the pores would be long gone before the needed Si is etched away. Using 25 % TMAH at 70 °C (standard processing bath in the cleanroom) instead, seems feasible at first since its selectivity for Si versus SiO_2 is preferable, but with an etchrate of 300 nm/min for $\langle 100 \rangle$ Si, the two-side etching of a 525 μm thick wafer would take 14 h 35 min while the SiO_2 etches at a speed of 0.7 nm/h [44], meaning 10.1 nm of SiO_2 could be etched, fully removing the 10 nm SiO_2 layer.

Because of this a 50 nm layer of SiN was left on both sides to protect the in SiN embedded pillars. By protecting top side of the wafer with a photoresist mask, the SiN at the bottom side can be etched by using RIE, reaching the embedded layer of SiO_2 that was formed during the oxidation of the sacrificial pillars. This layer is then removed using BHF after which the Si at the bottom side is accessible for etching, while the SiN still protects to top side.

Si Etching (Step 20-21)

As described in the previous section, there is a big difference in Si and SiO_2 selectivity for 25 % TMAH at 70 °C and 25 % KOH at 75 °C while KOH also etches the Si much faster, so for a shorter processing time, it is desired to etch most of the Si with KOH. However since the KOH would severely damage the SiO_2 layer, a 80 μm is left after the KOH etching for protecting the embedded pillars. The last 80 μm is then etched away by using TMAH with a little overetching to be sure sacrificial pillars are fully etched away, leaving the SiO_2 layer virtually intact.

Single Sided Hard Mask (Step 22-27)

The remaining SiN protection layer at the top side with the wafer will be etched using 85 % H_3PO_4 at 180 °C. This has an etchrate of about 4.5 nm/min for SiN, but also an etchrate of 0.47 nm/min for SiO_2 . This means that without extra steps, the now exposed SiO_2 layer that will form the coating of the final pores, would be damaged during the etching. To prevent this a layer of poly-Si is deposited and oxidised on both sides of the wafer.

Then dicing foil is used to create a protection layer on the bottom of the wafer after which the SiO_2 layer on the topside is etched away using BHF. After removal of the dicing foil, now having only a poly-Si layer on the topside of the wafer, while having a poly-Si layer with an SiO_2 layer on the bottom side, the poly-Si on the top side is etched away. Now the SiN can be etched by the H_3PO_4 while the filled up pores at the bottom side of the wafer stay intact.

Removing the Protective SiN Layer (Step 28)

This is one the most crucial steps of the process needing high precision. The etch time needs to be long enough to fully free up all the tops of the embedded pillars, else they can never become pores. For this some overetching is preferred to be sure all tops are free, also taking non-uniformity into account for the protective SiN layer that still covers them.

However, the thickness and thus the total strength of the membrane is determined by the thickness of SiN, so for this aspect, overetching is not preferred since it means weakening the membrane. Also if there are any inclusions as found and described in section 3.5.1, the overetching should be minimised as much as possible to prevent them from opening up or

etching much larger. Therefore this step needs a high precision for etching just the right amount of SiN.

4.3 MASKS

Whereas batch 1 was based on a mask which 3 cm by 3 cm areas on a full 4inch wafer could be prepared with sacrificial pillars, the technique was for the second batch optimised within the group, allowing for full wafer exposure. The new mask set, allows for 37 square 1 cm chips per wafer instead of 9.

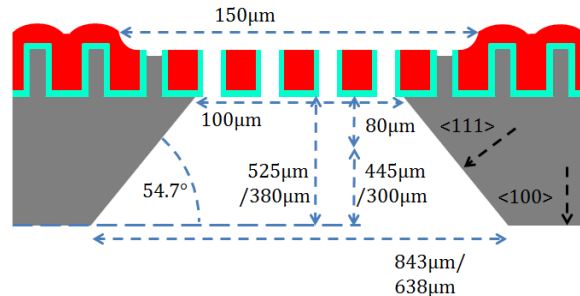


Figure 27: Sketch for calculations on the mask for etching.

Top Side Mask

The new design only consists of 100 µm square membranes since the rectangular membranes of the previous design, only resulted in broken membranes during production. Since the top 500 nm SiN layer does not add significantly to the strength of the whole structure, compared to the 525 µm or 380 µm wafer, it is decided to make the etched windows in the SiN 150 µm squares instead of 100 µm. This will make sure no effective pump area can be lost when accidental misalignment might take place. The windows are still preferred over a fully etched top surface, since the remaining SiN layer will make for a smooth and even finish, which is preferable for sealing and cleaning. The spacing of these windows depends on the alignment with the bottom mask.

Bottom Side Mask

It has been decided to make 2 masks for both 525 µm and 380 µm thick wafers. For the exact dimensions, the angle between the <100> and <111> of 54.7 °, the etch dept and the different etch speeds for the different planes need to be taken into account.

In total 80 µm will be etched by means of 25 % TMAH at 70 °C. This has an etch speed of 300 nm/min in the <100> direction and an etch speed of 25 nm/min in the <111> direction. This gives a ratio of 12 and thus the <111> direction will be etched for 6.67 µm. Multiplying this by $\sin(54.7^\circ)$ gives 5.44 µm of sideways etching and thus a window widening of a total of 10.9 µm.

In total 300 µm or 445 µm will be etched by means of 25 % KOH at 75 °C. This has an etch speed of 1 µm/min in the <100> direction and an etch speed of 12.5 nm/min in the <111> direction. This gives a ratio of 80 and thus the <111> direction will be etched for 3.75 µm or 5.56 µm respectively. This results in 3.06 µm and 4.54 µm of sideways etching respectively and thus a window widening of 6.12 µm and 9.08 µm respectively, so for compensation for sideways etching, the mask opening needs to be reduced by 17 µm or 20 µm respectively.

It is been decided that for strength, including the option of bonding the wafer to a carrier wafer for extra strength in future designs, but also for making sure that the photoresist can easily meet the resolution, that the bottom surface of the beams needs to be at least 150 µm wide which means the mask needs to be at least 170 µm wide. For the 525µm wafers that means the diagonal slope on the <111> plane has a width of 372 µm, meaning the beams will be 893 µm wide and that the windows will have a spacing of 993 µm.

For the 380 µm diagonal slope on the <111> plane has width of 269 µm. Taking the same spacing of 993 µm, this results in a mask width of $993 \mu\text{m} - 100 \mu\text{m} - 2 \cdot 269 \mu\text{m} + 17 \mu\text{m} = 372 \mu\text{m}$.

4 - Design Batch 2

With these dimensions, a pattern was made to fit within the 9mm diameter circle that is needed to be flat at both sides for good sealing by the O-ring in the chipholder. Coincidentally this gave the same pattern of the pattern of the chips on the wafer, resulting in a total of 37 membranes.

Dicing Trenches

Since most of the membranes from batch 1 did not survive the production process, it was decided not to use the present dicing machine since its vibrations might pose a risk to breaking the membranes. Instead it was decided to add dicing trenches to the design along which the wafer might be carefully broken apart into individual chips. The trenches are made by using the KOH and TMAH etching by means of self limiting trenches.

For the trenches it is important that they do not penetrate too much of the wafer because of the handling strength of the wafer during the production. Also they should not be too wide since it will take away part of the surface needed for sealing by the O-ring. For a trench of 150µm deep in a 380 µm thick wafer, a total of $\cos(54.7^\circ) \cdot (6.67 \mu\text{m} + 3.75 \mu\text{m}) = 6 \mu\text{m}$ will be etched due to the etching in the <111> direction, so a remaining total of 144 µm still needs to be etched. The needed width in the mask for this is $2 \cdot 14 \mu\text{m} / \tan(54.7^\circ) = 204 \mu\text{m}$.

The trenches are extend beyond the chips towards the edge of the wafer to make prevent breaking lines starting at the wrong location and breaking through the chips. To add some little strength to the wafers for during the processing, the corners of the chips are connected without trenches passing through by sections/squares 250 µm in the mask. The resulting three masks can be found in Appendix C.

5 RESULT AND DISCUSSION

5.1 FABRICATION BATCH 2

During inspection after processing step 20 (after the Si has been mostly removed by KOH, leaving a 80 μm layer), it turned out that a large part of the SiN on the top of the wafers had been damaged before the KOH etching took place, causing penetration of the membrane during the KOH etching. An example of how it is supposed to look and how a damaged membrane area looks, can be seen in Figure 29. The etching has not stopped before reaching the membrane, since the etchant also passed through the membrane, starting to etch from the back, removing all Si and the SiO₂ coating. Not only are the holes visible, but at the right focus dept, the edge is visible where the two etching fronts (coming from the bottom and top/membrane side of the wafer) meet.

Unfortunately by now already over 75 % of the chips turned out to be unusable. It is not fully certain what caused this, but it is possible that due to non-uniformity of the SiN layer thickness over the wafer (due to etching and maybe in combination with the deposition), a part was already much thinner than the intended 50 nm, if not yet already gone in some areas. If the H₃PO₄ did not yet fully remove the SiN layer and reaching the SiO₂, the KOH etching time needed for the Si, was long enough to etch 4.3 nm of SiN and theoretically 1.3 μm of SiO₂, but the SiO₂ layer was no more than 10 nm thick. Meaning that theoretically the SiN could have been unpenetrated after the H₃PO₄ etching, but was locally already below 4.3 nm thick instead of the intended 50 nm and that the KOH also etched away the last thin layer of protecting SiN and the SiO₂ layer at the top of the embedded sacrificial pillars.

Once the sacrificial pillars are etched away, the Si below the pillars will be etched by the KOH forming gas and thus building up pressure under the SiN membrane layer. Once these etching pits connect and the membrane layer becomes disconnected from the Si, the build-up of pressure underneath the membrane could then blow out pieces of the membrane due to the high pressure build-up as has been illustrated in Figure 28.

The wafers were again inspected after processing step 28. The last H₃PO₄ etching, uncovering the tops of the oxide coated pillars in the SiN. SEM images of this can be seen in Figure 30. It shows there was a misalignment between the top and bottom mask. This can be seen by the two squares from the front side and back side etching, not being fully concentric and being under a different angle. This should cause no problem for the functionality however due to wider window etched in the SiN. Also the tops of the pillars are visible, but it also shows there are holes between the pillars again at the same location as was the case with the first batch of chips as can be read in section 3.5.1.

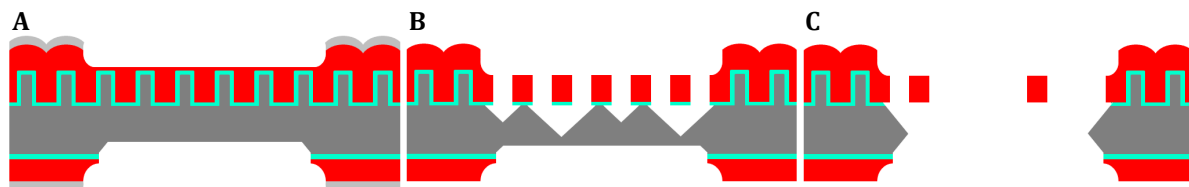


Figure 28: Illustration of the possibly cause for the penetration of the membranes after processing step 20, KOH etching of the Si. A: Ideal etching situation where only the Si is etched from the bottom side. B: Etching situation in which the top SiN layer has been penetrated and Si below the sacrificial pillars starts to etch and some etch pits already connect, generating a lot of gas while having an unsupported membrane. C: Blown out pieces of membrane after the unintentional double sided KOH etching.

5 - Result and Discussion

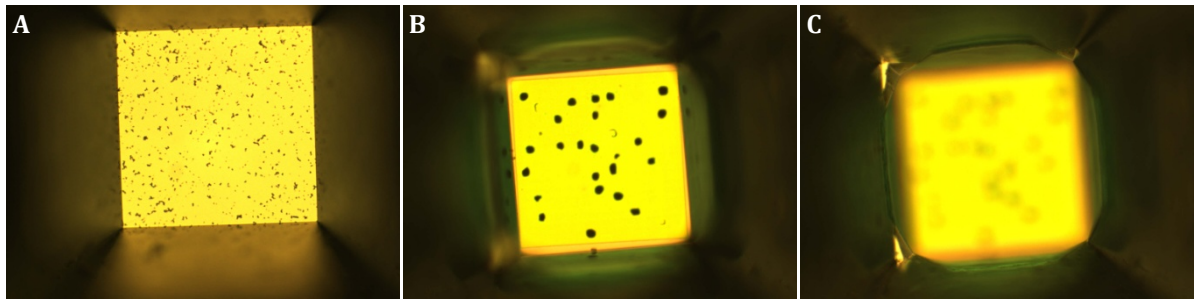


Figure 29: Images taken from the bottom side right after processing step 20, KOH etching of the Si. The visible square area, is about 100 μm wide and high. A: An undamaged pre-membrane as is illustrated in Figure 28 A. B: A membrane with holes in it (the black spots). C: The same image as B, but with the focus plane a bit higher, in the Si, showing the meeting edge of the two etching fronts. Both are illustrated in Figure 28 C.

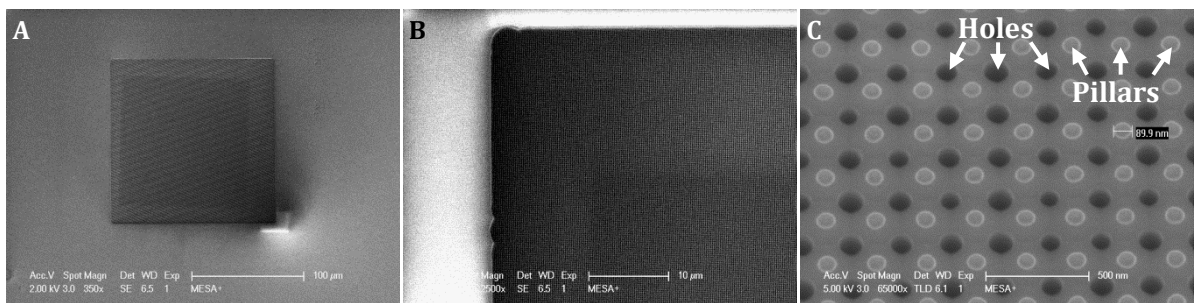


Figure 30: Pictures taken from the topside after step 28. A: a single membrane with the larger etching window from the top (larger square), and the Si etched away from the bottom (darker middle square), showing some misalignment. B: Corner of the membrane, showing the flat SiN (lightest area), the etched away SiN showing the pillar tops and the area which is also etched from the back (dark area on the bottom right). C: SiN with pillar tops and holes viewed under a slight tilt.

After the removal of the oxide in BHF, step 29, another wafer was inspected by removing a chip and breaking it across the membrane to perform a crosscut inspection. SEM images of this can be seen in Figure 31. Figure 31 A, B and C shows the difference between the cristalyine Si and the poly-Si as can be seen by the colour difference, meaning that during the last TMAH step, the sacrificial pillars were indeed fully etched away and that the SiO_2 pores have been filled up again with poly-Si. This can also be seen in Figure 31 F, where it can be seen that the bottom poly-Si layer is the same material as the material of the sacrificial pillars since there is no contrast in colour or texture, or a visible transition interface between these two.

Because of the roughness and odd angles of the breakline, as can be seen in Figure 31, it is hard to exactly estimate the angles of the walls of the extra etched holes, but they seem to be largely perpendicular or slightly negatively tapered towards the top. In Figure 31 E the SiN can be seen, that is not etched. The blue lines indicate the locations of covered pillars while the red lines indicate the locations of the elongated holes in the SiN. When looking closer, the in-plane shape of these holes seems to have the shape of a hole enclosed by four cylinders. This is expected since the SiN "grows" on the cylindrical pillars.

To prevent the formation of inclusions during the processing, a positive tapering has been chosen for the sacrificial pillars. However, probably during the start of the etching, there is a small area of negative tapering taking place right below the BARC, due to the BARC protecting the top part of the pillar. This wider top part of the pillar seems also present in Figure 25 and Figure 31 C and F. During the deposition of SiN this wider top part closed itself before the holes underneath were filled and during etching they opened up again, as is described in section 3.5.1.

In Figure 31 C and D it is visible that there is a gap between the SiN and the (poly-)Si pillars. This is caused by the SiO₂ layer that is etched away by the BHF prior to etching the poly-Si for opening up the pores. At a breakline where the top part of the pillar has broken off, it is visible that SiO₂ has been etched away for roughly 57 nm between the SiN and Si.

After the full production a chip was broken for a cross sectional SEM inspection. Examples of the SEM images can be seen in Figure 32. It is clear that for this chip there were multiple breaches through the SiN and SiO₂ and possibly all the pores were etched free. Because the edges under the SiN show a flat etching front coming from the membrane and it starts at the edge of the broader 150 µm window etched into the SiN. However the meeting of the two etch fronts was not in the middle of the Si layer, but near the membrane, suggesting a thin layer of SiN was still left at the beginning of the KOH, delaying the etching several hours until it reached the SiO₂ coating of the pillars, which was etched away in about 3.5 min after which the KOH started to etch crystalline Si of the pillars and later of the wafer underneath the pillars.

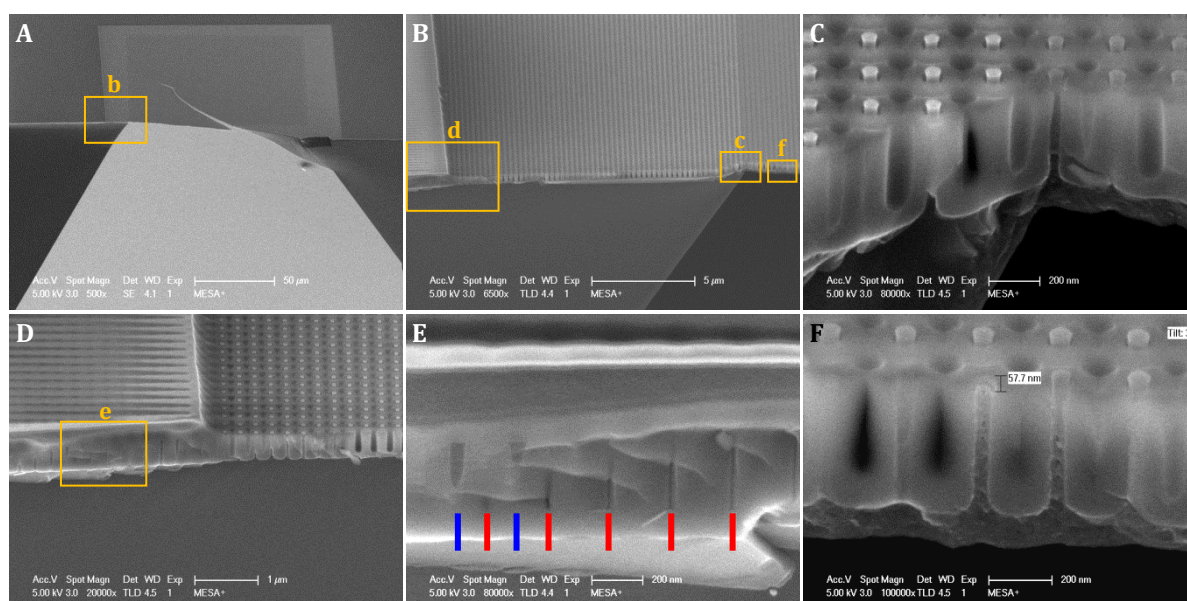


Figure 31: All images are taken under a tilt of 31 ° after processing step 29. The yellow rectangles show of which area close-up images are taken that can be found in the subfigure according to the labels above the rectangles. A: Close up of a membrane that snapped during breaking. B: Close up of the transition from SiN top-layer to the etched SiN with the Si below and to the free hanging SiN membrane. C: Close up of the edge of the actual membrane, showing the white Si pillars on the left and the darker grey poly-Si pillars on the right. D: Close up of the transition of the SiN top-layer to etched SiN with the Si below. E: Cross section of the un-etched part of the SiN layer. The blue lines indicate the locations of Si pillars. The red lines indicate the locations of holes in the SiN between the pillars. F: Close up of the free hanging membrane and measurement of how far the SiO₂ layer on the pillars has been etched away between the SiN and the poly-Si.

Figure 32 B, shows dimension measurements, including one for measuring the difference between the top of the SiN membrane, and the height at which the SiO₂ is still present, showing that the SiO₂ was etched back by roughly 40 nm. Also the thickness of the membrane at 442 nm and the width of the top of the pores of 91 nm. The SiN and SiO₂ layer forming the membrane at the bottom of the extra etched holes are together about 124 nm thick, meaning the SiN has an overall thickness or 114nm on the sides of the pillars. Also taking into account that the diagonal distance between the pores is 263nm (as described in section, it means that the extra etched holes should have a diameter of no more than 35nm .

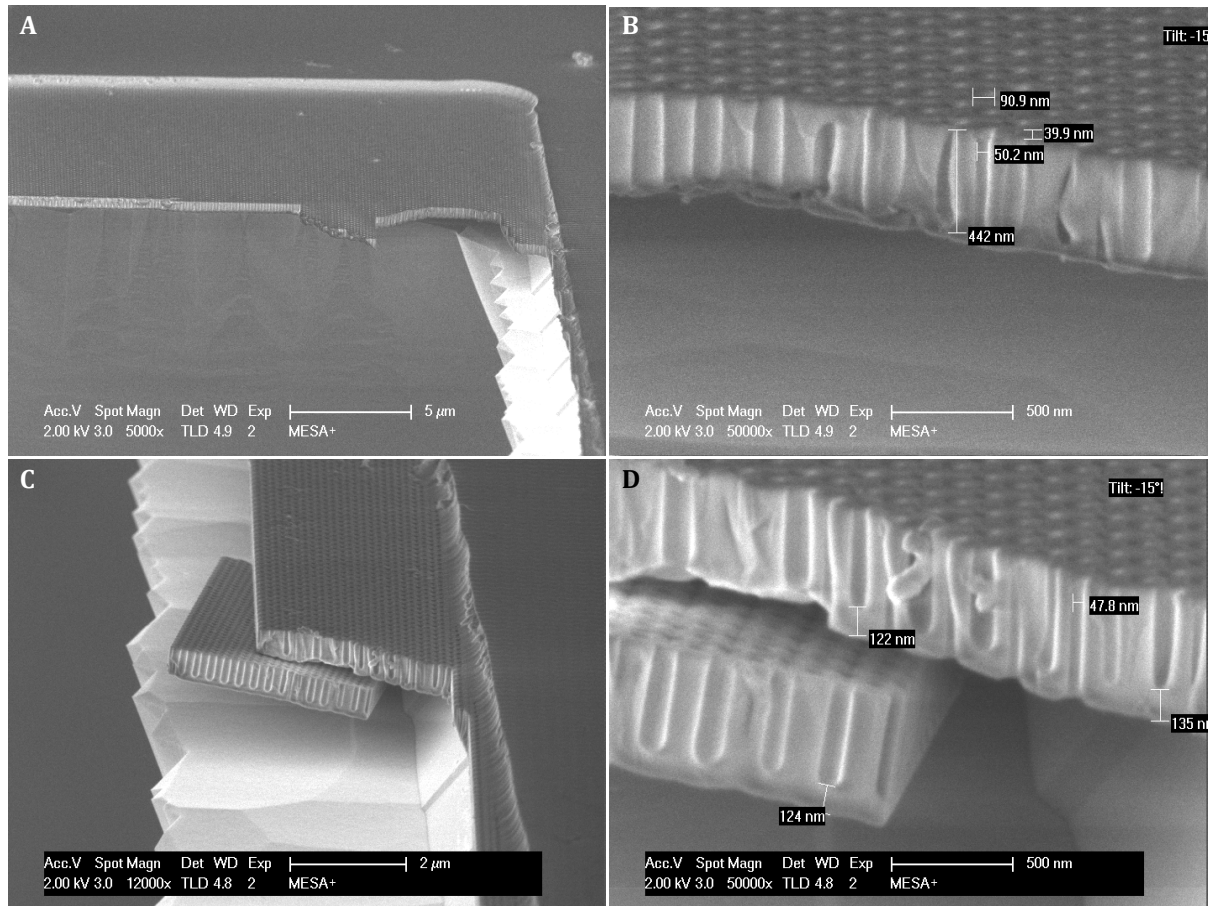


Figure 32: Images taken of a finished chip of which the SiN was damaged during the KOH etching. A: broken membrane with under etching. B: Close up of the side of the membrane as shown in A. C: Broken membrane with under etching. D: Close up of C.

5.2 MECHANICAL

5.2.1 HYDRAULIC RESISTANCE

For measuring the resistance, two types of measurements have been undertaken. One with a constant pressure of 1 bar and one with an gradually increasing pressure. For the latter however, the increasing flow did not follow a linear increase with the pressure at some point and later one did not noticeable increase anymore with increasing pressure. After inspection it turned out the chip had become clogged. Thus instead of the 4h test, a shorter 15 min test at 1 bar was performed.

At a constant pressure of 1.002 bar, a hydraulic resistance of $6.6 \cdot 10^{13} \text{ Pa} \cdot \text{s} / \text{m}^3$ was found, which is the exact same value as was expected according to

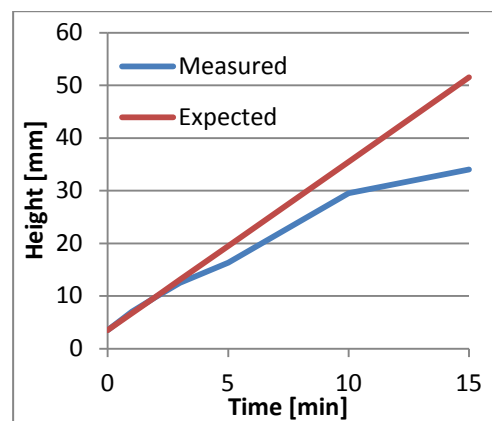


Figure 33: 1 bar pressure measurement showing the height increase the measurement column (so volume) over time.

the calculated value, using F. 8. This resistance gives an increase of 3.2 mm/min in the 6 mm diameter height column. The result of the pressure measurement can be seen in Figure 33. As can be seen, the height increases with an average of 3.2 mm/min in the first 2 minutes, but this already decreases to 3 mm/min in the 3rd minute and becomes lower after. The first minutes show that the geometry of the membrane is indeed as expected, however the decreasing curve also shows that the membrane clogs up relatively fast, even when using extra filtered H₂O.

5.2.2 MAXIMUM PRESSURE

Starting at 5 kPa, the pressure was gradually increased with steps of 5 kPa. For the given membrane with a thickness of 455 nm and a span of 100 μ m, the maximum calculated pressure, using F. 8, is 155 kPa. During the test the membrane broke at a 180 kPa, 16 % more than expected. this is already close, but the fracture strength of 6.9 GPa was an assumption.

As mentioned in 2.2.2, values of 6.4 GPa up to 12.1 GPa have been mentioned in literature, which is a range of 7.2 % lower and 75 % higher than the assumed value of 6.9 GPa, so the 180 kPa breaking pressure, giving a fracture strength of 8 GPa is well within the range of what could be expected. However the unintended non-penetrating holes in the SiN membrane should have weakened the structure, meaning that probably the actual fracture strength of the produced SiN, might be even more than can be directly calculated from these results.

5.3 EOF

5.3.1 VOLTAGE CONTROLLED

When using the voltage controlled setup with a concentration of 0.1 M KNO₃, as has been used for the first batch, it turned out that the current in the first minutes would increase rapidly, most likely due to initial settling effects. This resulted in currents of over 85 mA for several minutes before lowering again. Though this seemed promising for registering EOF, there were no clear results showing EOF in the order of what was expected and it was evident that during most of these measurements at least one of the membranes would rupture or be totally blown out.

As found in section 5.2.2, the maximum pressure that the membrane can withstand is 180 kPa. Based on this strength, an estimate of the maximum values involved caused by the EOF can be made. The calculations for the estimation of these values for a single chip can be found in Appendix C. When the breaking strength of the membrane is achieved by EOF, there is an expected maximum velocity of the plug flow of 7.8 mm/s, which for this chip relates to a maximum flow of 66 μ l/s at and effective potential over the membrane of 140 mV and a maximum current of 14.2 mA. Since the recorded currents go up to 6 times as high, it seems plausible that the EOF forces are breaking the membranes.

Examples of these measurements can be seen in Appendix I with the expected EOF and the measured EOF. When looking at the first minutes, it seems that the height increase is as expected, but most likely most of this increase is caused by bubbles. Only after the high current peak has past and the current is settling, there seems to be some EOF, but lower than expected and settling to a maximum height. The latter is most surely caused by the ripped away membrane(s). The lower measured EOF, will also be caused by the broken out membranes, but also possibly by the faradaic polarisation effect, described in the next section.

5.3.2 CURRENT CONTROLLED

One Hour Faradaic Concentration Polarisation

Since in general the currents of batch 1 and also the couple of voltage controlled measurements of batch 2 would eventually settle around 10 mA to 20 mA, it was decided to set the actuation current at 10 mA. However after several 1 h long measurements at this current, it seemed virtually no EOF took place. Only an initial increase in height was observed, but since the initial increase is always dominated by the bubbles settling on the walls, it cannot be determine how much or if at all any EOF took place.

However one long measurement was attempted (and can be found in Appendix I), 36 min at 10 mA and with no result, this was increased to 20 mA. With the bubbles constantly forming, the exact timing is hard to determine, but after roughly 1.5 h EOF started to take place. For another 5 measurements at 20 mA, the same happened, but it took roughly 1 h before the EOF started to take place, but all with an EOF that was about 1/4 of the expected value according to F. 7, using F. 15 to calculate the effective voltage from the current.

This suggests a form of faradaic ion concentration polarisation where a certain total charge delivered to the system is needed to reach the right concentration polarisation for the system to work. This is also supported by the couple of measurements made with the chips of which the membranes were eventually blown out. Here A big current peak was observed after which EOF started taking place. The earlier described measurement that started at 10 mA also supports this as explained below.

Assuming a certain charge or amount electrons is needed, roughly estimated 20 mA is for 1 h, is needed to "charge" the system, which is about 72 C (coulomb), depending on the exact volumes in the reservoirs and height columns. For the 10 mA measurement; the 10 mA at 36 min gives 21.6 C, so at 20 mA, another 42 minutes would be needed to reach 72 C, which would give a total of 78 min after which the EOF would take place, which is close to the 1.5 h that was registered.

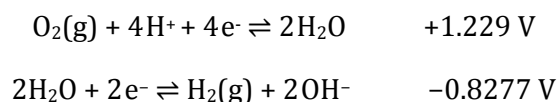
Several times after a test that eventually showed EOF taking place, the test was stopped by turning off the power supply, which for this supply meant it would disconnect and thus not cause current leakage via the output connector. After this the setup was left alone for several minutes up to 15 h overnight for several times. When the power supply would be reconnected again, EOF was immediately observed with the standard uncertainty during the first minutes due to the bubbles settling in the walls. The EOF measured after the first few minutes when the bubbles would have settled, had similar values as the EOF measured during the preceding test.

As also described in section 3.5.3, what possibly happened is that the channels acidified due to the H^+ production in the reservoir at the positive side, which also would be pumped into the channel due to EOF, stopping the EOF when the pH got below 3. However when the pH at the alkaline side got high enough, the gradient driven diffusion caused enough OH^- to go into the channel to create a section with a pH above 3. This would then start the EOF to take place in part of the channel at the side of the negative electrode. For EOF to keep taking place, there would be an equilibrium by the amount of OH^- going into the channel by diffusion and the amount of H^+ going into the channel by both diffusion and transport due to EOF.

Aqueous Battery

After inspection after later measurements, it turned out that the buffer solution at the reservoir with the positive electrode, would have a pH of a little over 1, while the buffer solution at the reservoir with the negative electrode would have a pH of around 13.5. After turning off the

power source, it was also noticed that the voltage would rapidly drop to a potential a little under 2.1 V and then gradually lower over the hours. This potential matches the reduction potentials of the half reactions of (dissolved) oxygen (gas) at high acidity and (dissolved) hydrogen (gas) at low acidity at potential of 2.0567 V [17], so this seems a plausible explanation for the found potential:



After about 15 h, this potential would still be around 0.9 V while still decreasing and the pH was still the same. Effectively an acid base battery on oxygen hydrogen basis might have been created. To demonstrate this, a red low power light emitting diode (LED) was connected to the electrodes. After "charging" the system with the power supply, the LED could light for about 2 to 3 seconds at 100 μA . After disconnecting and reconnecting, the LED would slightly light up again. The latter caused by the local depletion of redox species at the electrodes, where after time due to diffusion, there would again be enough redox species for partially powering the LED.

Buffered Solution

The charging effect clearly causes opposite extreme pH values in the reservoirs, meaning that when the EOF starts taking place after one hour, it is unclear what the pH of the solution in the pores of the membrane is and thus it is impossible to make a prediction for the expected EOF. To still test EOF, it has been decided to use a buffer solution with a pH of 7.908 and a conductivity of 2.44 S/m to stay as close to the original test as possible.

There is a lot of uncertainty about the exact zeta potential, especially at higher salt concentrations. Virtually no data about the zeta potential at concentrations higher than 0.1 M were available and not at all with the buffer used, so the zeta potential will be assumed the same as for a 0.1 M KNO_3 solution, though it might in reality be lower due to the higher concentration. Other relevant properties are also assumed to be similar to the KNO_3 solution with the clear exception of the conductivity that is measured. The six successful resulting measurements that could still be taken within the time that was left, can be seen in Appendix I.

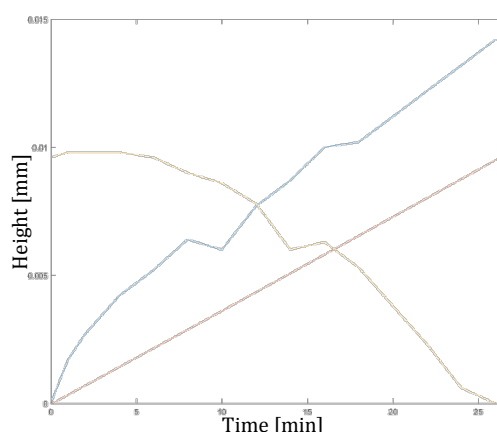


Figure 34: Representative example of the EOF measurements with the buffered solution. Time in [min] in the X-axis, height in [m] on the Y-axis. Blue: Measured increase. Yellow: Measured decrease. Red: Calculated increase.

One representative example is also visible in Figure 34. As can be seen, the measured and calculated values are in the same order. The data of these 6 measurements have been collected, normalised and fitted, and the results can be seen in Figure 35. The data have been fitted with a second order polynomial which is assumed to fit for the bubble-caused increase at the start of the measurement after which a linear regime is reached due to the EOF. In reality the ends of these curves would be a bit steeper for the increasing column and a bit more levelled for the decreasing column, but since the data did not extend beyond these points, the fitting does not take the expected values into account.

5 - Result and Discussion

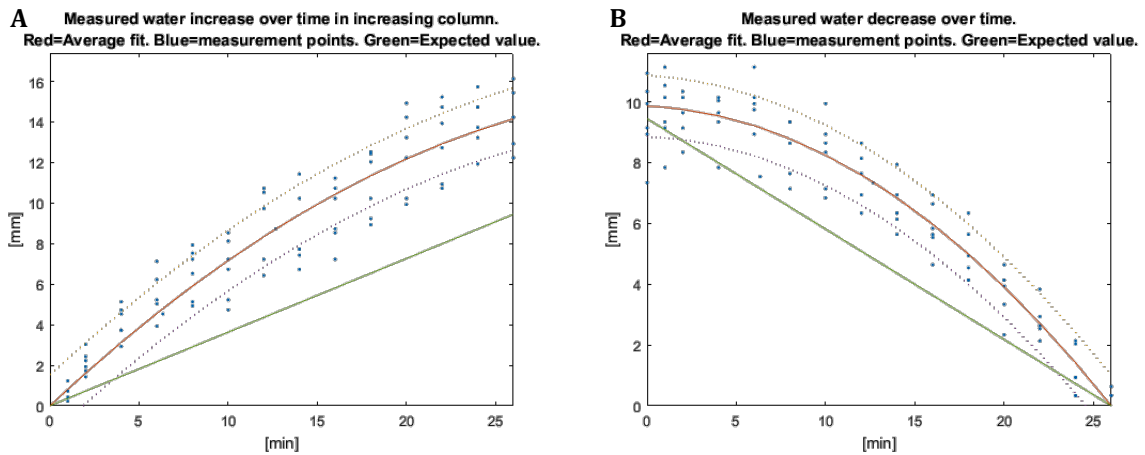


Figure 35: Normalised results of the buffered measurements. A: Increasing height column. B: decreasing height column. The expected value is based on F. 7, using F. 15 to calculate the effective membrane potential, while compensating for the average temperature as described in section 2.3.1.1.

As can be seen, the final value of EOF over 26 minutes is off from the predicted values by 50 % at the increasing column and only 4 % at the decreasing column. However a significant part of the initial increase will be caused by bubbles settling on the wall. This is also the case in the decreasing column, causing the more levelled slope at the beginning, but at a lower rate due to the lower interaction of the oxygen bubbles with the plexiglass than the hydrogen bubbles at the increasing water column. If the curves are compared starting after 10 minutes, it can be seen that the increasing curve only differs by 25 % and the decreasing curve differs by 27 % of the expected curves, as can also be seen in Figure 36.

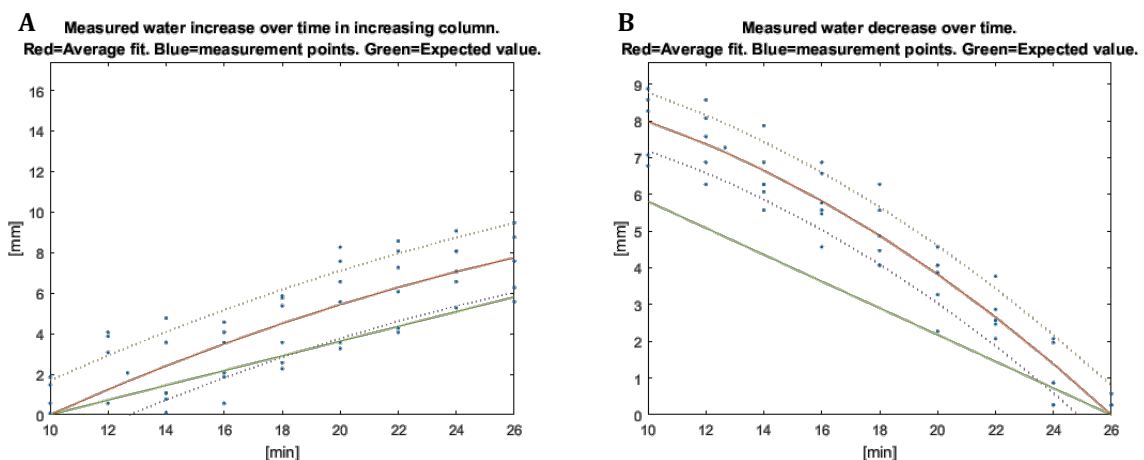


Figure 36: Normalised results of the buffered measurements after 10min. A: Increasing height column. B: decreasing height column. The expected value is based on F. 7, using F. 15 to calculate the effective membrane potential, while compensating for the average temperature as described in section 2.3.1.1.

There are too many uncertainties to fully accurately explain the deviation. Likely the zeta potential of the 0.2 M buffer solution could be lower than that of the expected 0.1 M KNO_3 solution. However the zeta potential for the latter, was also already estimated taking several sources into account while they did not all agree, so it is unsure to say whether it should be higher or lower than the used 36 mV.

What is certain, is that the bubbles do cause a volume increase at both sides right from the start as they become part of the total volume. This increases the height at the start, but there will also be more bubbles, settling on the wall that is gained by the water front in the column, making the volume seem to rise faster than purely due to EOF. At the other side, the volume will seem to go

down faster than purely the volume pumped by the EOF due to bubbles on the walls disappearing after the water front went passes them.

Since at this time the exact volume of the bubbles cannot be accounted for (though the influence was optically shown to be well below 50 % of the volume in the columns), it will be taken as part of the EOF to make an estimate. Also since the increasing and decreasing height columns, do not have the same difference per minute, the average of these two will be taken, which resulted in a flow of 13.05 $\mu\text{l}/\text{min}$ or 0.218 $\mu\text{l}/\text{s}$ or $2.18 \cdot 10^{-10} \text{ m}^3/\text{s}$ where 10.27 $\mu\text{l}/\text{min}$ or $1.72 \cdot 10^{-10} \text{ m}^3/\text{s}$ would be expected according to F. 7, using F. 15 to calculate the effective membrane potential of 117 mV, while compensating for the average temperature as described in section 2.3.1.1. This means that for an equivalent effective chip area of 1 cm^2 , this would result in a flow of 3.5 ml/min or 58.9 $\mu\text{l}/\text{s}$ or $5.89 \cdot 10^{-8} \text{ m}^3/\text{s}$.

At the end of the measurements the pH was also measured, showing that the pH in the reservoir of the positive electrode, dropped to a little over 7 while the pH at the negative side, increased to about 12.5. Looking at the buffer characteristics, this was expected and not directly problematic for the EOF. The more neutral solution at the positive side was pumped into the membrane by the membrane itself meaning that the pores should have been filled with the neutral solution, or are largely neutral with a smaller part filled with an alkaline solution. In both cases EOF should be able to take place.

5.3.3 FLOW AND PRESSURE CHARACTERISTICS

Since there was no time to do proper flow versus pressure testing, the output power has not been directly measured. However for the buffered solution the flow has been measured. The whole membrane can be modelled by a Norton equivalent circuit with a flow source and a parallel impedance which on its term can be modelled as a Thévenin equivalent circuit, which gives the expected pressure for an ideal pump. The measured flow was $2.18 \cdot 10^{-10} \text{ m}^3/\text{s}$ and the hydraulic resistance was as expected $6.6 \cdot 10^{13} \text{ Pa} \cdot \text{s}/\text{m}^3$ giving an estimated pressure of 14.4 kPa. Assuming all does indeed scale linearly with the potential over the membrane, this gives a flow of 29,9 ml/min or 503 $\mu\text{l}/\text{s}$ or 30.2 ml/(min V cm^2) and would result in a pressure of 123 kPa/V.

The flow and pressure are about 35 % of the calculated values found in section 2.3.4.3. Part of it might be explained by the uncertainties that are also described in the previous section. However in the original calculations, room temperature is assumed whereas with quite some of the measurements the temperature increased close to 30 °C, as can be seen in the individual measurements of the buffered solution EOF measurements, this on its turn will change a lot of the properties of the system, as described in section 2.3.1. To properly account for this, the individual measurements should also be normalised for temperature, or more measurements should be taken to see if one average temperature can be taken as the equivalent for calculating the values.

5.3.4 POWER AND EFFICIENCY

The total theoretical hydraulic power of the pump is 3.14 μW . The measurements were taken at 20mA and the average calculated voltage over the membrane was 117 mV. This means the electrical input power was 2.34 mW leading to an efficiency of 0.134 % or 1.34 ‰. For the 0.1 M KNO_3 solution at 117 mV the expected efficiency can be calculated by using F. 27 which is based on F. 23 from in section 2.3.6, but compensated for the measured and calculated output power. The found 0.134 % for the buffered solution is only 12 % of what would expected of the KNO_3 ,

5 - Result and Discussion

but this is in accordance with the measured flow and calculated pressure, that are both at 35 % of what was expected. Multiplied for the output power, this also results in only 12 % of the expected output power.

Most reasons for these lower numbers have already been given in the previous sections, however in the dissipated power, it is relevant to mention that the buffered solution had a 68 % higher conductivity of 2.44 S/m versus the 1.45 S/m of the KNO₃, which on its own would already make up decreasing the efficiency to 0.67 % instead of the expected 1.1 % for KNO₃.

$$\begin{aligned} efficiency &= \frac{1.2 U_{eff}^2 \cdot 10^{-3}}{0.10 U_{eff}^2 + 2.0 U_{eff} \cdot 10^{-4} + 1.2 U_{eff}^2 \cdot 10^{-3}} \\ &= \frac{1.6 \cdot 10^{-5}}{1.4 \cdot 10^{-3} + 2.3 \cdot 10^{-5}} = 0.011 = 1.1\% \end{aligned} \quad \text{F. 27}$$

6 SUMMARY, CONCLUSION AND RECOMMENDATIONS

Based on an existing design, two functional EOF pump chips have been created by sacrificial moulding. With these chips a proof of concept was demonstrated, after which a redesign has been made and another batch of chips has been created. These chips were used for more extensive testing which yielded indicative results for EOF pumping performance during which some unexpected but interesting phenomena have been found.

6.1 FABRICATION

Based on a partially existing design and production process, a novel production process has been developed and carried out for producing nanopore SiO₂ covered SiN membranes by means of sacrificial moulding. For the mould a novel technique is used to create the sacrificial nanopillars in Si. The pores have a length of 455 µm, but are with the current state of art extendable to 1 µm depending on their geometry. The profile of the pillars is tuneable in diameter with up to now a minimum diameter of 10 nm as long as wet etching is used, but for future processing, possible lower dimensions could be achieved by using other types of etching [8].

The process flow seems to produce usable chips, however a large area of the wafers was damaged during the KOH etching, possibly due to earlier damage during the H₃PO₄ etching. Also with the chips of batch 2, there were still a lot of fully broken away or partially ripped 100 µm square windows before dicing. The manual dicing also caused more windows to break, but that might have been due to not dicing careful enough. In the end about 5 % to 10 % of the chips made it through the full production process including the dicing.

For future productions, a thicker SiN layer could be left during H₃PO₄ of processing step 14 to create a thicker protection layer. This would result in longer RIE-etching after at processing step 17. Also it might be interesting to briefly inspect all the membranes under a microscope for cracks and broken out membranes after every processing step past the KOH etching of processing step 20, to see at which step most windows are damaged and what might be changed to yield a higher success rate.

The end result did still contain undesired non-penetrating holes in the SiN membrane. This should have a weakening effect on the whole structure, leading to a lower maximum strength. For this optimisation could be desired, meaning that the top of the sacrificial Si pillars will need to have a different profile.

6.2 MECHANICAL

From the pressure tests it is shown that the hydraulic resistance of the chips from batch 2 was exactly as expected at $6.6 \cdot 10^{13} \text{ Pa} \cdot \text{s} / \text{m}^3$, indicating that the exact geometry of the membrane is also exactly or at least very close to the expected geometry. This is also backed up by the images taken with the SEM.

Maximum Pressure

The maximum pressure that the membranes of batch 2 could withstand was found to be 180 kPa, which is only 16 % more than expected, but possibly this could have been more if the membrane would not contain the extra holes.

6.3 EOF

6.3.1 CHIPHOLDER

During the first EOF test with batch 1, it has been shown that the EOF takes place in the chips. These tests were also used to develop a chipholder for the actual testing. The chipholder was custom made out of plexiglass with plexiglass height columns for measuring the solution displacement caused by the EOF. The tail ends of the chipholder have been fitted with removable plexiglass plates for easy electrode exchanging. The chipholder has been fitted with two 2 0.5mm spiral platinum wires optimised for the minimal bubble agglomeration on the electrodes.

However partially due to the roughness of the fabrication and partially due to the chosen material, there are still a lot of bubbles accumulating on the walls, generating a high measurement error in the data. This could be improved by remaking the chipholder of another material or coating the current chipholder with another material to make it more hydrophilic, making the bubbles interact less thus not stick to the walls.

This was not yet attempted due to the lack of time and the uncertainty of a material that is suitable. Next to being suitable for coating the plexiglass and being hydrophilic, it should not in any amount dissolve in the solutions since the low salt concentrations are easily disturbed by low concentrations of other materials. Also as shown for the metal tube fittings, the material should be able to withstand relatively large electrical potentials without dissolving.

6.3.2 VOLTAGE CONTROLLED MEASUREMENTS

During the voltage controlled measurements high current peaks were reached that broke the membranes. This is most likely not caused by heating since the whole system has been produced at temperatures much higher than are possible within water. What might have happened is that the flow was too strong and due to the viscosity of the water, locally the forces got large enough to rip the membrane. Meaning that the flows locally created a pressure of more than 180 kPa.

This is supported by the already mentioned results and calculations of section 5.3.1. This pressure might theoretically already be reached at an effective potential over the membrane of just 140 mV, which occurs at 14.2 mA, causing a flow of 66 $\mu\text{l/s}$. However more tests would need to be performed to confirm if this indeed holds.

6.3.3 CURRENT CONTROLLED MEASUREMENTS

Because of the breaking membranes, a current controlled setup was used. This showed there is an initial faradaic concentration polarisation effect that at 20 mA in a 0.1 M KNO_3 solution takes about 1 hour. This had not been noticed before, possibly because the high current peaks in the first several minutes, made the effect only last several minutes and during the first minutes it is impossible to determine presence of EOF due to the bubbles still settling on the walls. After the faradaic concentration polarisation of roughly 1h, EOF would take place. However, based on the few successful measurements made, the EOF was only 25 % of what was expected purely from the calculated EOF, while not compensating for the presence of the gas bubbles.

It turned out that the reservoir at the positive electrode, where the O_2 is produced, became highly acidic with a pH of 1 due to the removal of O^{2-} in the form of O_2 . The other reservoir where the H_2 is produced, became highly basic due to the removal of H^+ in the form of H_2 . This on itself creates a type of battery with H_2 in a highly basic solution on one side and with O_2 in a highly

acidic solution at the other side. The O_2 and H_2 will escape relatively fast from the water, but test showed, that the pH difference stayed present for at least 15 h.

This on itself might be interesting to perform more research on to possibly create a new type of rechargeable battery based on these membranes. The main challenge would be keeping as much of the gas dissolved or else in direct contact with the water as possible, also without it escaping. This could possibly partially be solved by creating a structure with microtraps in which microscaled bubbles will be trapped, while staying in direct contact with the solution.

A possible explanation for the 1 h delay after which EOF still takes place, is that EOF does take place in the very beginning. At the positive electrode acid is created and the EOF flows the acidic solution into the channels. When the pH gets too low (around 3) the EOF stops, but the decrease of pH on one side and the increase of pH on the other side continues. After about 1 hour, the concentration of the OH^- is so high, that it recombines into water again somewhere inside the pores. This makes part of the pore work as an EOF pump again while the high concentration still causes a faster diffusion back into the membrane than the pumping flows it out again.

6.3.4 BUFFERED SOLUTION AND POWER AND EFFICIENCY

To overcome the problems with the pH, a K_2HPO_4 - KH_2PO_4 solution with concentration of 0.2 M and a pH of 7.907 was used. This showed instant results in the form of instant EOF, shown by both the increasing height column at one side and the decreasing height column at the other side. This resulted in a pumping action of 13.1 $\mu\text{l}/\text{min}$ or 0.218 $\mu\text{l}/\text{s}$ for the chip at 20 mA and 117 mV or 3.5 ml/min or 58.9 $\mu\text{l}/\text{s}$ for a 1 cm^2 chip at the same voltage. The deduced pressure from this flow was 14.4 kPa.

This means that at 1 V an effective membrane of 1 cm^2 would generate a flow of 29,9 ml/min or 503 $\mu\text{l}/\text{s}$ at a maximum backpressure of 132 kPa. This was 65 % lower than expected for a 0.1 M KNO_3 solution, but close enough to state that the test was successful and seems largely in accordance with the theory. Also with the current mechanical strength this means the maximum allowed backpressure is 180 kPa which can be reached at 1.36 V when there is no effective output flow of the system present. This actuation potential also corresponds to a maximum flow 40.7 ml/min or 686 $\mu\text{l}/\text{s}$ for an effective membrane of 1 cm^2 .

When normalising the results, the membrane produces a flow of 30 ml/(min V cm^2) and a pressure of 123 kPa/V. This is better than any of the other performances found in literature that are mentioned in chapter 1.2. However it should be noted that the current maximum mechanical pressure is only 180 kPa, meaning it is in its current form not suitable for really high pressure applications such as the 40 MPa pump mentioned in chapter 1.2.

The whole system had an efficiency of 0.13 % which was only 12 % of the expectation, which corresponds to 65 % lower pressure and flow would explain. Also the conductivity of the buffered solution was 67 % higher than that of the 0.1M KNO_3 and the increasing temperatures changed many of the values involved, such as the zeta potential and conductivity. To determine the exact deviation in results compared to the theory and the cause(s), more tests will be needed in order to be able to normalise and average to remove the large measurement error caused by the bubbles.

It must be noted however that as mentioned in section 5.3.1 and 6.3.2, that the membrane might already break due to the forces of the EOF flow itself. This would occur when an effective potential of 140 mV is reached, which for the buffered solution in a chip happens at a current of 24 mA. This results in a flow of 15.7 $\mu\text{l}/\text{min}$ or 0.261 $\mu\text{l}/\text{min}$. For an effective membrane area of 1 cm^2 this would be 4.2 ml/min or 70.5 $\mu\text{l}/\text{s}$. Based on just the resulting EOF flow, the deduced

6 - Summary, Conclusion and Recommendations

maximum backpressure would then be 17 kPa, but as mentioned before, more tests are needed to verify if this is actually the case, including pressure tests with EOF taking place.

All in all the results look promising to confirm that the created EOF pump seems to meet up closely to the theoretical expectations meaning, a low voltage high flow high pressure EOF pump has been realised. Setting the basis for further research and optimisation, including strengthening the membrane, so it will be able to take higher pressures than the found 180 kPa.

However only a small amount of tests have been performed and thus more test would be needed to fully confirm this. Ideally the expected values would then be recalculated with all the right constants and values for the buffered solution, or the pH difference problem would need to be solved differently.

This latter can theoretically be done by means of a Nafion membrane which is a known material for creating proton exchanging membranes while not allowing (high pressured) water. Also when the pump would be placed in a closed system, the solution from the basic reservoir would be pumped through the system and recombine again at the acidic side once it passed the whole system, removing a large part of the problem. However it is advisable to select an effective buffer to keep the pH in the desired range [4].

For using the chip as a real pump, the creation of gas would also need to be solved. Ideally the pump could be used in a closed system, but that means that the gasses need to be recombined without creating leaks for the fluids. One solution would be using a gas permeable polytetrafluorethene (PTFE) membrane to let the hydrogen gas pass back to the lower pressured side and meet with the oxygen gas to recombine. For promoting the recombination of the hydrogen and oxygen gas, a platinum catalyst could be used. Both solutions are already shown by Yao et al. [4].

7 LIST OF ABBREVIATIONS

BARC	Bottom anti reflective coating
BHF	Buffered hydrofluoric acid
C ₄ F ₄	Octafluorocyclobutane
CHF ₃	Fluoroform
DTL	Displacement Talbot lithography
EOF	Electro-osmotic flow
EDL	Electrical double layer
HF	Hydrofluoric acid
HNO ₃	Nitric acid
H ₃ PO ₄	Phosphoric acid
pH	Measure to specify acidity
KOH	Potassium hydroxide
KCl	Potassium chloride
KH ₂ PO ₄	Monopotassium phosphate
K ₂ HPO ₄	Dipotassium phosphate
KNO ₃	Potassium nitrate
O ₂	Oxygen
OH	Hydroxyl or hydrogen oxide
PTFE	Polytetrafluorethene
M	Molar concentration in mol/l
N ₂	Nitrogen (gas)
NaCl	Sodium chloride
RIE	Reactive-ion etching
SEM	Scanning electron microscope
SF ₆	Sulphur hexafluoride
Si	Silicon
SiN	Silicon nitride
SiO ₂	Silicon dioxide
SiOH	Silanol
TMAH	Tetramethylammonium hydroxide
USB	Universal serial bus
VI	Virtual instrument

8 REFERENCES

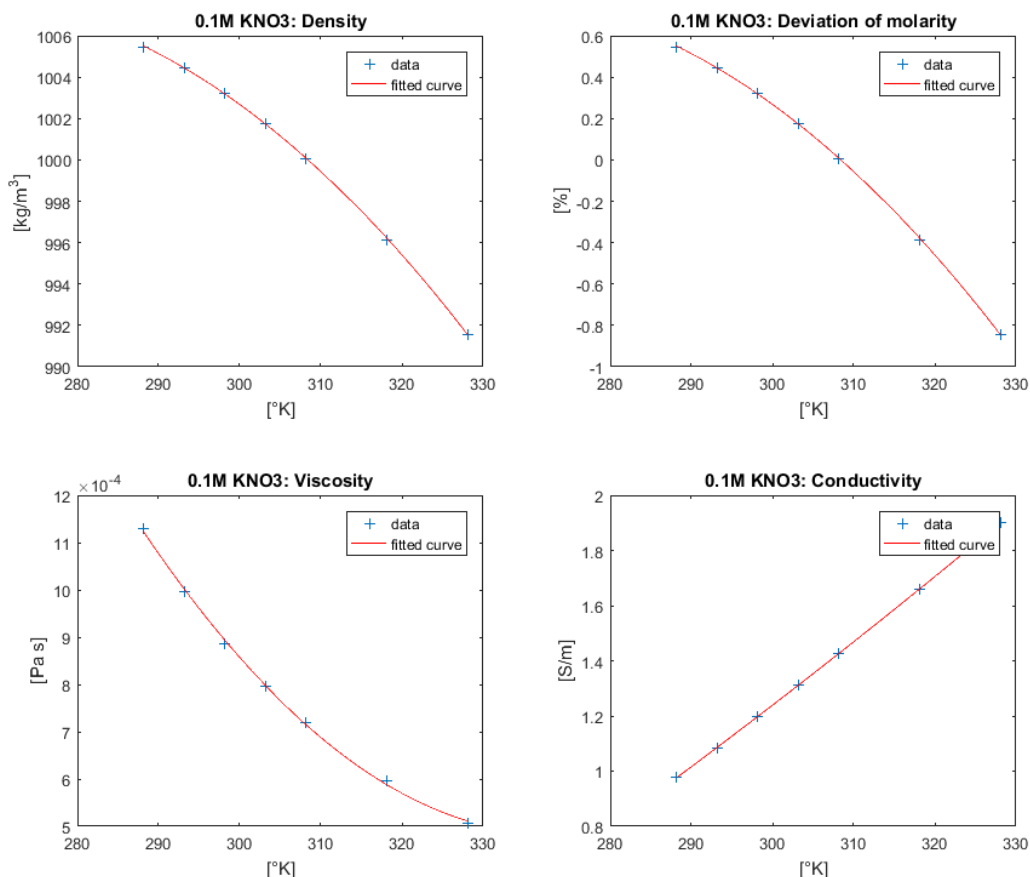
- [1] X. Wang, C. Cheng, S. Wang and S. Liu, "Electroosmotic pumps and their applications in microfluidic systems," vol. 6, 2009.
- [2] L. Jiang, J. Mikkelsen, J.-M. Koo, D. Huber, S. Yao, L. Zhang, P. Zhou, J. G. Maveety, R. Prasher, J. G. Santiago, T. W. Kenny and K. E. Goodson, "Closed-Loop Electroosmotic Microchannel Cooling System for VLSI Circuits," vol. 25, no. 3, 2002.
- [3] V. Singhal, S. V. Garimella and A. Raman, "Microscale pumping technologies for microchannel cooling systems," vol. 57, no. 33, 2004.
- [4] S. Yao, D. E. Hertzog, S. Zeng, J. C. J. Mikkelsen and J. G. Santiago, "Porous glass electroosmotic pumps: design and experiments," vol. 268, 2003.
- [5] S. Zeng, C.-H. Chen, J. G. Santiago, J.-R. Chen, R. N. Zare, J. A. Tripp, F. Svec and J. M. Fréchet, "Electroosmotic flow pumps with polymer frits," vol. 82, 2002.
- [6] J. Berenschot, X. Sun, H. Le The, E. Sarajlic, R. Tiggelaar, M. de Boer, J. Eijkel, H. Gardeniers and N. Tas, "Massive parallel nanostructure formation inside vertical nano-pores," in *Poster Mesa+ Meeting 2016*, 2016.
- [7] J. Berenschot, X. Sun, H. Le The, R. Tiggelaar, M. de Boer, J. Eijkel, J. Gardeniers and N. Tas, "Wafer-scale Nano Formation Inside Vertical Nano-pores," in *12th IEEE International Conference on Nano/Micro Engineered and Molecular Systems*, Los Angeles, 2017.
- [8] K. Hamaguchi, .. Tsuchiya, K. Shimaoka and H. Funabashi, "3-nm Gap Fabrication Using Gas Phase Sacrificial Etching for Quantum Devices," in *17th IEEE International Conference on Micro Electro Mechanical Systems. Maastricht MEMS 2004 Technical Digest*, Maastricht, 2004.
- [9] M. Kooijman and M. Pallada, *Leerboek materiaalkunde voor technici*, Enschede: Boon, 2017.
- [10] J. G. E. Gardeniers and H. A. C. Tilmans, "LPCVD silicon-rich silicon nitride films for applications in micromechanics, studied with statistical experimental design," *Journal of vacuum science and technology A: vacuum, surfaces, and films*, vol. 14, 1996.
- [11] C. J. M. van Rijn, *Membrane Science and Technology Series 10*, Elsevier, 2004.
- [12] W.-H. Chuang, T. Luger, R. K. Fettig and R. Ghodssi, "Mechanical Property Characterization of LPCVD Silicon Nitride Thin Films at Cryogenic Temperatures," vol. 13, no. 5, 2004.
- [13] D. C. Webb, K. Kormi and S. T. S. Al-Hassani, "Use of FEM. in performance assessment of perforated plate subject to general loading conditions," vol. 64, 1995.
- [14] K. Sadek, J. Lueke and W. Moussa, "A Coupled Field Multiphysics Modeling Approach to Investigate RF MEMS Switch Failure Modes under Various Operational Conditions," *Sensors*, vol. 9, pp. 7988-8006, 2009.

- [15] W. C. Young and R. G. Budynas, Roark's Formulas for Stress and Strain, 7th ed., McGraw-Hill, 2002.
- [16] M. Aryarad and M. Heshmati, "Evaluation and analysis of the stress concentration factor reduction techniques on perforated plates using finite element method," vol. 36, no. 4, 2015.
- [17] D. Lide, CRC handbook of Chemistry and Physics 86th ed., CRC Press, 2005.
- [18] D. R. Lide, CRC Handbook of Chemistry and Physics 74th Edition 1993-1994 Special Student Edition, CRC Press, 1993.
- [19] A. V. Bandura and S. N. Lvov, "The Ionization Constant of Water over Wide Ranges of Temperature and Density," *Journal of Physical and Chemical Reference Data* 35, vol. 15, 2006.
- [20] M. A. Brown, Z. Abbas, K. Kleibert, R. G. Green, A. Goel, S. May and T. M. Squires, "Determination of Surface Potential and Electrical Double-Layer Structure at the Aqueous Electrolyte-Nanoparticle Interface," *Physical Review X*, no. 6, 2016.
- [21] U. N. I. o. S. a. Technology, "CODATA Value: electric constant," in *The NIST Reference on Constants, Units, and Uncertainty*, June 2015.
- [22] R. Zimmermann, D. Küttner, L. Renner, M. Kaufmann, J. Zitzmann and M. Müller, "Charging and structure of zwitterionic supported bilayer lipid membranes studied by streaming current measurements, fluorescence microscopy, and attenuated total reflection Fourier transform infrared spectroscopy," *Biointerphases*, vol. 4, no. 1, 2009.
- [23] A. Revil and P. A. Pezard, "Streaming potential in porous media 1. Theory of zeta potential," *Journal of Geophysical Research*, vol. 104, no. B9, pp. 20021-20031, 1999.
- [24] B. J. Kirby and E. F. J. Hasselbrink, "Zeta potential of microfluidic substrates: 1. Theory, experimental techniques, and effects on separations," *Electrophoresis*, vol. 25, pp. 187-202, 2004.
- [25] C.-H. Chen and J. G. Santiago, "A Planar Electroosmotic Micropump," *Journal of Microelectromechanical Systems*, vol. 11, no. 6, 2002.
- [26] A. J. Bard and L. R. Faulkner, *Electrochemical Methods Fundamentals and Applications* Second Edition, John Wiley & Sons, 2001.
- [27] A. W. Adamson, "Solutions of Electrolytes, 12-3A. Strong Electrolytes," in *A textbook of physical chemistry 2nd Ed.*, Academic Press, 1973, p. 437.
- [28] A. Catenaccio, Y. Daruich and C. Magallanes, "Temperature dependence of the permittivity of water," *Chemical Physics Letters*, vol. 367, p. 669-671, 2003.
- [29] T. Isono, "Density, Viscosity, and Electrolytic Conductivity of Concentrated Aqueous Electrolyte Solutions at Several Temperatures. Alkaline-Earth Chlorides, LaCl₃, Na₂SC₄, NaNC₃, NaBr, KNC₃, KBr, and Cd(NO₃)₂," vol. 29, no. 1, pp. 45-52, 1984.
- [30] K. G. H. Janssen, H. T. Hoanh, J. Floris, J. de Vries, N. R. Tas, J. C. T. Eijkel and T. Hankemeier, "Solution Titration by Wall Deprotonation during Capillary Filling of Silicon Oxide

8 - References

- Nanochannels," vol. 80, pp. 8095-8101, 2008.
- [31] R. B. M. Schasfoort, S. Schlautmann, J. Hendrikse and A. van den Berg, "Field-Effect Flow Control for Microfabricated Fluidic Networks," vol. 286, no. 5441, pp. 942-945, 1999.
- [32] D. Laser and S. J.G., "A Review of Micropumps," *Journal of Micromechanics and Microengineering*, vol. 14, pp. 35-64, 2004.
- [33] . M. A. Parashchenko, N. S. Filippov, V. V. Kirienko and S. I. Romanov, "Electroosmotic pump based on asymmetric silicon microchannel membranes," *Optoelectronics Instrumentation and Data Processing*, vol. 50, no. 3, p. 315-322, 2014.
- [34] S. Zeng, C.-H. Chen, J. C. J. Mikkelsen and J. G. Santiago, "Fabrication and characterization of electroosmotic micropumps," *Sensors and Actuators B*, vol. 79, 2001.
- [35] J. Lyklema, "Surface Conduction," *Journal of Physics: Condensed Matter*, vol. 13, pp. 5027-5034, 2001.
- [36] R. B. Byron, W. E. Stewart and E. N. Lightfoot, "The Equations of Change of Nonisothermal Systems, The Equations of Energy," in *Transport Phenomena - International Edition*, Wiley, 1960.
- [37] G. L. Morini, "Viscous Dissipation," in *Encyclopedia of Microfluidics and Nanofluidics*, New York, Springer Science+Business Media, 2013.
- [38] Hiroyuki Oshima, *Electrical Phenomena at Interfaces and Biointerfaces - Fundamentals and Applications in Babo-, Bio-, and Environmental Sciences*, Wiley, 2012.
- [39] V. M. Starov, *Nanoscience: Colloidal and Interfacial Aspects*, vol. Surfactant Science Series Volume 147, CRC Press, 2010.
- [40] D. Stein, M. Kruithof and C. Dekker, "Surface-Charge-Governed Ion Transport in Nanofluidic Channels," *Physical Review Letters*, vol. 93, no. 3, 2004.
- [41] E. T. Urbansky and M. R. Schock, "Understanding, Deriving, and Computing Buffer Capacity," *Journal of chemical education*, vol. 77, 2000.
- [42] N. R. Tas, J. Haneveld, J. H. V., M. Elwenspoek and A. van den Berg, "Capillary Filling Speed of Water in Nanochannels," *Applied Physics Letters*, vol. 85, pp. 3274-3276, 2004.
- [43] H. H. Solak, C. Dais and F. Clube, "Displacement Talbot lithography: a new method for high-resolution patterning of large areas," *Optic Express*, vol. 19, 2011.
- [44] A. Merlos, M. Acero, M. H. Bao, J. Bausells and J. Esteve, "TMAH/IPA anisotropic etching characteristics," *Sensors and Actuators A*, Vols. 37-38, pp. 737-743, 1993.

APPENDIX A CURVE FITTINGS FOR TEMPERATURE DEPENDENT DENSITY, VISCOSITY AND CONDUCTIVITY



Resulting parameters:

dens_KNO3_01_fit =

Linear model Poly2:

$$\text{dens_KNO3_01_fit}(x) = p1 \cdot x^2 + p2 \cdot x + p3$$

Coefficients (with 95% confidence bounds):

$$p1 = -0.003978 \quad (-0.004281, -0.003675)$$

$$p2 = 2.102 \quad (1.915, 2.289)$$

$$p3 = 730.1 \quad (701.4, 758.9)$$

mol_dev_KNO3_01_fit =

Linear model Poly2:

$$\text{mol_dev_KNO3_01_fit}(x) = p1 \cdot x^2 + p2 \cdot x + p3$$

Coefficients (with 95% confidence bounds):

$$p1 = -0.0003978 \quad (-0.0004281, -0.0003675)$$

$$p2 = 0.2102 \quad (0.1915, 0.2289)$$

$$p3 = -26.99 \quad (-29.86, -24.11)$$

vis_KNO3_01_fit =

Linear model Poly2:

$$\text{vis_KNO3_01_fit}(x) = p1 \cdot x^2 + p2 \cdot x + p3$$

Coefficients (with 95% confidence bounds):

$$p1 = 2.536e-07 \quad (2.01e-07, 3.062e-07)$$

$$p2 = -0.0001716 \quad (-0.000204, -0.0001391)$$

$$p3 = 0.02951 \quad (0.02451, 0.0345)$$

cond_KNO3_01_fit =

Linear model Poly2:

$$\text{cond_KNO3_01_fit}(x) = p1 \cdot x^2 + p2 \cdot x + p3$$

Coefficients (with 95% confidence bounds):

$$p1 = 3.309e-05 \quad (2.754e-05, 3.864e-05)$$

$$p2 = 0.002781 \quad (-0.0006408, 0.006203)$$

$$p3 = -2.573 \quad (-3.1, -2.047)$$

APPENDIX B CALCULATIONS - PLUG FLOW HEATING

Q_{plug} is the flow of a single EOF plug flow in a single pore. The other variables and constants can be found in 2.3.1 and 2.3.5.1.

$$V_z(r) = \begin{cases} V_{max} & 0 \leq r \leq R_\lambda \\ \frac{V_{max}}{\lambda_D} (R_c - r) & R_\lambda \leq r \leq R_c \end{cases}, R_\lambda = R_c - \lambda_D$$

$$Q_{plug} = \int_0^{R_c} 2\pi r V_z(r) dr = \int_0^{R_\lambda} 2\pi r V_{max} dr + \int_{R_\lambda}^{R_c} 2\pi r \frac{V_{max}}{\lambda_D} (R_c - r) dr = Q_1 + Q_2$$

$$Q_1 = [\pi V_{max} r^2]_0^{R_\lambda} = \pi V_{max} (R_c^2 - 2R_c \lambda_D + \lambda_D^2)$$

$$Q_2 = \left[2\pi \frac{V_{max}}{\lambda_D} \left(\frac{1}{2} R_c r^2 - \frac{1}{3} r^3 \right) \right]_{R_\lambda}^{R_c} = 2\pi \frac{V_{max}}{\lambda_D} \left(\frac{1}{6} R_c^3 - \frac{1}{2} R_c (R_c - \lambda_D)^2 + \frac{1}{3} (R_c - \lambda_D)^3 \right)$$

$$= 2\pi \frac{V_{max}}{\lambda_D} \left(\frac{1}{6} R_c^3 - \frac{1}{2} R_c^3 + R_c^2 \lambda_D - \frac{1}{2} R_c \lambda_D^2 + \frac{1}{3} R_c^3 - R_c^2 \lambda_D + R_c \lambda_D^2 - \frac{1}{3} \lambda_D^3 \right)$$

$$= 2\pi \frac{V_{max}}{\lambda_D} \left(\frac{1}{2} R_c \lambda_D^2 - \frac{1}{3} \lambda_D^3 \right) = \pi V_{max} \left(R_c \lambda_D - \frac{2}{3} \lambda_D^2 \right)$$

$$Q_{plug} = \pi V_{max} \left(R_c^2 - 2R_c \lambda_D + \lambda_D^2 + R_c \lambda_D - \frac{2}{3} \lambda_D^2 \right) = \pi V_{max} \left(R_c^2 - R_c \lambda_D + \frac{1}{3} \lambda_D^2 \right)$$

$$V_{max} = \frac{Q_{plug}}{\pi (R_c^2 - R_c \lambda_D + \frac{1}{3} \lambda_D^2)}$$

$$W_{plug.vis.unit} = -\frac{\mu}{\rho} \left(\frac{\delta v_z}{\delta r} \right)^2 = -\frac{\mu}{\rho} \left(\frac{V_{max}}{\lambda_D} \right)^2$$

APPENDIX C CALCULATIONS - MEMBRANE BLOW-OUT CURRENT

This appendix contains the calculations used for calculating the theoretical voltage and current needed to create enough force for the membranes to be blown out for batch 2.

All used constants and values are the same as mentioned in section 2.3.1 for a 0.1M KNO₃ solution. For the flow a plug flow is assumed as is described in section 2.3.5.1. The maximum pressure P is found in section 5.2.2 and is 180kPa. The channel length $l_{channel}$ is 455nm, the radius of the channel $r_{channel}$ is 41.5nm and the maximum flow velocity is v_{EOF} which is labelled v_{max} in section 2.3.5.1.

The pressure on the membrane as a result of the EOF actuation is given by:

$$P = \frac{A \eta}{\pi r_{channel}^2} l_{channel} 2 \pi r_{channel} \frac{v_{EOF}}{\lambda_D}$$

So the maximum flow velocity is given by:

$$v_{eff} = \frac{P \lambda_D \pi r_{channel}^2}{A \eta l_{channel} 2 \pi r_{channel}} = 7.8 \text{mm/s}$$

As can be derived from Appendix B, the flow is then given by:

$$Q = A \eta v_{EOF} \left(\pi \left(r_{channel}^2 - r_{channel} \cdot \lambda_D + \frac{1}{3} \lambda_D^2 \right) \right) = 66 \mu\text{l/s}$$

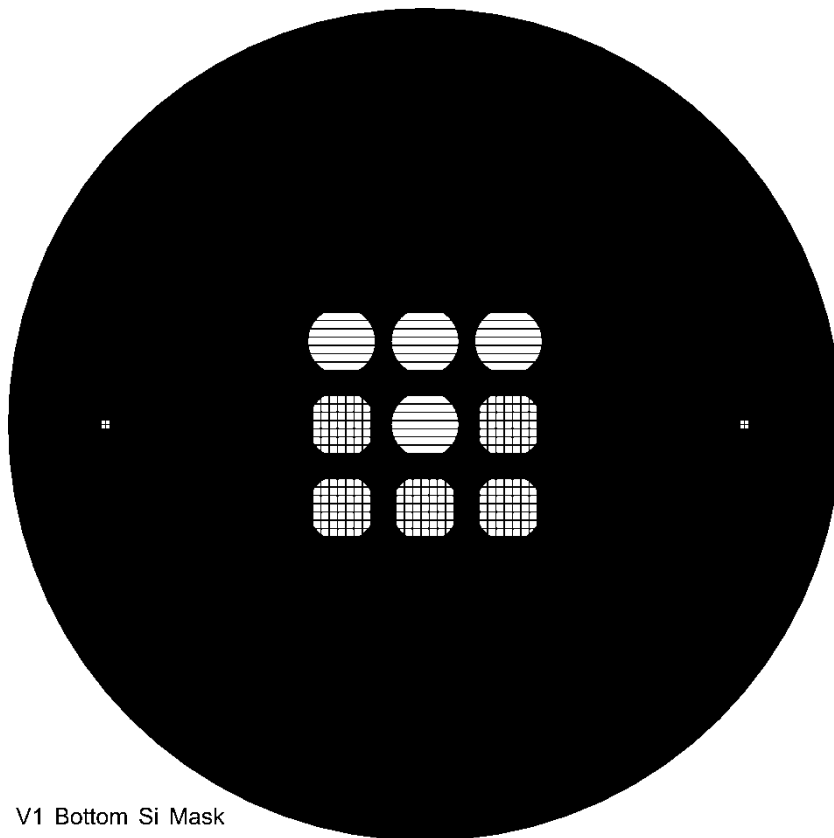
Using F. 7, the effective potential over the membrane can be derived:

$$U_{eff} = Q_{max} \frac{\mu l}{\eta A A_0 \varepsilon_0 \zeta} = 140 \text{mV}$$

Since the current is measured, it is interesting to know the corresponding current, which is given by:

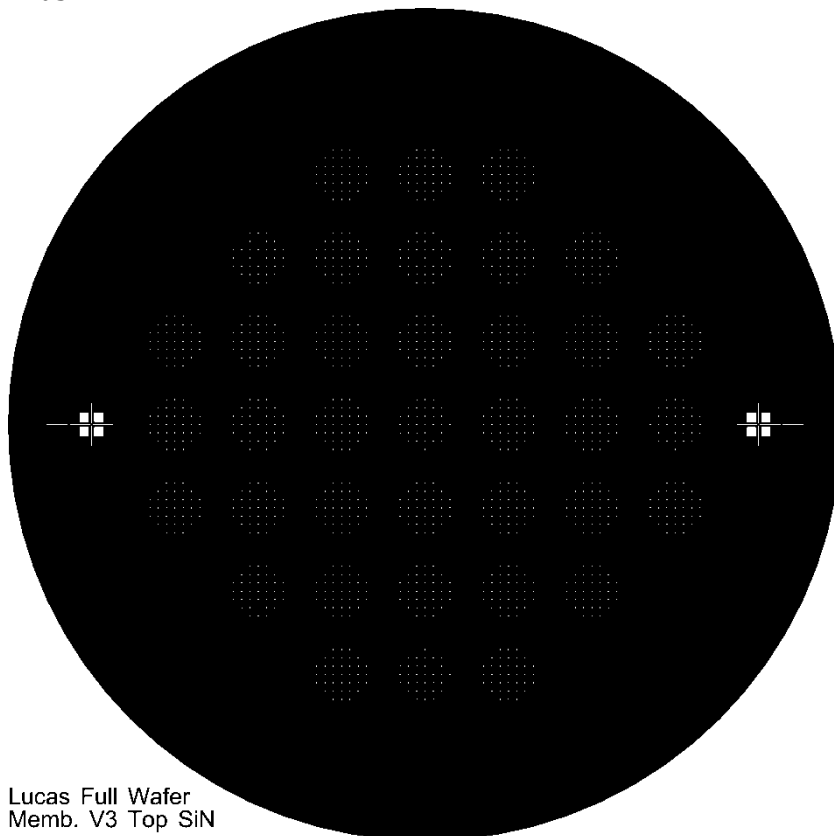
$$I = \frac{U_{eff}}{R} = \frac{U_{eff} \kappa_{cond} l_{channel}}{\pi r_{channel}^2} = 14.2 \text{mA}$$

APPENDIX D MASKS



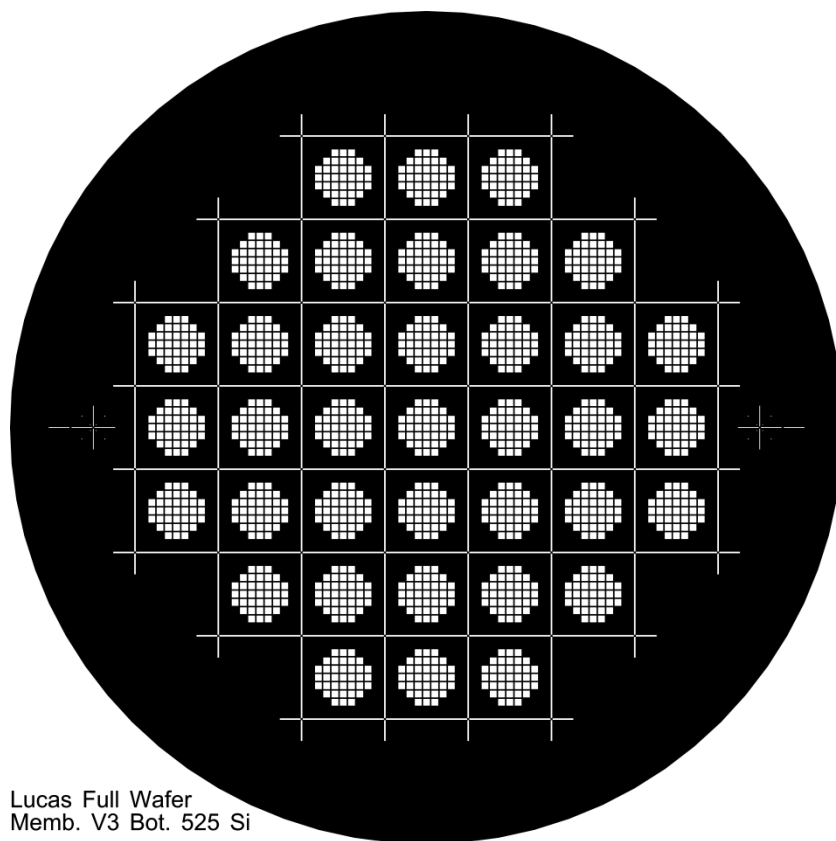
V1 Bottom Si Mask

Batch 1 bottom mask



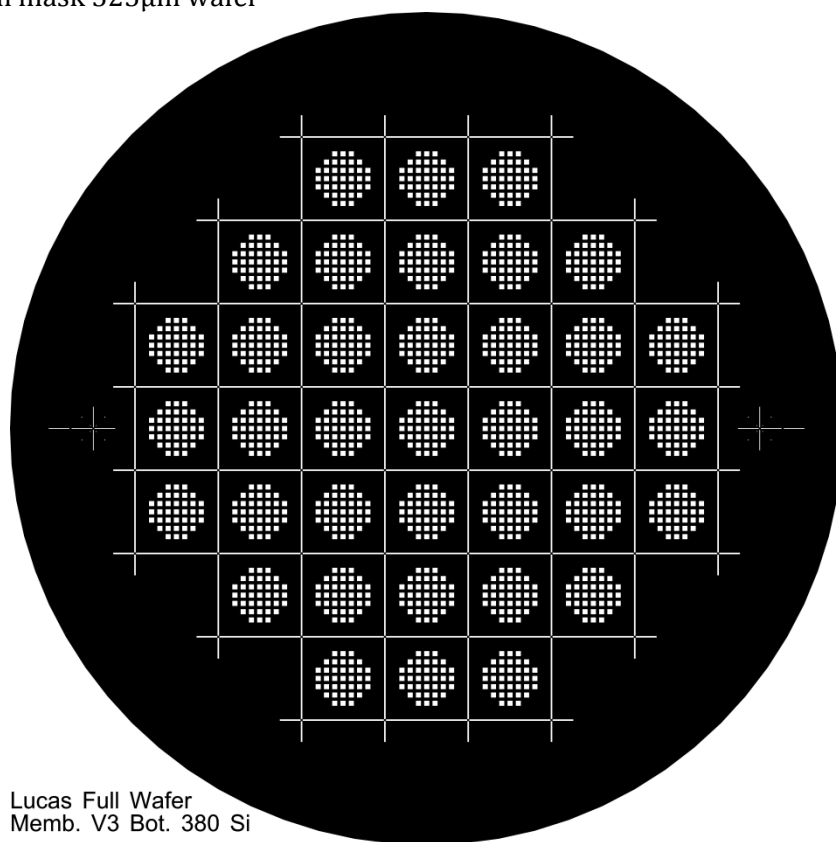
Lucas Full Wafer
Memb. V3 Top SiN

Batch 2 top mask: Due to resolution, the pattern seems non-homogeneous, but every cell consists of 37 square 150 μ m windows.



Lucas Full Wafer
Memb. V3 Bot. 525 Si

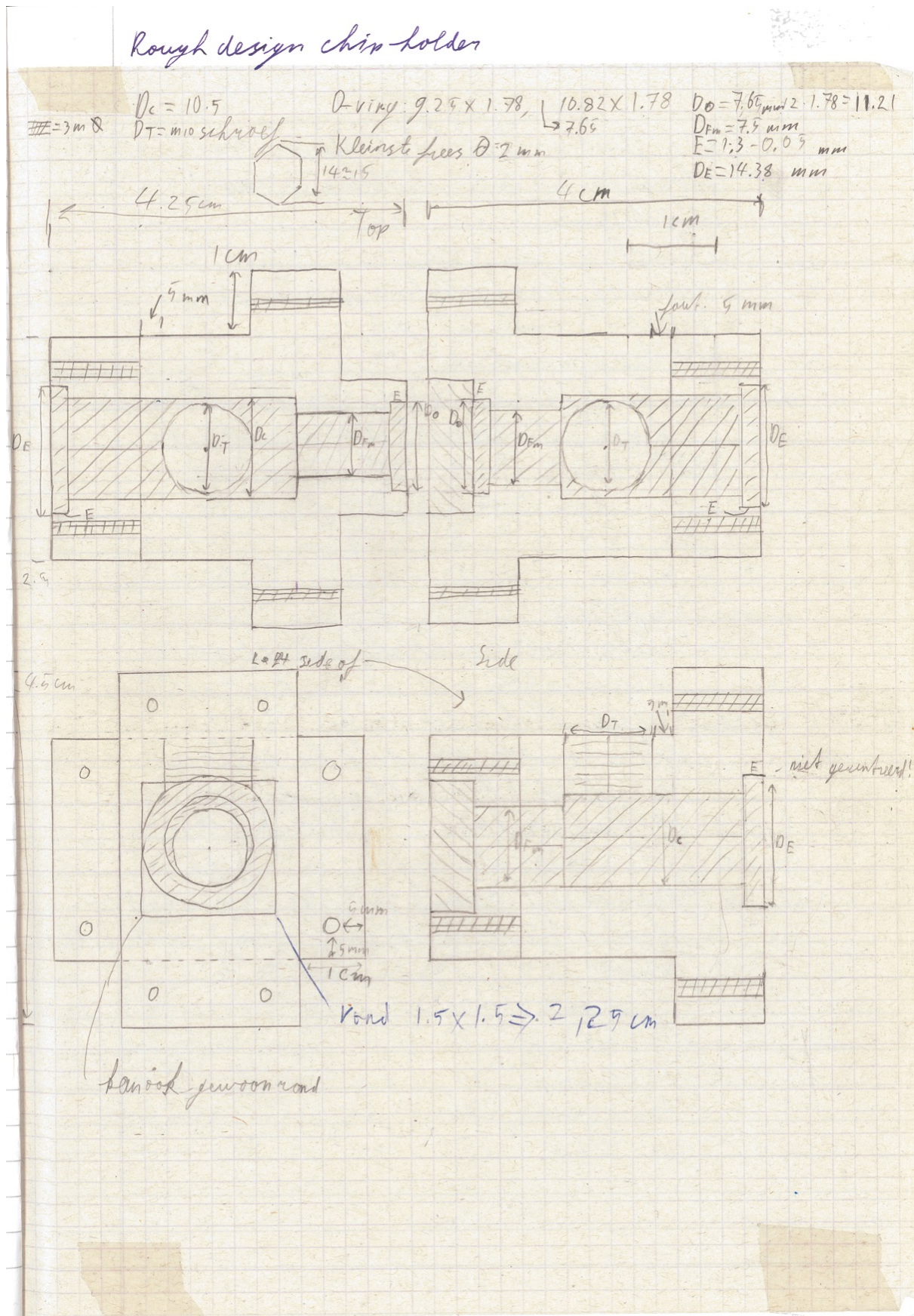
Batch 2 bottom mask 525 μ m wafer



Lucas Full Wafer
Memb. V3 Bot. 380 Si





Batch 2 bottom mask 380 μ m wafer

APPENDIX E CHIPHOLDER DESIGN


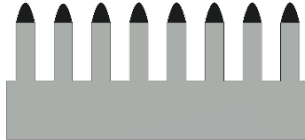



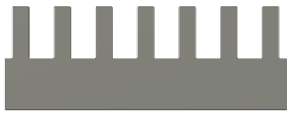
APPENDIX F DETAILED PROCESS FLOW: FROM WAFER TO PILLARS

Please note that the first section contains an illustrated process flow with all the used settings, while the second section contains the process flow as is composed using the cleanroom process flow composer. Both are complimentary. This process flow has been developed with and was created and performed by the venerable Yasser Pordeli.

Step	Process Description	Cross-section after process
1	Substrate Selection Orientation: <100> Diameter: 100mm Thickness: 385μm Polished: one side polished (OSP) Resistivity: 1-10Ωcm Type: P/phosphor	
Pillar formation		
8 – 11	Spin coating of BARC <ul style="list-style-type: none"> - Barli-II 200 - Spin program: 3000 (3000 rpm, 45sec) - ~180 nm Pre-bake of Barli-II 200 <ul style="list-style-type: none"> - 60 sec @185 °C 	
	Spin coating of PFI88 <ul style="list-style-type: none"> - PFI88 (1:1 diluted in PGMEA) - Spin program: 4000 (4000 rpm, 45sec) - ~160 nm Pre-bake of PFI88 <ul style="list-style-type: none"> - 60 sec @90 °C 	
12 – 15	Phabler 100C <ul style="list-style-type: none"> - Double Exposure <ul style="list-style-type: none"> • Intensity: 1mW/cm² • DTL-range: 3μm • Target cycle: 20s (1 precycle) • Gap: ~65 μm • Polarizer: Black slider in (Red slider out) • Spacer: 50 μm for LIL 144 (25 μm for LIL 053) 	

Appendix F - Detailed Process Flow: From Wafer to Pillars

	<ul style="list-style-type: none"> • Exposure time Dots: 45 s <p>Postbake @110 °C for 60 sec</p> <p>Development in OPD4262</p> <p>Beaker 1: 30 sec + beaker 2: 30 sec</p> <p>SEM inspection</p>	
16 – 20	<p>RIE etching of BARC</p> <ul style="list-style-type: none"> - P = 10 mTorr - N₂ flow: 50 sccm - Power= 25 W - t = 8 min ○ 1%HF dip for 30 sec 	
21	<p>DRIE Si in Estrelas</p> <p>ICP: 800 W</p> <p>RF Power: 38 W</p> <p>Pressure: 22 mTorr</p> <p>Temperature: 0 °C</p> <p>For tapered pillars:</p> <p>SF6: 29 sccm</p> <p>C4F8: 50 sccm</p> <p>Etch time: 87 seconds</p> <p>DC Bias: 208 V</p> <p>Etch rate: 5.23 nm/s</p>	
	<p>In-situ oxygen plasma cleaning (Estrelas)</p> <p>ICP: 2000 W</p> <p>Pressure: 10 mTorr</p> <p>O2: 100 sccm</p> <p>Temperature: 0 °C</p> <p>time: 60 seconds</p>	
	<p>RCA – 2 Clean</p> <ul style="list-style-type: none"> - 15 min 	

22 – 25	Strip BARC and Resist - 10 min in self-made 99% HNO ₃	
--------------------	--	--

Appendix F - Detailed Process Flow: From Wafer to Pillars

ILP: In-line Processing	MFP: Metal-free Processing	UCP: Ultra Clean Processing	Removal of Residues
-------------------------	----------------------------	-----------------------------	---------------------

Step	Level	Process/Basic flow	User comments
1		Substrate Silicon (#subs101) NL-CLR-Wafer Storage Cupboard Orientation: <100> Diameter: 100mm Thickness: 525µm +/- 25µm Polished: Single side (OSP) Resistivity: 5-10Ωcm Type: p/boron	5 dummy wafer for testing Estrelas. x device wafers
clean1001: In-line cleaning (WB06-ILP)			
2	ILP	Cleaning in 99% HNO₃ (#clean004) NL-CLR-WB06 Purpose: removal of organic traces. <ul style="list-style-type: none"> • Beaker 1: 99% HNO₃ • Time = 5 min 	Skip
3	ILP	Quick Dump Rinse (QDR) (#rinse001) NL-CLR-Wetbenches Purpose: removal of traces of chemical agents. Recipe 1 Quick dump rinsing (QDR) Recipe 2 Cascade rinsing for fragile wafers Rinse until message 'End of rinsing process' is shown on the touchscreen of the QDR, else repeat the rinsing process.	
4	MFP	Substrate drying (WB06-WB08) (#dry020) NL-CLR-WB06 to WB08 Single substrate drying: <ol style="list-style-type: none"> 1. Use the single-wafer spinner Settings: 2500 rpm, 60 sec (including 45 sec nitrogen purge) 2. Use the nitrogen gun (fragile wafers or small samples) Batch drying of substrates: The Semitool uses the following standard procedure: <ul style="list-style-type: none"> • Rinse: 30 sec (600 rpm) 	

- Q-rinse: 10.0 MΩ (600 rpm)
- Purge: 10 sec (600 rpm)
- Drying: 280 sec (1600 rpm)

Note: it is obligatory to apply a single rinsing step in the QDR before using the Semitool!

etch1201: HF etch 1 % (WB06)

5	ILP	Etching in 1% HF (#etch210)	NL-CLR-WB06 Strip native SiO ₂ in 1% HF. Beaker: 1% HF • Time: 1 min Strip until hydrofobic surface.	Skip
6	ILP	Quick Dump Rinse (QDR) (#rinse001)	NL-CLR-Wetbenches Purpose: removal of traces of chemical agents. Recipe 1 Quick dump rinsing (QDR) Recipe 2 Cascade rinsing for fragile wafers Rinse until message 'End of rinsing process' is shown on the touchscreen of the QDR, else repeat the rinsing process.	
7	ILP	Substrate drying (#dry001)	NL-CLR-WBs (ILP) Single substrate drying: 1. Use the single-wafer spinner Settings: 2500 rpm, 60 sec (including 45 sec nitrogen purge) 2. Use the nitrogen gun (fragile wafers or small samples)	

litho1310: Lithography of PFI88

8	ILP	Coating of Barli-II 200 (#litho113)	NL-CLR-WB21 Primus spinner • Barli-II 200 • Spin program: 3000 (3000rpm, 45sec) Under these conditions, the thickness of the Barli-II 200 is about 180 nm.	
9	ILP	Prebake of Barli-II 200 (#litho020)	NL-CLR-WB22 Hotplate • Temperature: 185°C • Time: 60s	

Appendix F - Detailed Process Flow: From Wafer to Pillars

10	ILP	Coating of PFI88 (#litho114)	NL-CLR-WB21 Coating: Primus spinner • PFI88 (1:1 diluted in PGMEA) • Spin program: 4000 (4000rpm, 45sec) Under these conditions, the thickness of the PFI88 is about 160 nm. Contact Huib van Vossen in case the bottle with resist is almost empty, since this is an in-house resist solution.
11	ILP	Prebake of PFI88 (#litho021)	NL-CLR-WB22 Prebake: hotplate • Temperature: 90°C • Time: 60s
12	ILP	Alignment & exposure of PFI88 (#litho330)	NL-CLR-PhableR 100C • Mask: Test mask of Phabler • Exposure dose: 250mJ • Hg-lamp: 2mW/cm ² • Exposure time: 125s • Target cycle: 30s (1 precycle) • No polarizer • DTL-range: 8µm • Gap: ~88µm (spacer = 25µm) The exposure settings are optimal for the hole test patterns on the mask.
13	ILP	Postbake of PFI88 (#litho022)	NL-CLR-WB22 Postbake: hotplate • Temperature: 110°C • Time: 60s
14	ILP	Development of PFI88 (#litho220)	NL-CLR-WB21 Developer: OPD4262 • Time: 30sec in beaker 1 • Time: 30sec in beaker 2 The development time of PFI88 in OPD4262 is not critical (no dark erosion).
15	ILP	SEM inspection (#metro103)	NL-CLR-SEM • JEOL JSM 5610 SEM • FEI Sirion HR-SEM

- High resolution SEM LEO (Mark Smithers)

etch1735: Transfer of nanopatterns in Barli-II 200 by N2 plasma (TEtske)

16	ILP	Chamber clean (TEtske) (#etch198)	<p>NL-CLR-TEtske Application: removal of organic and fluorocarbon residues on the chamber wall.</p> <p>Select the correct etch chamber and electrode for your etch process (see next step).</p> <ul style="list-style-type: none"> • Electrode temperature: 10°C • Pressure: 50mTorr • O2 flow: 50sccm • Power: 100Watt • Time: 10 min • DC bias: -600Volt • Load: 65 • Tune: 35 <p>The etch chamber is clean at the moment the plasma color is white.</p>
17	ILP	Directional Etching of Barli-II 200 (#etch240)	<p>NL-CLR-TEtske Application: transfer of nanopatterns by N2 plasma.</p> <p>Select the dirty chamber and the styros electrode.</p> <ul style="list-style-type: none"> • Electrode temperature: 10°C • Pressure: 13mTorr • N2 flow: 50sccm • Power: 25Watt • DC bias: ... <p>Etch rate Barli-II 200: 26 nm/min. For more details: H. Le-The, E. Berenschot, R.M. Tiggelaar, N.R. Tas, A. van den Berg, J.C.T. Eijkel, <i>Adv. Mater. Technol.</i> 2017, 1600238.</p>

etch1201: HF etch 1 % (WB06)

18	ILP	Etching in 1% HF	<p>NL-CLR-WB06</p> <p>Strip native SiO2 in 1% HF.</p> <p>30 sec</p>
----	-----	-------------------------	---

Appendix F - Detailed Process Flow: From Wafer to Pillars

		(#etch210)	Beaker: 1% HF • Time: 1 min Strip until hydrofobic surface.													
19	ILP	Quick Dump Rinse (QDR) (#rinse001)	NL-CLR-Wetbenches Purpose: removal of traces of chemical agents. Recipe 1 Quick dump rinsing (QDR) Recipe 2 Cascade rinsing for fragile wafers Rinse until message 'End of rinsing process' is shown on the touchscreen of the QDR, else repeat the rinsing process.													
20	ILP	Substrate drying (#dry001)	NL-CLR-WBs (ILP) Single substrate drying: 1. Use the single-wafer spinner Settings: 2500 rpm, 60 sec (including 45 sec nitrogen purge) 2. Use the nitrogen gun (fragile wafers or small samples)													
etch1804: High-Precision Nano-Scale Pillar Etch C-SF6/C4F8 - STD (Oxford Estrelas)																
21	ILP	High-Precision Nano-Scale Etch C-SF6/C4F8 (#etch804)	NL-CLR-Oxford Estrelas Application: etching of nanopillars (with a diameter of 100nm and 200 pitch) in Silicon Process name: Performance: • Etch rate: >150nm/min (at <10% loading) • Selectivity: >10 (with respect to PFI88) • Selectivity: >15 (with respect to t-SiO2) • Pillar height: 500nm • Profile control: 90±1° Ref. document: PT6683.04	Pillar length ~450 nm												
22	ILP	Stripping of Resists (#strip101)	NL-CLR-TePla360 Application: stripping of resist by O2 plasma. WARNING: in case of stripping of resist on chromium, then use recipe 041 on the TePla360 (strip1130)!													
<table><tr><th>Step</th><th>O2 (sccm)</th><th>Ar (sccm)</th><th>P (mbar)</th><th>Powe r (W)</th><th>Time (h:mm:ss)</th></tr><tr><td> </td><td> </td><td> </td><td> </td><td> </td><td> </td></tr></table>					Step	O2 (sccm)	Ar (sccm)	P (mbar)	Powe r (W)	Time (h:mm:ss)						
Step	O2 (sccm)	Ar (sccm)	P (mbar)	Powe r (W)	Time (h:mm:ss)											

Preheating	0	600	0.6	1000	0:10:00
Stripping of resist	360	160	0.6	800	*

* Select one of the following recipes to strip the resist, depending on the thickness of the resist, treatment of the resist and the number of wafers.

Recipe 011: time = 10min

Recipe 012: time = 20min

Recipe 013: time = 30min

Recipe 014: time = 40min

Recipe 016: time = 60min

BACKUP: If the TePla360 is down, contact the administrator on how to continue your processing on the TePla300.

PLEASE NOTE It is mandatory to remove metal traces originating from plasma tools in RCA-2 (residue1505), e.g. plasma etching or stripping in O2 plasma, in case you:

- continue with UCP processing
- continue with high-temperature processing (MFP)

23

Rem
Res

Removal of metal traces in RCA-2
(#residue504)

NL-CLR-WB09

Purpose: removal of metal traces originating from plasma tools in order to protect the cleaning efficiency of the wet benches. For this reason, RCA-2 is compulsory in case you continue:

- cleaning in the Pre-Furnace Clean (WB14-MFP)
- processing in the Ultra-Clean Line - Front End (WB12-UCP)
- processing in the Ultra-Clean Line - Back End (WB13-UCP)

Chemicals: HCl:H2O2:H2O (1:1:5 vol.%)

PLEASE NOTE

1. CAUTION: do not process substrates with metal patterns in RCA-2.

2. NO REUSE: reuse of RCA-2 is forbidden!

Contact the administrator in case there is no empty RCA-2 beaker available in WB09.

Procedure:

Appendix F - Detailed Process Flow: From Wafer to Pillars

			<ul style="list-style-type: none"> • Pour 1500ml* of DI water into the beaker • Turn on the stirrer • Add 300ml* of Hydrogen Chloride (HCl) • Heat up the solution to 70°C (setpoint heater = 80°C) • Slowly add 300ml* of Hydrogen Peroxide (H2O2) • Submerge your samples as soon as the temperature is above 70°C • Time = 15min <p>* Use a glass graduated cylinder of 500ml to measure the volume of the chemicals.</p>
24	ILP	Quick Dump Rinse (QDR) (#rinse001)	NL-CLR-Wetbenches Purpose: removal of traces of chemical agents. Recipe 1 Quick dump rinsing (QDR) Recipe 2 Cascade rinsing for fragile wafers Rinse until message 'End of rinsing process' is shown on the touchscreen of the QDR, else repeat the rinsing process.
25	ILP	Substrate drying (#dry001)	NL-CLR-WBs (ILP) Single substrate drying: 1. Use the single-wafer spinner Settings: 2500 rpm, 60 sec (including 45 sec nitrogen purge) 2. Use the nitrogen gun (fragile wafers or small samples)

APPENDIX G DETAILED PROCESS FLOW: FROM PILLARS TO MEMBRANE

Print date: 2019-01-17

Name of process flow:	Pillars to Membrane
Platform:	Fluidics
Creation date:	2018-06-14
Personal information	
User name:	Kooijman, L.
Email address:	l.j.kooijman@student.utwente.nl
Company/Chair:	Masterstudenten
Function:	Student
Project:	EOF Pump
Name of supervisor:	Niels Tas/Erwin Berenschot
Process planning	
Process start:	
Process end:	
Status	
Name of advisor:	
Last revision:	2019-01-17
Approval:	
Approval date:	
Expiration date:	

ILP: In-line Processing	MFP: Metal-free Processing	UCP: Ultra Clean Processing	Removal of Residues
--------------------------------	-----------------------------------	------------------------------------	----------------------------

Step Level Process/Basic flow			User comments
film1960: Dry Oxidation of Silicon (B3)			
1	MFP	Cleaning in 99% HNO₃ (#clean001)	NL-CLR-WB14 BEAKER 1 Purpose: removal of organic traces. Chemical: 99% HNO ₃ • Time: 5 min
2	MFP	Cleaning in 99% HNO₃ (#clean002)	NL-CLR-WB14 BEAKER 2 Purpose: removal of organic traces. Chemical: 99% HNO ₃ • Time: 5 min

Appendix G - Detailed Process Flow: from Pillars to Membrane

3	MFP	Rinsing (#rinse002)	<p>NL-CLR-WBs QDR Purpose: removal of traces of chemical agents.</p> <p>Choose one of the two rinsing modes: QDR = Quick dump rinsing mode Cascade = Overflow rinsing mode for fragile substrates</p> <p>Rinse until message 'End of rinsing process' is shown on the touchscreen of the QDR, else repeat the rinsing process.</p>
4	MFP	Cleaning in 69% HNO₃ (95 °C) (#clean003)	<p>NL-CR-WB14 BEAKER 3A/3B Purpose: removal of metallic traces.</p> <p>Chemical: 69% HNO₃ • Temperature: 95 °C • Time: 10 min</p>
5	MFP	Rinsing (#rinse002)	<p>NL-CLR-WBs QDR Purpose: removal of traces of chemical agents.</p> <p>Choose one of the two rinsing modes: QDR = Quick dump rinsing mode Cascade = Overflow rinsing mode for fragile substrates</p> <p>Rinse until message 'End of rinsing process' is shown on the touchscreen of the QDR, else repeat the rinsing process.</p>
6	MFP	Substrate drying (WB14) (#dry022)	<p>NL-CLR-WB14 Optional drying step. After the QDR, you can transfer your substrates directly to a Teflon carrier and strip the native SiO₂ in 1% HF (WB15).</p> <p>Single substrate drying: 1. Use the single-wafer spinner Settings: 2500 rpm, 60 sec (including 45 sec nitrogen purge). 2. Use the nitrogen gun (fragile wafers or small samples).</p> <p>Batch drying of substrates: Use the Semitool for drying up to 25 substrates at once.</p>
7	MFP	Etching in 1% HF (#etch127)	<p>NL-CLR-WB15 Beaker 1 Purpose: remove native SiO₂ from Silicon.</p> <p>Chemical: 1% HF • Temperature: room temperature • Time: 1 min</p> <p>This step is obligatory for the MESA+ monitor wafer (if applicable, see Equipment database).</p>
8	MFP	Rinsing (#rinse002)	<p>NL-CLR-WBs QDR Purpose: removal of traces of chemical agents.</p>

Detailed Process Flow: from Pillars to Membrane - Appendix G

			<p>Choose one of the two rinsing modes: QDR = Quick dump rinsing mode Cascade = Overflow rinsing mode for fragile substrates</p> <p>Rinse until message 'End of rinsing process' is shown on the touchscreen of the QDR, else repeat the rinsing process.</p>	
9	MFP	Substrate drying (WB15) (#dry023)	<p>NL-CLR-WB15</p> <p>Single substrate drying: 1. Use the single-wafer spinner Settings: 2500 rpm, 60 sec (including 45 sec nitrogen purge). 2. Use the nitrogen gun (fragile wafers or small samples).</p> <p>Batch drying of substrates: Use the Semitool for drying up to 25 substrates at once.</p>	
10	MFP	Dry Oxidation of Silicon (#film960)	<p>NL-CLR-B3 Furnace Recipe: OXxxx°C (xxx= temperature setting)</p> <p>Settings: • Standby temperature: 800°C • Temperature range: 800-1100°C • Ramp: 10°C/min • O₂ flow: 2slm</p> <p>Please mention the following settings in the User Comments: • Target thickness: nm • Temperature:°C • Time:min</p>	10nm
film1206: LPCVD of low-stress SiRN (G4-250 MPa)				
11	MFP	Cleaning in 99% HNO₃ (#clean001)	<p>NL-CLR-WB14 BEAKER 1 Purpose: removal of organic traces.</p> <p>Chemical: 99% HNO₃ • Time: 5 min</p>	Skip. Already done for thermal oxidation.
12	MFP	Cleaning in 99% HNO₃ (#clean002)	<p>NL-CLR-WB14 BEAKER 2 Purpose: removal of organic traces.</p> <p>Chemical: 99% HNO₃ • Time: 5 min</p>	Skip. Already done for thermal oxidation.
13	MFP	Rinsing (#rinse002)	<p>NL-CLR-WBs QDR Purpose: removal of traces of chemical agents.</p> <p>Choose one of the two rinsing modes: QDR = Quick dump rinsing mode Cascade = Overflow rinsing mode for fragile substrates</p>	Skip. Already done for thermal oxidation.

Appendix G - Detailed Process Flow: from Pillars to Membrane

			Rinse until message 'End of rinsing process' is shown on the touchscreen of the QDR, else repeat the rinsing process.	
14	MFP	Cleaning in 69% HNO₃ (95 °C) (#clean003)	NL-CR-WB14 BEAKER 3A/3B Purpose: removal of metallic traces. Chemical: 69% HNO ₃ • Temperature: 95 °C • Time: 10 min	Skip. Already done for thermal oxidation.
15	MFP	Rinsing (#rinse002)	NL-CLR-WBs QDR Purpose: removal of traces of chemical agents. Choose one of the two rinsing modes: QDR = Quick dump rinsing mode Cascade = Overflow rinsing mode for fragile substrates Rinse until message 'End of rinsing process' is shown on the touchscreen of the QDR, else repeat the rinsing process.	Skip. Already done for thermal oxidation.
16	MFP	Substrate drying (WB14) (#dry022)	NL-CLR-WB14 Optional drying step. After the QDR, you can transfer your substrates directly to a Teflon carrier and strip the native SiO ₂ in 1% HF (WB15). Single substrate drying: 1. Use the single-wafer spinner Settings: 2500 rpm, 60 sec (including 45 sec nitrogen purge). 2. Use the nitrogen gun (fragile wafers or small samples). Batch drying of substrates: Use the Semitool for drying up to 25 substrates at once.	Skip. Already done for thermal oxidation.
17	MFP	Etching in 1% HF (#etch127)	NL-CLR-WB15 Beaker 1 Purpose: remove native SiO ₂ from Silicon. Chemical: 1% HF • Temperature: room temperature • Time: 1 min This step is obligatory for the MESA+ monitor wafer (if applicable, see Equipment database).	Skip. Already done for thermal oxidation.
18	MFP	Rinsing (#rinse002)	NL-CLR-WBs QDR Purpose: removal of traces of chemical agents. Choose one of the two rinsing modes: QDR = Quick dump rinsing mode Cascade = Overflow rinsing mode for fragile substrates Rinse until message 'End of rinsing process' is shown on the touchscreen of the QDR, else repeat the rinsing	Skip. Already done for thermal oxidation.

Detailed Process Flow: from Pillars to Membrane - Appendix G

			process.	
19	MFP	Substrate drying (WB15) (#dry023)	NL-CLR-WB15 Single substrate drying: 1. Use the single-wafer spinner Settings: 2500 rpm, 60 sec (including 45 sec nitrogen purge). 2. Use the nitrogen gun (fragile wafers or small samples). Batch drying of substrates: Use the Semitool for drying up to 25 substrates at once.	Skip. Already done for thermal oxidation.
20	MFP	LPCVD of SiRN (250 MPa) (#film206)	NL-CLR-G4 Furnace Program: N2 Settings: <ul style="list-style-type: none"> • SiH₂Cl₂ flow: 150sccm • NH₃ flow: 50 sccm • Temperature: 830/850/870°C • Pressure: 200 mTorr Load your wafers within 4 hours after cleaning!	500nm at 8.3nm/min, 60min
21	ILP	Particle inspection (#metro201)	NL-CLR-Cold Light Source (SEM room) Shine the light onto the surface at an angle in a dark room to check for particles, haze and scratches in the coating(s) on the substrate. Please warn the administrator in case a thermal SiO ₂ or LPCVD coating contains a lot of particles! Contact Christaan Bruinink for questions.	
22	ILP	Layer thickness measurement (#metro401)	NL-CLR-Woollam M-2000UI ellipsometer Consult the user manual to perform a single point or a raster measurement. Use one of the available optical models to determine the layer thickness and optical constants of the coating on your substrate. Provide the following results in the digital logbook: thickness, refractive index (n) at 632.8nm and the nonuniformity of the layer (%range) of a 5-point scan.	
film1203: LPCVD of poly-Silicon (F2-590 °C)				
23	MFP	Cleaning in 99% HNO₃ (#clean001)	NL-CLR-WB14 BEAKER 1 Purpose: removal of organic traces. Chemical: 99% HNO ₃ • Time: 5 min	Skip. Already done for thermal oxidation.
24	MFP	Cleaning in 99% HNO₃ (#clean002)	NL-CLR-WB14 BEAKER 2 Purpose: removal of organic traces. Chemical: 99% HNO ₃ • Time: 5 min	Skip. Already done for thermal oxidation.

Appendix G - Detailed Process Flow: from Pillars to Membrane

25	MFP	Rinsing (#rinse002)	<p>NL-CLR-WBs QDR Purpose: removal of traces of chemical agents.</p> <p>Choose one of the two rinsing modes: QDR = Quick dump rinsing mode Cascade = Overflow rinsing mode for fragile substrates</p> <p>Rinse until message 'End of rinsing process' is shown on the touchscreen of the QDR, else repeat the rinsing process.</p>	Skip. Already done for thermal oxidation.
26	MFP	Cleaning in 69% HNO₃ (95 °C) (#clean003)	<p>NL-CR-WB14 BEAKER 3A/3B Purpose: removal of metallic traces.</p> <p>Chemical: 69% HNO₃ • Temperature: 95 °C • Time: 10 min</p>	Skip. Already done for thermal oxidation.
27	MFP	Rinsing (#rinse002)	<p>NL-CLR-WBs QDR Purpose: removal of traces of chemical agents.</p> <p>Choose one of the two rinsing modes: QDR = Quick dump rinsing mode Cascade = Overflow rinsing mode for fragile substrates</p> <p>Rinse until message 'End of rinsing process' is shown on the touchscreen of the QDR, else repeat the rinsing process.</p>	Skip. Already done for thermal oxidation.
28	MFP	Substrate drying (WB14) (#dry022)	<p>NL-CLR-WB14 Optional drying step. After the QDR, you can transfer your substrates directly to a Teflon carrier and strip the native SiO₂ in 1% HF (WB15).</p> <p>Single substrate drying: 1. Use the single-wafer spinner Settings: 2500 rpm, 60 sec (including 45 sec nitrogen purge). 2. Use the nitrogen gun (fragile wafers or small samples).</p> <p>Batch drying of substrates: Use the Semitool for drying up to 25 substrates at once.</p>	Skip. Already done for thermal oxidation.
29	MFP	Etching in 1% HF (#etch127)	<p>NL-CLR-WB15 Beaker 1 Purpose: remove native SiO₂ from Silicon.</p> <p>Chemical: 1% HF • Temperature: room temperature • Time: 1 min</p> <p>This step is obligatory for the MESA+ monitor wafer (if applicable, see Equipment database).</p>	Skip. Already done for thermal oxidation.
30	MFP	Rinsing (#rinse002)	<p>NL-CLR-WBs QDR Purpose: removal of traces of chemical agents.</p>	Skip. Already done for thermal oxidation.

Detailed Process Flow: from Pillars to Membrane - Appendix G

				oxidation.
			Choose one of the two rinsing modes: QDR = Quick dump rinsing mode Cascade = Overflow rinsing mode for fragile substrates	
			Rinse until message 'End of rinsing process' is shown on the touchscreen of the QDR, else repeat the rinsing process.	
31	MFP	Substrate drying (WB15) (#dry023)	NL-CLR-WB15 Single substrate drying: 1. Use the single-wafer spinner Settings: 2500 rpm, 60 sec (including 45 sec nitrogen purge). 2. Use the nitrogen gun (fragile wafers or small samples). Batch drying of substrates: Use the Semitool for drying up to 25 substrates at once.	Skip. Already done for thermal oxidation.
32	MFP	LPCVD of poly-Silicon (590 °C) (#film203)	NL-CLR-F2 Furnace Program: Senspoly Settings: • SiH ₄ flow: 50 sccm • N ₂ low: 250sccm • Temperature: 590°C • Pressure: 250mTorr Maximum thickness: 2.5 um. Load your wafers within 4 hours after cleaning!	50nm, recipe N5
33	ILP	Particle inspection (#metro201)	NL-CLR-Cold Light Source (SEM room) Shine the light onto the surface at an angle in a dark room to check for particles, haze and scratches in the coating(s) on the substrate. Please warn the administrator in case a thermal SiO ₂ or LPCVD coating contains a lot of particles! Contact Christaan Bruinink for questions.	
34	ILP	Layer thickness measurement (#metro401)	NL-CLR-Woollam M-2000UI ellipsometer Consult the user manual to perform a single point or a raster measurement. Use one of the available optical models to determine the layer thickness and optical constants of the coating on your substrate. Provide the following results in the digital logbook: thickness, refractive index (n) at 632.8nm and the nonuniformity of the layer (%range) of a 5-point scan.	
film1940: Wet Oxidation of Silicon (B2)				
35	MFP	Cleaning in 99% HNO₃ (#clean001)	NL-CLR-WB14 BEAKER 1 Purpose: removal of organic traces.	Skip. Already done for thermal oxidation.

Appendix G - Detailed Process Flow: from Pillars to Membrane

			Chemical: 99% HNO ₃ • Time: 5 min	
36	MFP	Cleaning in 99% HNO₃ (#clean002)	NL-CLR-WB14 BEAKER 2 Purpose: removal of organic traces. Chemical: 99% HNO ₃ • Time: 5 min	Skip. Already done for thermal oxidation.
37	MFP	Rinsing (#rinse002)	NL-CLR-WBs QDR Purpose: removal of traces of chemical agents. Choose one of the two rinsing modes: QDR = Quick dump rinsing mode Cascade = Overflow rinsing mode for fragile substrates Rinse until message 'End of rinsing process' is shown on the touchscreen of the QDR, else repeat the rinsing process.	Skip. Already done for thermal oxidation.
38	MFP	Cleaning in 69% HNO₃ (95 °C) (#clean003)	NL-CR-WB14 BEAKER 3A/3B Purpose: removal of metallic traces. Chemical: 69% HNO ₃ • Temperature: 95 °C • Time: 10 min	Skip. Already done for thermal oxidation.
39	MFP	Rinsing (#rinse002)	NL-CLR-WBs QDR Purpose: removal of traces of chemical agents. Choose one of the two rinsing modes: QDR = Quick dump rinsing mode Cascade = Overflow rinsing mode for fragile substrates Rinse until message 'End of rinsing process' is shown on the touchscreen of the QDR, else repeat the rinsing process.	Skip. Already done for thermal oxidation.
40	MFP	Substrate drying (WB14) (#dry022)	NL-CLR-WB14 Optional drying step. After the QDR, you can transfer your substrates directly to a Teflon carrier and strip the native SiO ₂ in 1% HF (WB15). Single substrate drying: 1. Use the single-wafer spinner Settings: 2500 rpm, 60 sec (including 45 sec nitrogen purge). 2. Use the nitrogen gun (fragile wafers or small samples). Batch drying of substrates: Use the Semitool for drying up to 25 substrates at once.	Skip. Already done for thermal oxidation.
41	MFP	Etching in 1% HF (#etch127)	NL-CLR-WB15 Beaker 1 Purpose: remove native SiO ₂ from Silicon. Chemical: 1% HF	Skip. Already done for thermal oxidation.

Detailed Process Flow: from Pillars to Membrane - Appendix G

			<ul style="list-style-type: none"> • Temperature: room temperature • Time: 1 min <p>This step is obligatory for the MESA+ monitor wafer (if applicable, see Equipment database).</p>	
42	MFP	Rinsing (#rinse002)	<p>NL-CLR-WBs QDR Purpose: removal of traces of chemical agents.</p> <p>Choose one of the two rinsing modes: QDR = Quick dump rinsing mode Cascade = Overflow rinsing mode for fragile substrates</p> <p>Rinse until message 'End of rinsing process' is shown on the touchscreen of the QDR, else repeat the rinsing process.</p>	Skip. Already done for thermal oxidation.
43	MFP	Substrate drying (WB15) (#dry023)	<p>NL-CLR-WB15</p> <p>Single substrate drying:</p> <ol style="list-style-type: none"> 1. Use the single-wafer spinner Settings: 2500 rpm, 60 sec (including 45 sec nitrogen purge). 2. Use the nitrogen gun (fragile wafers or small samples). <p>Batch drying of substrates: Use the Semitool for drying up to 25 substrates at once.</p>	Skip. Already done for thermal oxidation.
44	MFP	Wet Oxidation of Silicon (#film940)	<p>NL-CLR-B2 furnace Application: wet oxidation of Silicon. Programs: WET900, WET950, WET1000, WET1050, WET1150.</p> <p>Settings:</p> <ul style="list-style-type: none"> • Standby temperature: 800°C • Temperature range: 900-1150°C • Gas: wet N₂ (bubbler) • Flow: 1slm • Ramp: 10°C/min <p>Please mention the following settings in the User Comments:</p> <ul style="list-style-type: none"> • Target thickness: nm • Temperature:°C • Time:min 	<p>Target thickness: 7-8nm</p> <p>Temperature: 800°C</p> <p>Time: 15min</p>
45	ILP	Layer thickness measurement (#metro401)	<p>NL-CLR-Woollam M-2000UI ellipsometer</p> <p>Consult the user manual to perform a single point or a raster measurement. Use one of the available optical models to determine the layer thickness and optical constants of the coating on your substrate. Provide the following results in the digital logbook: thickness, refractive index (n) at 632.8nm and the nonuniformity of the layer (%range) of a 5-point scan.</p>	

Appendix G - Detailed Process Flow: from Pillars to Membrane

ILP)				
46	ILP	Priming HMDS (#litho600)	OPTION 1 Liquid HMDS priming NL-CLR-WB21/22 Hotplate Purpose: dehydration bake Settings: <ul style="list-style-type: none"> • Temperature: 120°C • Time: 5min After the dehydration bake, perform the liquid priming with minimum delay! NL-CLR-WB21 Primus SB15 Spinner Primer: HexaMethylDiSilazane (HMDS) Settings: <ul style="list-style-type: none"> • Spin mode: static • Spin speed: 4000rpm • Spin time: 30s OPTION 2 Vapor HMDS priming NL-CLR-WB28 Lab-line Duo-Vac Oven Primer: HexaMethylDiSilazane (HMDS) Settings: <ul style="list-style-type: none"> • Temperature: 150°C • Pressure: 25inHg • Dehydration bake: 2min • HMDS priming: 5min CAUTION: let the substrates cool down before handling with your tweezer!	
47	ILP	Coating of Olin OiR 908-35 (#litho102)	NL-CLR- WB21 Coating: Primus coater <ul style="list-style-type: none"> • Olin OiR 908-35 • Spin program: 4000 (4000rpm, 30sec) 	Bottom side, 3.5µm resist
48	ILP	Prebake of Olin OiR 908-35 (#litho004)	NL-CLR-WB21 Prebake: Hotplate <ul style="list-style-type: none"> • Temperature: 95°C • Time: 120s 	
49	ILP	Alignment & exposure of Olin OiR 908-35 (#litho302)	NL-CLR- EV620 <ul style="list-style-type: none"> • Electronic Vision Group EV620 Mask Aligner • Hg lamp: 12 mW/cm² • Exposure time: 9sec 	
50	ILP	After exposure bake of Olin OiR resists (#litho005)	NL-CLR-WB21 After exposure bake: Hotplate <ul style="list-style-type: none"> • Temperature: 120°C • Time: 60s 	
51	ILP	Development of Olin OiR resists (#litho200)	NL-CLR-WB21 Development: OPD4262 <ul style="list-style-type: none"> • Beaker 1: 30sec • Beaker 2: 15-30sec 	

Detailed Process Flow: from Pillars to Membrane - Appendix G

52	ILP	Quick Dump Rinse (QDR) (#rinse001)	NL-CLR-Wetbenches Purpose: removal of traces of chemical agents. Recipe 1 Quick dump rinsing (QDR) Recipe 2 Cascade rinsing for fragile wafers Rinse until message 'End of rinsing process' is shown on the touchscreen of the QDR, else repeat the rinsing process.
53	ILP	Substrate drying (#dry001)	NL-CLR-WBs (ILP) Single substrate drying: 1. Use the single-wafer spinner Settings: 2500 rpm, 60 sec (including 45 sec nitrogen purge) 2. Use the nitrogen gun (fragile wafers or small samples)
54	ILP	Postbake of Olin OiR resists (#litho008)	NL-CLR-WB21 Postbake: Hotplate • Temperature: 120°C • Time: 10min
55	ILP	Inspection by Optical Microscopy (#metro101)	NL-CLR-Nikon Microscope Use the Nikon microscope for inspection.

litho1801: Lithography of Olin OiR 907-17 (positive resist - ILP)

56	ILP	Priming HMDS (#litho600)	OPTION 1 Liquid HMDS priming NL-CLR-WB21/22 Hotplate Purpose: dehydration bake Settings: • Temperature: 120°C • Time: 5min After the dehydration bake, perform the liquid priming with minimum delay! NL-CLR-WB21 Primus SB15 Spinner Primer: HexaMethylDiSilazane (HMDS) Settings: • Spin mode: static • Spin speed: 4000rpm • Spin time: 30s OPTION 2 Vapor HMDS priming NL-CLR-WB28 Lab-line Duo-Vac Oven Primer: HexaMethylDiSilazane (HMDS) Settings: • Temperature: 150°C • Pressure: 25inHg • Dehydration bake: 2min
----	-----	------------------------------------	---

Appendix G - Detailed Process Flow: from Pillars to Membrane

			<ul style="list-style-type: none"> • HMDS priming: 5min 	
			CAUTION: let the substrates cool down before handling with your tweezer!	
57	ILP	Coating of Olin OiR 907-17 (#litho101)	NL-CLR-WB21 Coating: Primus spinner <ul style="list-style-type: none"> • Olin OiR 907-17 • Spin program: 4000 (4000rpm, 30sec) 	Top side, 1.7µm resist
58	ILP	Prebake of Olin OiR 907-17 (#litho003)	NL-CLR-WB21 Prebake: Hotplate <ul style="list-style-type: none"> • Temperature: 95°C • Time: 90s 	
59	ILP	Alignment & exposure of Olin OiR 907-17 (#litho301)	NL-CLR- EV620 Electronic Vision Group EV620 Mask Aligner <ul style="list-style-type: none"> • Hg-lamp: 12 mW/cm² • Exposure time: 4sec 	
60	ILP	After exposure bake of Olin OiR resists (#litho005)	NL-CLR-WB21 After exposure bake: Hotplate <ul style="list-style-type: none"> • Temperature: 120°C • Time: 60s 	
61	ILP	Development of Olin OiR resists (#litho200)	NL-CLR-WB21 Development: OPD4262 <ul style="list-style-type: none"> • Beaker 1: 30sec • Beaker 2: 15-30sec 	
62	ILP	Quick Dump Rinse (QDR) (#rinse001)	NL-CLR-Wetbenches Purpose: removal of traces of chemical agents. Recipe 1 Quick dump rinsing (QDR) Recipe 2 Cascade rinsing for fragile wafers Rinse until message 'End of rinsing process' is shown on the touchscreen of the QDR, else repeat the rinsing process.	
63	ILP	Substrate drying (#dry001)	NL-CLR-WBs (ILP) Single substrate drying: 1. Use the single-wafer spinner Settings: 2500 rpm, 60 sec (including 45 sec nitrogen purge) 2. Use the nitrogen gun (fragile wafers or small samples)	
64	ILP	Postbake of Olin OiR resists (#litho008)	NL-CLR-WB21 Postbake: Hotplate <ul style="list-style-type: none"> • Temperature: 120°C • Time: 10min 	
65	ILP	Inspection by Optical Microscopy (#metro101)	NL-CLR-Nikon Microscope Use the Nikon microscope for inspection.	
surf1100: Surface Modification by UV Ozone (PRS100-ILP)				
66	ILP	Surface Modification by UV	NL-CLR-UV PRS 100 reactor Purpose: modify the surface to increase the wetting of	Bottom side, 5min. To

Detailed Process Flow: from Pillars to Membrane - Appendix G

		Ozone (#surf100)	resist for wet-chemical etching or activate the surface for monolayer formation. • Time = 300 s	enhance wetting.
surf1100: Surface Modification by UV Ozone (PRS100-ILP)				
67	ILP	Surface Modification by UV Ozone (#surf100)	NL-CLR-UV PRS 100 reactor Purpose: modify the surface to increase the wetting of resist for wet-chemical etching or activate the surface for monolayer formation. • Time = 300 s	Top side, 5min. To enhance wetting.
etch1207: Etching in BHF (WB06 - ILP)				
68	ILP	Etching in BHF (#etch117)	NL-CLR-WB06 Use dedicated beaker BHF (1:7) Temp.: Room temperature Etch rates: Thermal SiO ₂ :60-80 nm/min PECVD SiO ₂ :125 nm/min	20s to etch SiO ₂
69	ILP	Quick Dump Rinse (QDR) (#rinse001)	NL-CLR-Wetbenches Purpose: removal of traces of chemical agents. Recipe 1 Quick dump rinsing (QDR) Recipe 2 Cascade rinsing for fragile wafers Rinse until message 'End of rinsing process' is shown on the touchscreen of the QDR, else repeat the rinsing process.	
70	ILP	Substrate drying (#dry001)	NL-CLR-WBs (ILP) Single substrate drying: 1. Use the single-wafer spinner Settings: 2500 rpm, 60 sec (including 45 sec nitrogen purge) 2. Use the nitrogen gun (fragile wafers or small samples)	Skip if directly proceeding to next step.
strip1000: Stripping of resists in 99% HNO₃ (WB06 - ILP)				
71	ILP	Stripping polymers and resists (#strip001)	NL-CLR-WB06 Purpose: stripping of polymers and resists. • Beaker 0: 99% HNO ₃ • Time: continue until complete removal of resist	1min
72	ILP	Quick Dump Rinse (QDR) (#rinse001)	NL-CLR-Wetbenches Purpose: removal of traces of chemical agents. Recipe 1 Quick dump rinsing (QDR) Recipe 2 Cascade rinsing for fragile wafers Rinse until message 'End of rinsing process' is shown on the touchscreen of the QDR, else repeat the rinsing process.	
73	MFP	Substrate drying (WB06-WB08)	NL-CLR-WB06/07/08	Skip if directly proceeding to

Appendix G - Detailed Process Flow: from Pillars to Membrane

		(#dry020)	<p>Single substrate drying:</p> <ol style="list-style-type: none"> 1. Use the single-wafer spinner Settings: 2500 rpm, 60 sec (including 45 sec nitrogen purge) 2. Use the nitrogen gun (fragile wafers or small samples) <p>Batch drying of substrates: The Semitool uses the following standard procedure:</p> <ul style="list-style-type: none"> • Rinse: 30 sec (600 rpm) • Q-rinse: 10.0 MΩ (600 rpm) • Purge: 10 sec (600 rpm) • Drying: 280 sec (1600 rpm) <p><u>Note:</u> it is obligatory to apply a single rinsing step in the QDR before using the Semitool!</p>	next step.
etch1005: TMAH etch - standard (WB07)				
74	ILP	Etching in 1% HF (#etch210)	<p>NL-CLR-WB06 Strip native SiO₂ in 1% HF.</p> <p>Beaker: 1% HF</p> <ul style="list-style-type: none"> • Time: 1 min <p>Strip until hydrofobic surface.</p>	14s instead of 1min! To remove oxide due to the HNO ₃ .
75	ILP	Quick Dump Rinse (QDR) (#rinse001)	<p>NL-CLR-Wetbenches Purpose: removal of traces of chemical agents.</p> <p>Recipe 1 Quick dump rinsing (QDR) Recipe 2 Cascade rinsing for fragile wafers Rinse until message 'End of rinsing process' is shown on the touchscreen of the QDR, else repeat the rinsing process.</p>	
76	MFP	Etching in TMAH (25 wt%) (#etch147)	<p>NL-CLR-WB07 Standard double-wall vessel Chemical: 25wt.% TMAH</p> <p>Settings:</p> <ul style="list-style-type: none"> • Temperature: 70°C • Use stirrer <p>Etch rate is 300 nm/min for <100> Silicon and 25 nm/min for <111> Silicon.</p>	30s to etch poly-Si.
77	MFP	Quick Dump Rinse (QDR) (#rinse002)	<p>NL-CLR-Wetbenches Purpose: removal of traces of chemical agents.</p> <p>Recipe 1 Quick dump rinsing (QDR) Recipe 2 Cascade rinsing for fragile wafers Rinse until message 'End of rinsing process' is shown on the touchscreen of the QDR, else repeat the rinsing process.</p>	
78	MFP	Substrate drying (#dry002)	<p>NL-CLR-WBs (MFP)</p> <p>Single substrate drying:</p> <ol style="list-style-type: none"> 1. Use the single-wafer spinner Settings: 2500 rpm, 60 sec (including 45 sec 	Skip if directly proceeding to next step.

nitrogen purge)
 2. Use the nitrogen gun (fragile wafers or small samples)

etch1215: H3PO4 etch (WB08-standard)

79

MFP

**Etching in
H₃PO₄ Standard
(#etch153)**

NL-CLR-WB08

Use dedicated beaker with reflux lid for etching

Table 1 : Etchrates values old Cleanroom
(without reflux and without lid!)

Temperature [°C]	Er SiRN- G3 [nm/min]	Er SiO ₂ A2 [nm/min]
180	4.1	0.48
160	1.4	0.16
140	0.5	0.05

Etching of SiN at 180°C until 50nm is left. Use dummy and after 25 min, remove dummy (possibly with the rest) to determine the etch rate.

Table 2: Etchrate values fresh prepared H3PO4 in new CR
by Yiping (with lid and without lid cooling)

Temperature [°C]	Er SiRN- G3 [nm/min]	Er SiO ₂ [nm/min]
180	6.1-6.6	0.6
160	2.35	0.18
140		

Table 3: Etchrate values after 50 days in new Cleanroom
by Erwin (with lid and without lid cooling)

Temperature [°C]	Er SiRN- G3 [nm/min]	Er SiO ₂ 800°C [nm/min]
180	4.5	0.47
160		

Table 4: Si₃N₄ LPCVD-H₂ by Christiaan,
Etchrate values after 50 days in new Cleanroom

Temperature [°C]	Er Si ₃ N ₄ - H ₂ [nm/min]	
180	4,7	
160	1,8	

Appendix G - Detailed Process Flow: from Pillars to Membrane

80	MFP	Quick Dump Rinse (QDR) (#rinse002)	NL-CLR-Wetbenches Purpose: removal of traces of chemical agents. Recipe 1 Quick dump rinsing (QDR) Recipe 2 Cascade rinsing for fragile wafers Rinse until message 'End of rinsing process' is shown on the touchscreen of the QDR, else repeat the rinsing process.
81	MFP	Substrate drying (#dry002)	NL-CLR-WBs (MFP) Single substrate drying: 1. Use the single-wafer spinner Settings: 2500 rpm, 60 sec (including 45 sec nitrogen purge) 2. Use the nitrogen gun (fragile wafers or small samples)

litho1804: Spincoating of Olin OiR 907-17 (positive resist - ILP)

82	ILP	Priming HMDS (#litho600)	OPTION 1 Liquid HMDS priming NL-CLR-WB21/22 Hotplate Purpose: dehydration bake Settings: • Temperature: 120°C • Time: 5min After the dehydration bake, perform the liquid priming with minimum delay! NL-CLR-WB21 Primus SB15 Spinner Primer: HexaMethylDiSilazane (HMDS) Settings: • Spin mode: static • Spin speed: 4000rpm • Spin time: 30s OPTION 2 Vapor HMDS priming NL-CLR-WB28 Lab-line Duo-Vac Oven Primer: HexaMethylDiSilazane (HMDS) Settings: • Temperature: 150°C • Pressure: 25inHg • Dehydration bake: 2min • HMDS priming: 5min CAUTION: let the substrates cool down before handling with your tweezer!
83	ILP	Coating of Olin OiR 907-17 (#litho101)	NL-CLR-WB21 Coating: Primus spinner • Olin OiR 907-17 • Spin program: 4000 (4000rpm, 30sec)

Detailed Process Flow: from Pillars to Membrane - Appendix G

84	ILP	Prebake of Olin OiR 907-17 (#litho003)	NL-CLR-WB21 Prebake: Hotplate • Temperature: 95°C • Time: 90s	5min
85	ILP	Postbake of Olin OiR resists (#litho008)	NL-CLR-WB21 Postbake: Hotplate • Temperature: 120°C • Time: 10min	Skip
86	ILP	Inspection by Optical Microscopy (#metro101)	NL-CLR-Nikon Microscope Use the Nikon microscope for inspection.	

etch1731: Etching of thin nitrides, oxides and shallow Si by CHF3/O2 Plasma (TEtske)

87	ILP	Chamber clean (TEtske) (#etch198)	NL-CLR-TEtske Application: removal of organic and fluorocarbon residues on the chamber wall. Select the correct etch chamber and electrode for your etch process (see next step). • Electrode temperature: 10°C • Pressure: 50mTorr • O2 flow: 50sccm • Power: 100Watt • Time: 10 min • DC bias: -600Volt • Load: 65 • Tune: 35 The etch chamber is clean at the moment the plasma color is white.	
88	ILP	RIE with CHF3/O2 Plasma (#etch193)	NL-CLR-TEtske Application: plasma etching of thin layers of various oxides and nitrides, shallow etching (nm) in Silicon and pre-conditioning for XeF2 etching. Use Kapton tape or Kapton foil to protect the edge of the wafer and therefore avoid damage during processing in KOH or TMAH. Select the dirty chamber and the styros electrode. • Electrode temperature: 10°C • Pressure: 10mTorr • CHF3 flow: 25sccm • O2 flow: 5sccm • Power: 60Watt • DC bias: -500 up to - 540Volt Etch rate SiRN (G3-SiRN): 60 nm/min Etch rate SiO2: 30 nm/min Etch rate Si: 15-25 nm/min Etch rate Olin OiR resists: 50 nm/min	P=25W, O2=5sccm, CHF3 = 25sccm. Test on dummy for 1min to determine the etch rate. Over-etch the SiN very lightly to be sure all SiN is gone and you are in the SiO2 layer. Overetching into the Si is not a problem. The remaining SiN layer is thick enough and is coated with a poly-Si layer

89

ILP

Stripping of Resists
(#strip100)

NL-CLR-TePla300

Application: stripping of resists by O2 plasma after plasma etching.

which etches slower.

Use Recipe 02.
30 minutes of resist removal.

PLEASE NOTE

1. RESTRICTION: do not strip resists on chromium in the TePla300, but instead use the TePla360 (choose: recipe 041).

2. BACKUP: TePla300 down? Contact the administrator if you can continue your processing in the TePla360.

Step	O2 (sccm)	N2 (sccm)	P (mbar)	Power (W)	Time (h:mm:ss)
Preheating	0	500	1.0	800	0:10:00
Stripping of resist	500	0	1.0	800	*

* Select one of the following recipes to strip the resist, depending on the thickness of the resist, treatment of the resist and the number of wafers. Use the abort option in the last step if you sample requires a shorter stripping time.

Recipe 01: time = 10 min

Recipe 02: time = 30 min

Recipe 04: time = 60 min

90

Rem
Res

Removal of metal traces in RCA-2
(#residue504)

NL-CLR-WB09

Purpose: removal of metal traces originating from plasma tools in order to protect the cleaning efficiency of the wet benches. For this reason, RCA-2 is compulsory in case you continue:

- cleaning in the Pre-Furnace Clean (WB14-MFP)
- processing in the Ultra-Clean Line - Front End (WB12-UCP)
- processing in the Ultra-Clean Line - Back End (WB13-UCP)

Chemicals: HCl:H2O2:H2O (1:1:5 vol.%)

PLEASE NOTE

1. CAUTION: do not process substrates with metal patterns in RCA-2.

2. NO REUSE: reuse of RCA-2 is forbidden! Contact the administrator in case there is no empty RCA-2 beaker available in WB09.

Procedure:

- Pour 1500ml* of DI water into the beaker
- Turn on the stirrer
- Add 300ml* of Hydrogen Chloride (HCl)
- Heat up the solution to 70°C (setpoint heater = 80°C)
- Slowly add 300ml* of Hydrogen Peroxide (H2O2)
- Submerge your samples as soon as the

Detailed Process Flow: from Pillars to Membrane - Appendix G

			<p>temperature is above 70°C</p> <ul style="list-style-type: none"> • Time = 15min <p>* Use a glass graduated cylinder of 500ml to measure the volume of the chemicals.</p>	
91	ILP	Quick Dump Rinse (QDR) (#rinse001)	<p>NL-CLR-Wetbenches Purpose: removal of traces of chemical agents.</p> <p>Recipe 1 Quick dump rinsing (QDR) Recipe 2 Cascade rinsing for fragile wafers Rinse until message 'End of rinsing process' is shown on the touchscreen of the QDR, else repeat the rinsing process.</p>	
92	ILP	Substrate drying (#dry001)	<p>NL-CLR-WBs (ILP)</p> <p>Single substrate drying:</p> <ol style="list-style-type: none"> 1. Use the single-wafer spinner Settings: 2500 rpm, 60 sec (including 45 sec nitrogen purge) 2. Use the nitrogen gun (fragile wafers or small samples) 	
surf1100: Surface Modification by UV Ozone (PRS100-ILP)				
93	ILP	Surface Modification by UV Ozone (#surf100)	<p>NL-CLR-UV PRS 100 reactor Purpose: modify the surface to increase the wetting of resist for wet-chemical etching or activate the surface for monolayer formation.</p> <ul style="list-style-type: none"> • Time = 300 s 	Bottom side, 5min. To enhance wetting.
etch1207: Etching in BHF (WB06 - ILP)				
94	ILP	Etching in BHF (#etch117)	<p>NL-CLR-WB06 Use dedicated beaker BHF (1:7) Temp.: Room temperature</p> <p>Etch rates: Thermal SiO₂: 60-80 nm/min PECVD SiO₂: 125 nm/min</p>	20s to etch SiO ₂ .
95	ILP	Quick Dump Rinse (QDR) (#rinse001)	<p>NL-CLR-Wetbenches Purpose: removal of traces of chemical agents.</p> <p>Recipe 1 Quick dump rinsing (QDR) Recipe 2 Cascade rinsing for fragile wafers Rinse until message 'End of rinsing process' is shown on the touchscreen of the QDR, else repeat the rinsing process.</p>	
96	ILP	Substrate drying (#dry001)	<p>NL-CLR-WBs (ILP)</p> <p>Single substrate drying:</p> <ol style="list-style-type: none"> 1. Use the single-wafer spinner Settings: 2500 rpm, 60 sec (including 45 sec nitrogen purge) 2. Use the nitrogen gun (fragile wafers or small samples) 	Skip if directly proceeding to next step.

Appendix G - Detailed Process Flow: from Pillars to Membrane

etch1001: KOH etch - standard (WB17) with RCA-2 post cleaning (WB09)				
97	ILP	Etching in 1% HF (#etch192)	NL-CLR-WB16 Beaker: 1% HF <ul style="list-style-type: none"> • Temperature: 20 °C. • Time: depends on application 	Skip if previous HF step has just been taken.
98	ILP	Quick Dump Rinse (QDR) (#rinse001)	NL-CLR-Wetbenches Purpose: removal of traces of chemical agents. Recipe 1 Quick dump rinsing (QDR) Recipe 2 Cascade rinsing for fragile wafers Rinse until message 'End of rinsing process' is shown on the touchscreen of the QDR, else repeat the rinsing process.	
99	ILP	Silicon etching in KOH (#etch138)	NL-CLR-WB17 Beaker KOH-1 or KOH-2 Chemical: 25wt.% KOH Application: anisotropic etching of crystalline silicon. Settings: <ul style="list-style-type: none"> • Temperature: 75°C • Use stirrer Etch rates: Si <100> = 1µm/min Si <111> = 12.5nm/min SiO ₂ (thermal) = 180nm/hr SiRN < 0.6nm/hr	Use microscope after at least about 10 min to determine the etch rate. After some hours, test again for a more accurate etch rate. Etch Si to a remaining layer of 80µm.
100	ILP	Quick Dump Rinse (QDR) (#rinse001)	NL-CLR-Wetbenches Purpose: removal of traces of chemical agents. Recipe 1 Quick dump rinsing (QDR) Recipe 2 Cascade rinsing for fragile wafers Rinse until message 'End of rinsing process' is shown on the touchscreen of the QDR, else repeat the rinsing process.	
101	ILP	Substrate transport in demi-water (#trans003)	NL-CLR-WB17→WB09 Purpose: transport of wafers for cleaning in RCA-2 after etching in KOH (WB17). Wet transport of substrates in a beaker with demi-water. After transport, return the quartz wafer carrier back to WB17.	
102	Rem Res	Removal of residues in RCA-2 (#residue501)	NL-CLR-WB09 Purpose: removal of residues after wet-chemical processing (e.g. KOH and metal stripping) in order to protect the cleaning efficiency of the wet benches. For this reason, RCA-2 is compulsory in case you continue: <ul style="list-style-type: none"> • cleaning in the Pre-Furnace Clean (WB14-MFP) 	

Detailed Process Flow: from Pillars to Membrane - Appendix G

			<ul style="list-style-type: none"> • processing in the Ultra-Clean Line - Front End (WB12-UCP) • processing in the Ultra-Clean Line - Back End (WB13-UCP) . <p>Chemicals: HCl:H₂O₂:H₂O (1:1:5 vol%)</p> <p>PLEASE NOTE</p> <p>1. CAUTION: do not process substrates with metal patterns in RCA-2.</p> <p>2. NO REUSE: reuse of RCA-2 is forbidden! Contact the administrator in case there is no empty RCA-2 beaker available in WB09.</p> <p>Procedure:</p> <ul style="list-style-type: none"> • Pour 1500ml* of DI water into the beaker • Turn on the stirrer • Add 300ml* of Hydrogen Chloride (HCl) • Heat up the solution to 70°C (setpoint heater = 80°C) • Slowly add 300ml* of Hydrogen Peroxide (H₂O₂) • Submerge your samples as soon as the temperature is above 70°C • Time = 15min <p>* Use a glass graduated cylinder of 500ml to measure the volume of the chemicals.</p>	
103	ILP	Quick Dump Rinse (QDR) (#rinse001)	<p>NL-CLR-Wetbenches</p> <p>Purpose: removal of traces of chemical agents.</p> <p>Recipe 1 Quick dump rinsing (QDR)</p> <p>Recipe 2 Cascade rinsing for fragile wafers</p> <p>Rinse until message 'End of rinsing process' is shown on the touchscreen of the QDR, else repeat the rinsing process.</p>	
104	ILP	Substrate drying (#dry001)	<p>NL-CLR-WBs (ILP)</p> <p>Single substrate drying:</p> <ol style="list-style-type: none"> 1. Use the single-wafer spinner Settings: 2500 rpm, 60 sec (including 45 sec nitrogen purge) 2. Use the nitrogen gun (fragile wafers or small samples) 	Skip if directly proceeding to next step.
etch1005: TMAH etch - standard (WB07)				
105	ILP	Etching in 1% HF (#etch210)	<p>NL-CLR-WB06</p> <p>Strip native SiO₂ in 1% HF.</p> <p>Beaker: 1% HF</p> <ul style="list-style-type: none"> • Time: 1 min <p>Strip until hydrofobic surface.</p>	Skip if previous step has just been taken.
106	ILP	Quick Dump Rinse (QDR) (#rinse001)	<p>NL-CLR-Wetbenches</p> <p>Purpose: removal of traces of chemical agents.</p>	

Appendix G - Detailed Process Flow: from Pillars to Membrane

			<p>Recipe 1 Quick dump rinsing (QDR) Recipe 2 Cascade rinsing for fragile wafers Rinse until message 'End of rinsing process' is shown on the touchscreen of the QDR, else repeat the rinsing process.</p>	
107	MFP	Etching in TMAH (25 wt%) (#etch147)	<p>NL-CLR-WB07 Standard double-wall vessel Chemical: 25wt.% TMAH</p> <p>Settings: • Temperature: 70°C • Use stirrer</p> <p>Etch rate is 300 nm/min for <100> Silicon and 25 nm/min for <111> Silicon.</p>	Etch Si as a batch back to 5µm. Then one by one with 10 min of overetching or at least enough to etch 80% of the pore if it would still be willed with Si.
108	MFP	Quick Dump Rinse (QDR) (#rinse002)	<p>NL-CLR-Wetbenches Purpose: removal of traces of chemical agents.</p> <p>Recipe 1 Quick dump rinsing (QDR) Recipe 2 Cascade rinsing for fragile wafers Rinse until message 'End of rinsing process' is shown on the touchscreen of the QDR, else repeat the rinsing process.</p>	
109	MFP	Substrate drying (#dry002)	<p>NL-CLR-WBs (MFP)</p> <p>Single substrate drying: 1. Use the single-wafer spinner Settings: 2500 rpm, 60 sec (including 45 sec nitrogen purge) 2. Use the nitrogen gun (fragile wafers or small samples)</p>	
film1203: LPCVD of poly-Silicon (F2-590 °C)				
110	MFP	Cleaning in 99% HNO₃ (#clean001)	<p>NL-CLR-WB14 Purpose: removal of organic traces.</p> <p>• Beaker 1: 99% HNO₃ • Time = 5 min</p>	
111	MFP	Cleaning in 99% HNO₃ (#clean002)	<p>NL-CLR-WB14 Purpose: removal of organic traces.</p> <p>• Beaker 2: 99% HNO₃ • Time = 5 min</p>	
112	MFP	Quick Dump Rinse (QDR) (#rinse002)	<p>NL-CLR-Wetbenches Purpose: removal of traces of chemical agents.</p> <p>Recipe 1 Quick dump rinsing (QDR) Recipe 2 Cascade rinsing for fragile wafers Rinse until message 'End of rinsing process' is shown on the touchscreen of the QDR, else repeat the rinsing process.</p>	
113	MFP	Cleaning in 69%	NL-CR-WB14	

Detailed Process Flow: from Pillars to Membrane - Appendix G

		HNO₃ (95 °C) (#clean003)	Purpose: removal of metallic traces. <ul style="list-style-type: none"> • Beaker 3A or 3B: 69% HNO₃ • Temperature= 95 °C • Time = 10 min 	
114	MFP	Quick Dump Rinse (QDR) (#rinse002)	NL-CLR-Wetbenches Purpose: removal of traces of chemical agents. Recipe 1 Quick dump rinsing (QDR) Recipe 2 Cascade rinsing for fragile wafers Rinse until message 'End of rinsing process' is shown on the touchscreen of the QDR, else repeat the rinsing process.	
115	MFP	Substrate drying (WB14) (#dry022)	NL-CLR-WB14 Optional drying step. After the QDR, you can transfer your substrates directly to a Teflon carrier and strip the native SiO ₂ in 1% HF (WB15). Single substrate drying: <ol style="list-style-type: none"> 1. Use the single-wafer spinner Settings: 2500 rpm, 60 sec (including 45 sec nitrogen purge) 2. Use the nitrogen gun (fragile wafers or small samples) Batch drying of substrates: The Semitool uses the following standard procedure: <ul style="list-style-type: none"> • Rinse: 30 sec (600 rpm) • Q-rinse: 10.0 MΩ (600 rpm) • Purge: 10 sec (600 rpm) • Drying: 280 sec (1600 rpm) <u>Note:</u> it is obligatory to apply a single rinsing step in the QDR before using the Semitool!	Skip if directly proceeding to next step.
116	MFP	Etching in 1% HF (#etch127)	NL-CLR-WB15 Purpose: remove native SiO ₂ from silicon. Beaker: 1% HF Temperature: room temperature Time = 1 min This step is obligatory for the MESA+ monitor wafer (if applicable, see Equipment database).	Not for the structures! Only for the monitor wafer.
117	MFP	Quick Dump Rinse (QDR) (#rinse002)	NL-CLR-Wetbenches Purpose: removal of traces of chemical agents. Recipe 1 Quick dump rinsing (QDR) Recipe 2 Cascade rinsing for fragile wafers Rinse until message 'End of rinsing process' is shown on the touchscreen of the QDR, else repeat the rinsing process.	
118	MFP	Substrate drying (WB15) (#dry023)	NL-CLR-WB15 Single substrate drying:	

Appendix G - Detailed Process Flow: from Pillars to Membrane

			<p>1. Use the single-wafer spinner Settings: 2500 rpm, 60 sec (including 45 sec nitrogen purge)</p> <p>2. Use the nitrogen gun (fragile wafers or small samples)</p> <p>Batch drying of substrates: The Semitool uses the following standard procedure:</p> <ul style="list-style-type: none"> • Rinse: 30 sec (600 rpm) • Q-rinse: 10.0 MΩ (600 rpm) • Purge: 10 sec (600 rpm) • Drying: 280 sec (1600 rpm) <p><u>Note:</u> it is obligatory to apply a single rinsing step in the QDR before using the Semitool!</p>	
119	MFP	LPCVD of poly-Silicon (590 °C) (#film203)	<p>NL-CLR-F2 Furnace Program: Sensopoly</p> <p>Settings:</p> <ul style="list-style-type: none"> • SiH₄ flow: 50 sccm • N₂ low: 250sccm • Temperature: 590°C • Pressure: 250mTorr <p>Maximum thickness: 2.5 um. Load your wafers within 4 hours after cleaning!</p>	Deposit 100nm of poly-Si.
120	ILP	Particle inspection (#metro201)	<p>NL-CLR-Cold Light Source (SEM room)</p> <p>Shine the light onto the surface at an angle in a dark room to check for particles, haze and scratches in the coating(s) on the substrate. Please warn the administrator in case a thermal SiO₂ or LPCVD coating contains a lot of particles!</p> <p>Contact Christaan Bruinink for questions.</p>	
121	ILP	Layer thickness measurement (#metro401)	<p>NL-CLR-Woollam M-2000UI ellipsometer</p> <p>Consult the user manual to perform a single point or a raster measurement. Use one of the available optical models to determine the layer thickness and optical constants of the coating on your substrate. Provide the following results in the digital logbook: thickness, refractive index (n) at 632.8nm and the nonuniformity of the layer (%range) of a 5-point scan.</p>	
film1920: Dry Oxidation of Silicon (H1)				
122	MFP	Cleaning in 99% HNO₃ (#clean001)	<p>NL-CLR-WB14 Purpose: removal of organic traces.</p> <ul style="list-style-type: none"> • Beaker 1: 99% HNO₃ • Time = 5 min 	Skip. Already done for poly-Si LPCVD.
123	MFP	Cleaning in 99% HNO₃ (#clean002)	<p>NL-CLR-WB14 Purpose: removal of organic traces.</p> <ul style="list-style-type: none"> • Beaker 2: 99% HNO₃ 	Skip. Already done for poly-Si LPCVD.

Detailed Process Flow: from Pillars to Membrane - Appendix G

			<ul style="list-style-type: none"> • Time = 5 min 	
124	MFP	Quick Dump Rinse (QDR) (#rinse002)	NL-CLR-Wetbenches Purpose: removal of traces of chemical agents. Recipe 1 Quick dump rinsing (QDR) Recipe 2 Cascade rinsing for fragile wafers Rinse until message 'End of rinsing process' is shown on the touchscreen of the QDR, else repeat the rinsing process.	Skip. Already done for poly-Si LPCVD.
125	MFP	Cleaning in 69% HNO₃ (95 °C) (#clean003)	NL-CR-WB14 Purpose: removal of metallic traces. <ul style="list-style-type: none"> • Beaker 3A or 3B: 69% HNO₃ • Temperature= 95 °C • Time = 10 min 	Skip. Already done for poly-Si LPCVD.
126	MFP	Quick Dump Rinse (QDR) (#rinse002)	NL-CLR-Wetbenches Purpose: removal of traces of chemical agents. Recipe 1 Quick dump rinsing (QDR) Recipe 2 Cascade rinsing for fragile wafers Rinse until message 'End of rinsing process' is shown on the touchscreen of the QDR, else repeat the rinsing process.	Skip. Already done for poly-Si LPCVD.
127	MFP	Substrate drying (WB14) (#dry022)	NL-CLR-WB14 Optional drying step. After the QDR, you can transfer your substrates directly to a Teflon carrier and strip the native SiO ₂ in 1% HF (WB15). Single substrate drying: 1. Use the single-wafer spinner Settings: 2500 rpm, 60 sec (including 45 sec nitrogen purge) 2. Use the nitrogen gun (fragile wafers or small samples) Batch drying of substrates: The Semitool uses the following standard procedure: <ul style="list-style-type: none"> • Rinse: 30 sec (600 rpm) • Q-rinse: 10.0 MΩ (600 rpm) • Purge: 10 sec (600 rpm) • Drying: 280 sec (1600 rpm) <u>Note:</u> it is obligatory to apply a single rinsing step in the QDR before using the Semitool!	Skip. Already done for poly-Si LPCVD.
128	MFP	Etching in 1% HF (#etch127)	NL-CLR-WB15 Purpose: remove native SiO ₂ from silicon. Beaker: 1% HF Temperature: room temperature Time = 1 min This step is obligatory for the MESA+ monitor wafer (if applicable, see Equipment database).	Skip. Already done for poly-Si LPCVD.

Appendix G - Detailed Process Flow: from Pillars to Membrane

129	MFP	Quick Dump Rinse (QDR) (#rinse002)	NL-CLR-Wetbenches Purpose: removal of traces of chemical agents. Recipe 1 Quick dump rinsing (QDR) Recipe 2 Cascade rinsing for fragile wafers Rinse until message 'End of rinsing process' is shown on the touchscreen of the QDR, else repeat the rinsing process.	Skip. Already done for poly-Si LPCVD.
130	MFP	Substrate drying (WB15) (#dry023)	NL-CLR-WB15 Single substrate drying: 1. Use the single-wafer spinner Settings: 2500 rpm, 60 sec (including 45 sec nitrogen purge) 2. Use the nitrogen gun (fragile wafers or small samples) Batch drying of substrates: The Semitool uses the following standard procedure: • Rinse: 30 sec (600 rpm) • Q-rinse: 10.0 MΩ (600 rpm) • Purge: 10 sec (600 rpm) • Drying: 280 sec (1600 rpm) <u>Note:</u> it is obligatory to apply a single rinsing step in the QDR before using the Semitool!	Skip. Already done for poly-Si LPCVD.
131	MFP	Dry Oxidation of Silicon (#film920)	NL-CLR-H1 Furnace Recipe: DRYxxx°C (xxx= temperature setting) Settings: • Standby temperature: 700°C • Temperature range: 700-1100°C • Ramp: 10°C/min • O ₂ flow: 5l/min Please mention the following settings in the User Comments: • Target thickness: nm • Temperature:°C • Time:min	Oxidation of poly-Si. Less than 10nm.

132 Place dicing foil on the bottom.

surf1100: Surface Modification by UV Ozone (PRS100-ILP)

133	ILP	Surface Modification by UV Ozone (#surf100)	NL-CLR-UV PRS 100 reactor Purpose: modify the surface to increase the wetting of resist for wet-chemical etching or activate the surface for monolayer formation. • Time = 300 s	Top side, 5min. To enhance wetting.
-----	-----	---	---	--

etch1207: Etching in BHF (WB06 - ILP)

134	ILP	Etching in BHF (#etch117)	NL-CLR-WB06 Use dedicated beaker BHF (1:7) Temp.: Room temperature	20s
-----	-----	-------------------------------------	--	-----

Detailed Process Flow: from Pillars to Membrane - Appendix G

			Etch rates: Thermal SiO ₂ :60-80 nm/min PECVD SiO ₂ :125 nm/min	
135	ILP	Quick Dump Rinse (QDR) (#rinse001)	NL-CLR-Wetbenches Purpose: removal of traces of chemical agents. Recipe 1 Quick dump rinsing (QDR) Recipe 2 Cascade rinsing for fragile wafers Rinse until message 'End of rinsing process' is shown on the touchscreen of the QDR, else repeat the rinsing process.	
136	ILP	Substrate drying (#dry001)	NL-CLR-WBs (ILP) Single substrate drying: 1. Use the single-wafer spinner Settings: 2500 rpm, 60 sec (including 45 sec nitrogen purge) 2. Use the nitrogen gun (fragile wafers or small samples)	
137				Remove dicing foil
etch1005: TMAH etch - standard (WB07)				
138	ILP	Etching in 1% HF (#etch210)	NL-CLR-WB06 Strip native SiO ₂ in 1% HF. Beaker: 1% HF • Time: 1 min Strip until hydrofobic surface.	Skip
139	ILP	Quick Dump Rinse (QDR) (#rinse001)	NL-CLR-Wetbenches Purpose: removal of traces of chemical agents. Recipe 1 Quick dump rinsing (QDR) Recipe 2 Cascade rinsing for fragile wafers Rinse until message 'End of rinsing process' is shown on the touchscreen of the QDR, else repeat the rinsing process.	
140	MFP	Etching in TMAH (25 wt%) (#etch147)	NL-CLR-WB07 Standard double-wall vessel Chemical: 25wt.% TMAH Settings: • Temperature: 70°C • Use stirrer Etch rate is 300 nm/min for <100> Silicon and 25 nm/min for <111> Silicon.	30s to etch poly-Si.
141	MFP	Quick Dump Rinse (QDR) (#rinse002)	NL-CLR-Wetbenches Purpose: removal of traces of chemical agents. Recipe 1 Quick dump rinsing (QDR) Recipe 2 Cascade rinsing for fragile wafers Rinse until message 'End of rinsing process' is shown on the touchscreen of the QDR, else repeat the rinsing process.	

Appendix G - Detailed Process Flow: from Pillars to Membrane

142	MFP	Substrate drying (#dry002)	<p>process.</p> <p>NL-CLR-WBs (MFP)</p> <p>Single substrate drying:</p> <ol style="list-style-type: none"> 1. Use the single-wafer spinner Settings: 2500 rpm, 60 sec (including 45 sec nitrogen purge) 2. Use the nitrogen gun (fragile wafers or small samples) 	Skip if directly proceeding to next step.
-----	-----	-------------------------------	--	---

etch1215: H3PO4 etch (WB08-standard)

143

MFP

Etching in

H₃PO₄ Standard

(#etch153)

NL-CLR-WB08

Use dedicated beaker with reflux lid for etching

Table 1 : Etchrates values old Cleanroom (without reflux and without lid!)

Temperature [°C]	Er SiRN-G3 [nm/min]	Er SiO ₂ A2 [nm/min]
180	4.1	0.48
160	1.4	0.16
140	0.5	0.05

Table 2: Etchrate values fresh prepared H3PO4 in new CR by Yiping (with lid and without lid cooling)

Temperature [°C]	Er SiRN-G3 [nm/min]	Er SiO ₂ [nm/min]
180	6.1-6.6	0.6
160	2.35	0.18
140		

Table 3: Etchrate values after 50 days in new Cleanroom by Erwin (with lid and without lid cooling)

Temperature [°C]	Er SiRN-G3 [nm/min]	Er SiO ₂ 800°C [nm/min]
180	4.5	0.47
160		

Table 4: Si3N4 LPCVD-H2 by Christiaan, Etchrate values after 50 days in new Cleanroom

Temperature [°C]	Er Si3N4-H2 [nm/min]	

Etch the remaining 50nm of SiN at 180°C with about 10nm of overetching. Use a dummy to test the SiN thickness for determining the etch time. The etched part of the substrate should go from hydrofobe to hydrofyle.

Detailed Process Flow: from Pillars to Membrane - Appendix G

180	4,7	
160	1,8	

144	MFP	Quick Dump Rinse (QDR) (#rinse002)	NL-CLR-Wetbenches Purpose: removal of traces of chemical agents. Recipe 1 Quick dump rinsing (QDR) Recipe 2 Cascade rinsing for fragile wafers Rinse until message 'End of rinsing process' is shown on the touchscreen of the QDR, else repeat the rinsing process.	
145	MFP	Substrate drying (#dry002)	NL-CLR-WBs (MFP) Single substrate drying: 1. Use the single-wafer spinner Settings: 2500 rpm, 60 sec (including 45 sec nitrogen purge) 2. Use the nitrogen gun (fragile wafers or small samples)	At 2000RPM to protect the membrane.

surf1100: Surface Modification by UV Ozone (PRS100-ILP)

146	ILP	Surface Modification by UV Ozone (#surf100)	NL-CLR-UV PRS 100 reactor Purpose: modify the surface to increase the wetting of resist for wet-chemical etching or activate the surface for monolayer formation. • Time = 300 s	Bottom side, 5min. To enhance wetting.
-----	-----	---	---	--

surf1100: Surface Modification by UV Ozone (PRS100-ILP)

147	ILP	Surface Modification by UV Ozone (#surf100)	NL-CLR-UV PRS 100 reactor Purpose: modify the surface to increase the wetting of resist for wet-chemical etching or activate the surface for monolayer formation. • Time = 300 s	Top side, 5min. To enhance wetting.
-----	-----	---	---	-------------------------------------

etch1207: Etching in BHF (WB06 - ILP)

148	ILP	Etching in BHF (#etch117)	NL-CLR-WB06 Use dedicated beaker BHF (1:7) Temp.: Room temperature Etch rates: Thermal SiO ₂ :60-80 nm/min PECVD SiO ₂ :125 nm/min	20s
149	ILP	Quick Dump Rinse (QDR) (#rinse001)	NL-CLR-Wetbenches Purpose: removal of traces of chemical agents. Recipe 1 Quick dump rinsing (QDR) Recipe 2 Cascade rinsing for fragile wafers Rinse until message 'End of rinsing process' is shown on the touchscreen of the QDR, else repeat the rinsing	

Appendix G - Detailed Process Flow: from Pillars to Membrane

			process.	
150	ILP	Substrate drying (#dry001)	NL-CLR-WBs (ILP) Single substrate drying: 1. Use the single-wafer spinner Settings: 2500 rpm, 60 sec (including 45 sec nitrogen purge) 2. Use the nitrogen gun (fragile wafers or small samples)	At 2000RPM to protect the membrane. Skip if directly proceeding to next step.
etch1005: TMAH etch - standard (WB07)				
151	ILP	Etching in 1% HF (#etch210)	NL-CLR-WB06 Strip native SiO ₂ in 1% HF. Beaker: 1% HF • Time: 1 min Strip until hydrofobic surface.	Skip.
152	ILP	Quick Dump Rinse (QDR) (#rinse001)	NL-CLR-Wetbenches Purpose: removal of traces of chemical agents. Recipe 1 Quick dump rinsing (QDR) Recipe 2 Cascade rinsing for fragile wafers Rinse until message 'End of rinsing process' is shown on the touchscreen of the QDR, else repeat the rinsing process.	
153	MFP	Etching in TMAH (25 wt%) (#etch147)	NL-CLR-WB07 Standard double-wall vessel Chemical: 25wt.% TMAH Settings: • Temperature: 70°C • Use stirrer Etch rate is 300 nm/min for <100> Silicon and 25 nm/min for <111> Silicon.	Etching the poly-Si from the channels. There might be c-Si left in the channels. Take the etch time to remove the poly-Si plus the assumption that the channels are still filled with c-Si and need to be etched from both sides for 80% of the channel. (Around 10 min.)
154	MFP	Quick Dump Rinse (QDR) (#rinse002)	NL-CLR-Wetbenches Purpose: removal of traces of chemical agents. Recipe 1 Quick dump rinsing (QDR) Recipe 2 Cascade rinsing for fragile wafers Rinse until message 'End of rinsing process' is shown on the touchscreen of the QDR, else repeat the rinsing process.	
155	MFP	Substrate drying	NL-CLR-WBs (MFP)	At 2000RPM to

		(#dry002)	<p>Single substrate drying:</p> <ol style="list-style-type: none"> 1. Use the single-wafer spinner Settings: 2500 rpm, 60 sec (including 45 sec nitrogen purge) 2. Use the nitrogen gun (fragile wafers or small samples) 	protect the membrane.
strip1400: Stripping of resists in Piranha (WB09)				
156	ILP	Stripping polymers and resists (#strip400)	<p>NL-CLR-WB09 PIRANHA BEAKER</p> <p>Purpose: stripping of polymers and resists in Piranha. H₂SO₄:H₂O₂ (3:1) vol%</p> <p>Procedure:</p> <ul style="list-style-type: none"> • Put 1500 ml Sulfuric acid (H₂SO₄) in the beaker • SLOWLY ADD 500 ml Hydrogen peroxide (H₂O₂) in order to avoid a temperature rise above 95°C • Start processing your substrates at a temperature of 95 °C • Time = 15min <p>PIRANHA IS FOR ONE-TIME USE. ALWAYS PREPARE A FRESH SOLUTION BEFORE PROCESSING YOUR SUBSTRATES IN PIRANHA!</p> <p>OPERATIONAL TEMPERATURE IS 95 °C.</p>	At least 15 minutes. Not for stripping but cleaning and activating the silanol groups.
157	ILP	Rinsing (#rinse001)	<p>NL-CLR-WBs QDR</p> <p>Purpose: removal of traces of chemical agents.</p> <p>Choose one of the two rinsing modes: QDR = Quick dump rinsing mode Cascade = Overflow rinsing mode for fragile substrates</p> <p>Rinse until message 'End of rinsing process' is shown on the touchscreen of the QDR, else repeat the rinsing process.</p>	
158	ILP	Substrate drying (#dry001)	<p>NL-CLR-WBs (ILP)</p> <p>Single substrate drying:</p> <ol style="list-style-type: none"> 1. Use the single-wafer spinner Settings: 2500 rpm, 60 sec (including 45 sec nitrogen purge) 2. Use the nitrogen gun (fragile wafers or small samples) 	At 2000RPM to protect the membrane.
159				After the previous drying step, immediately place in vacuum for at least 10min for drying the pores and preventing forms of corrosion. This

Appendix G - Detailed Process Flow: from Pillars to Membrane

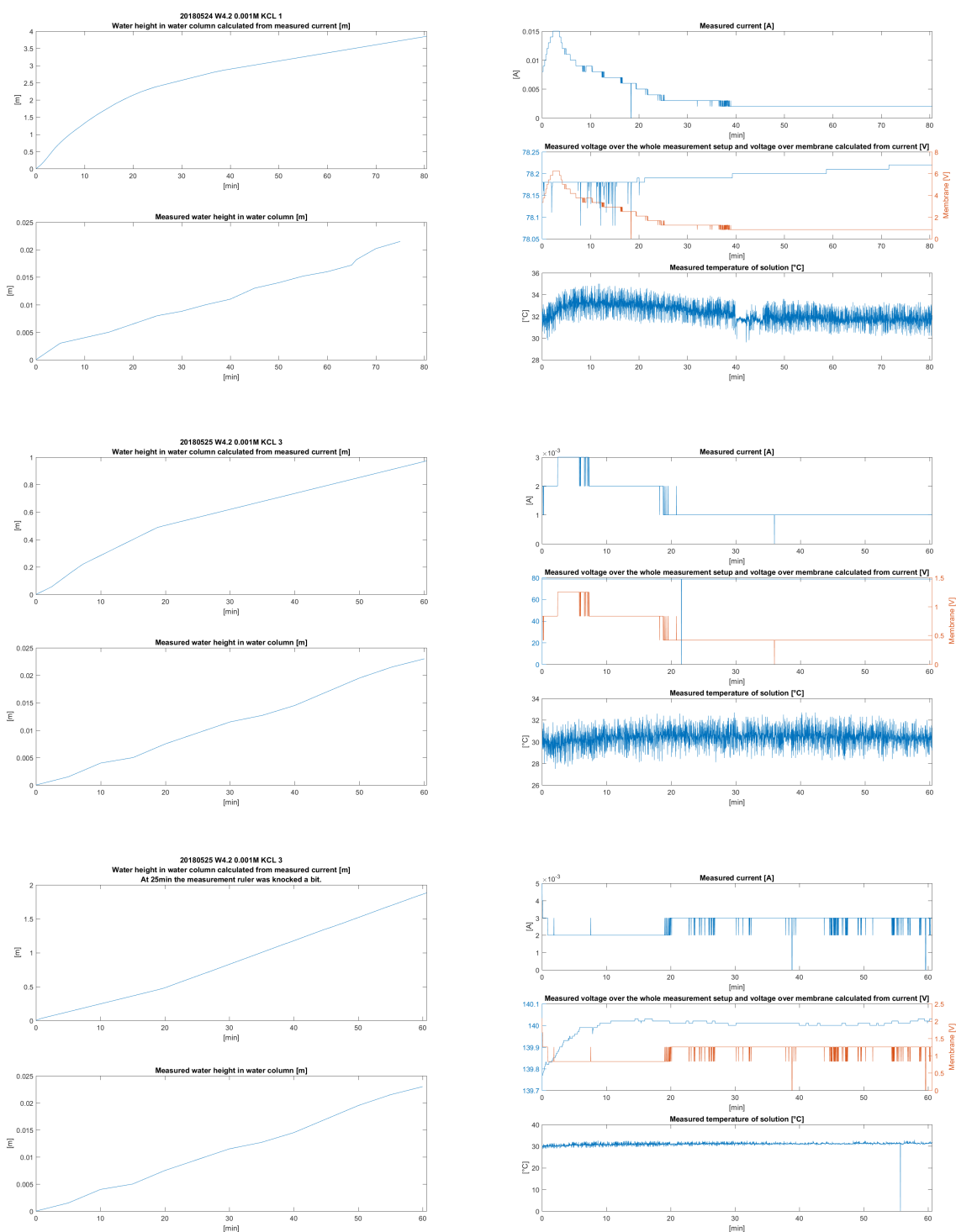
can be done in
the Heraeus
vacuum furnace
by just using its
vacuum and not
turning on the
furnace.

APPENDIX H MEASUREMENT RESULTS BATCH 1

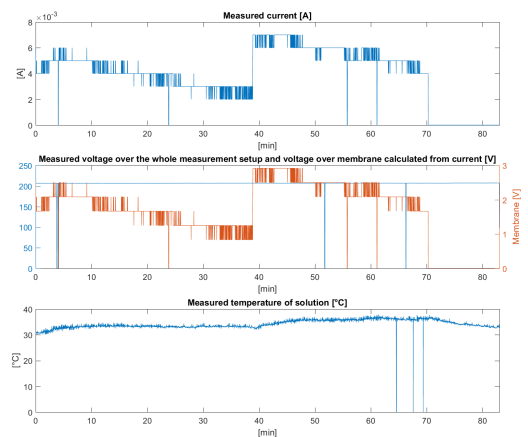
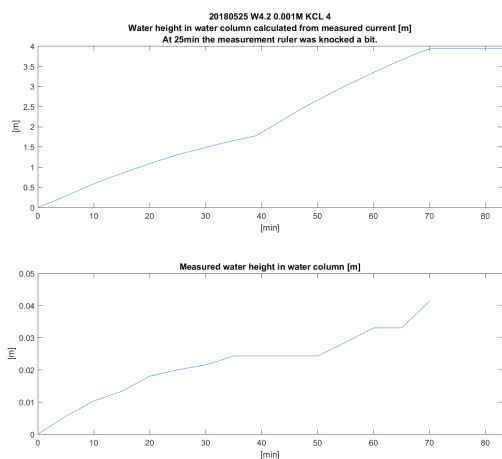
Only the more usable and noteworthy measurements are placed in this appendix.

The sudden negative peaks (of 0V) shown in the measured electrical data, are caused by data communication errors and should be disregarded. Also the labels mention KCl, however all measurements were performed using KNO_3 .

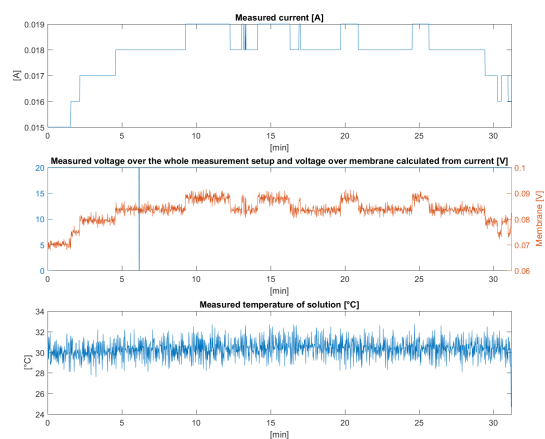
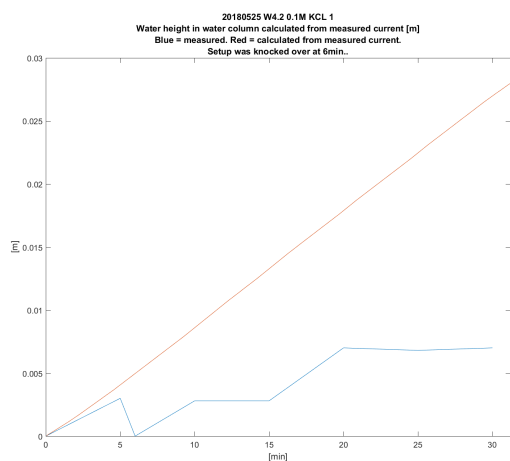
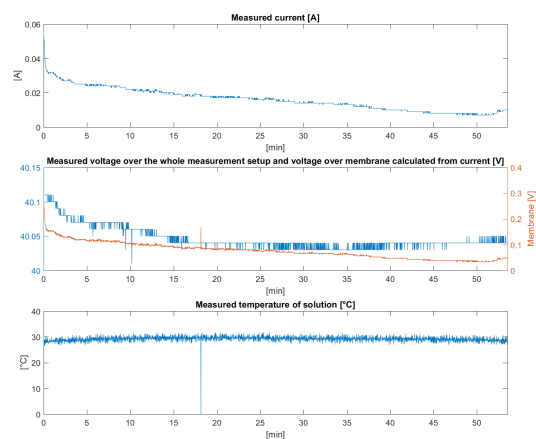
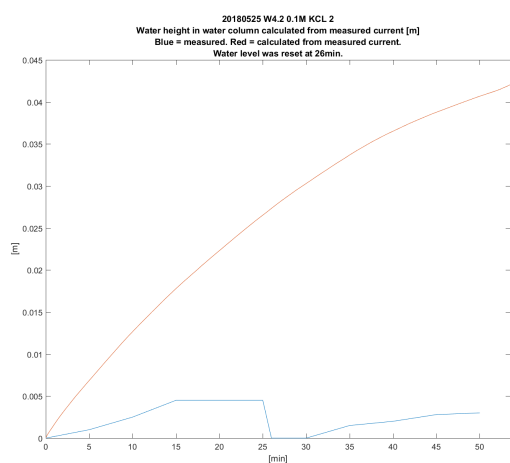
1mM



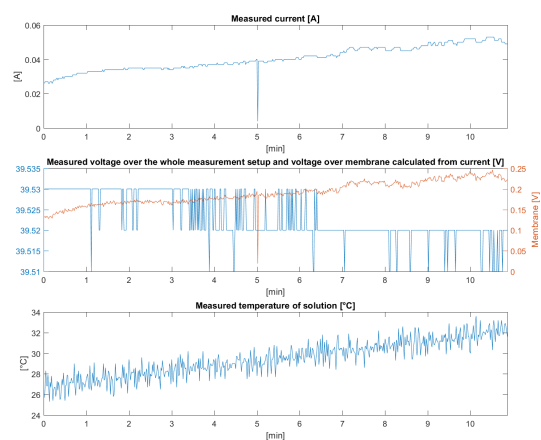
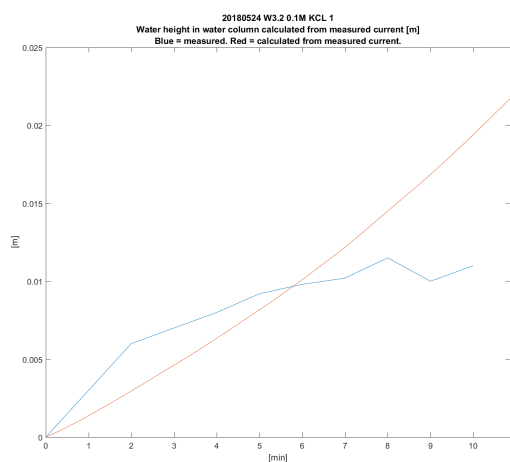
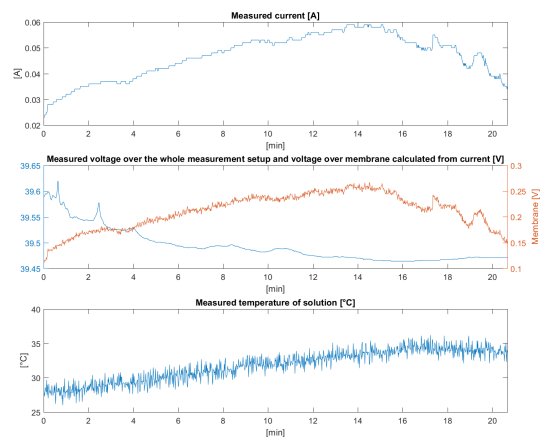
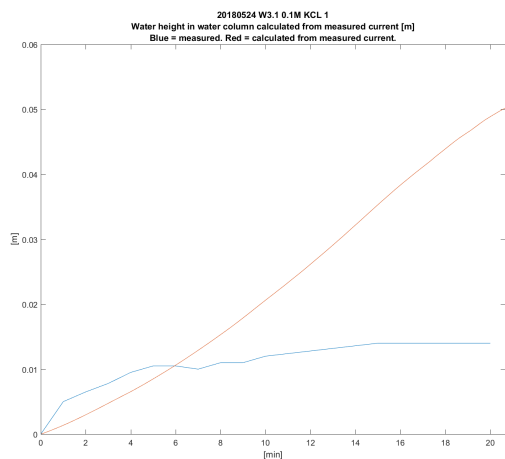
Appendix H - Measurement Results Batch 1



0.1M



Measurement Results Batch 1 - Appendix H

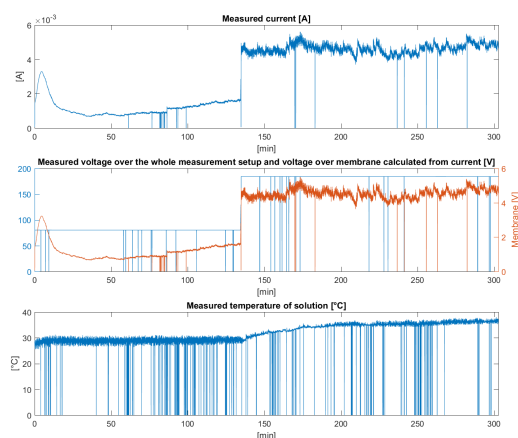


APPENDIX I MEASUREMENT RESULTS BATCH 2

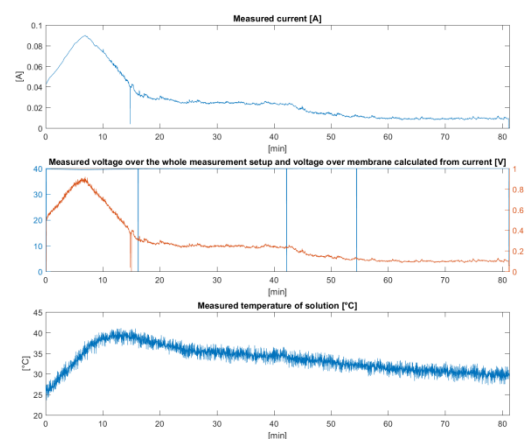
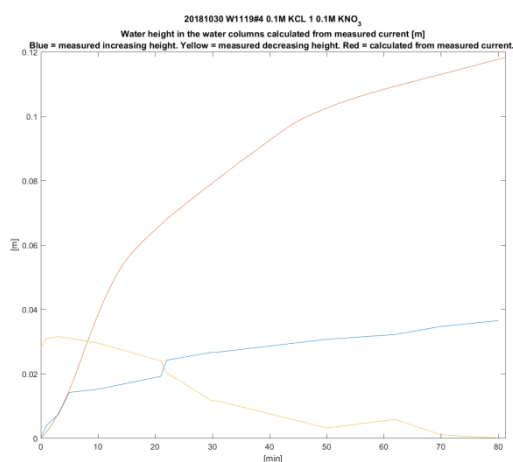
Only the more usable and noteworthy measurements are placed in this appendix.

Here are some of examples of the more relevant data of the measurements of the chips from batch 2. The sudden negative peaks (of 0V) shown in the measured electrical data, are caused by data communication errors and should be disregarded.

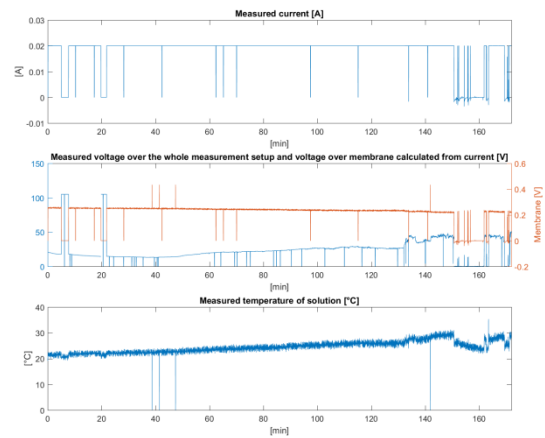
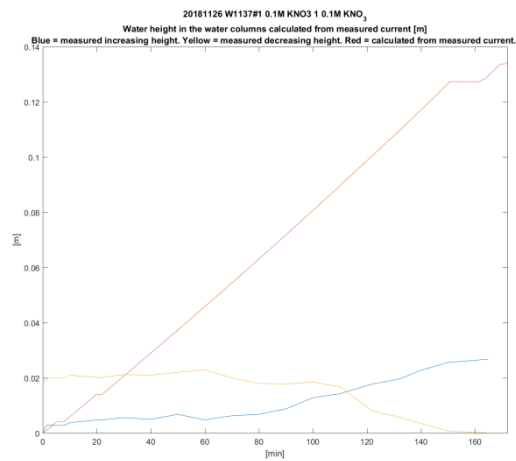
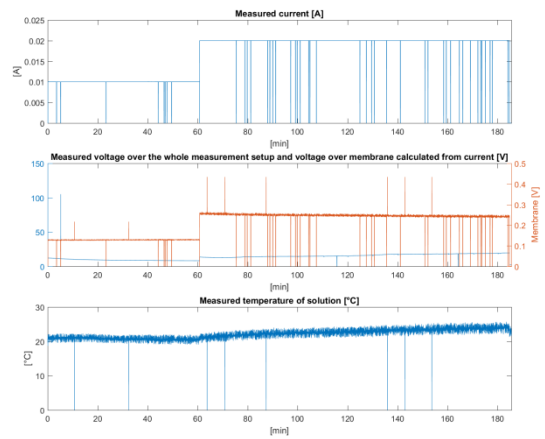
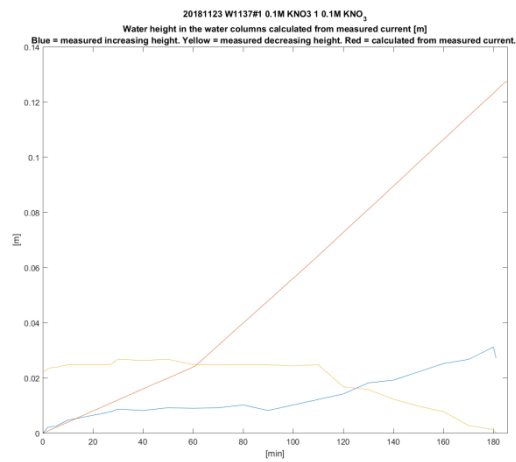
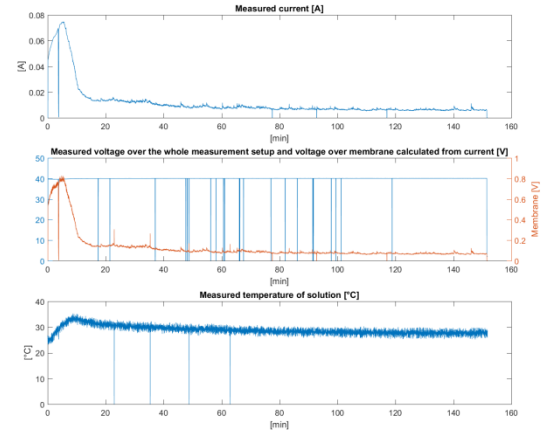
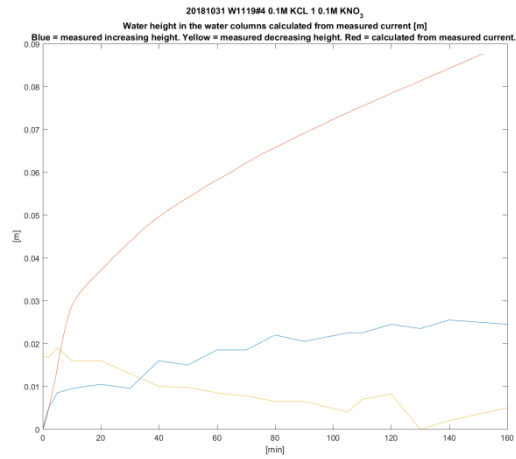
1mM



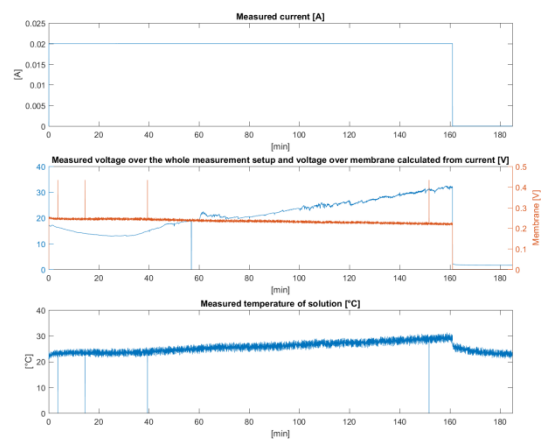
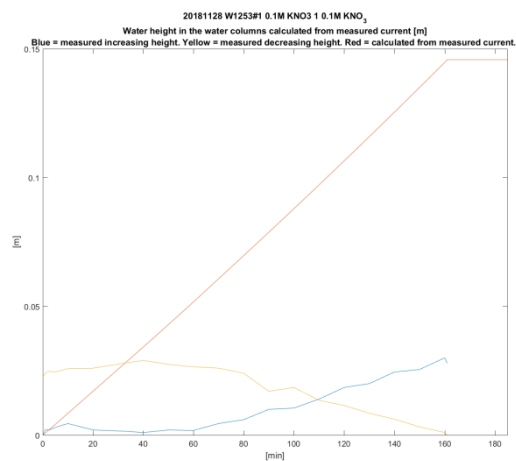
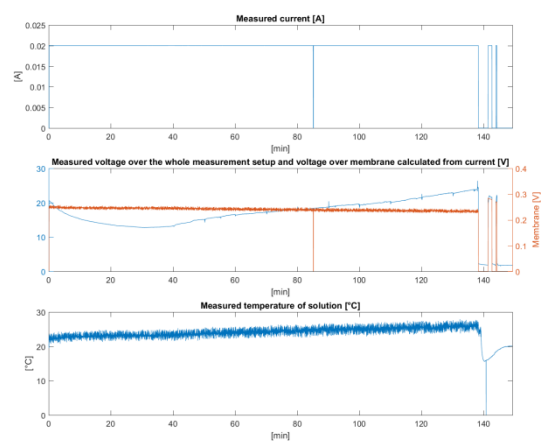
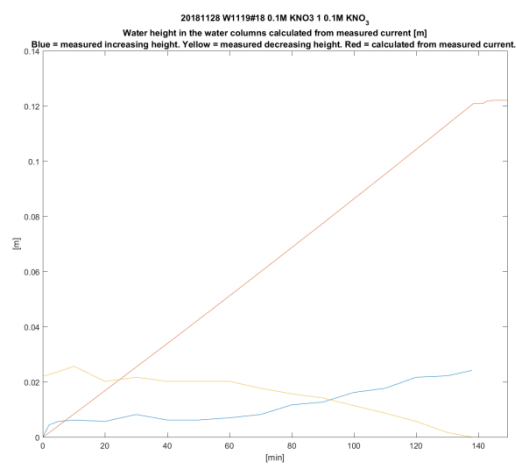
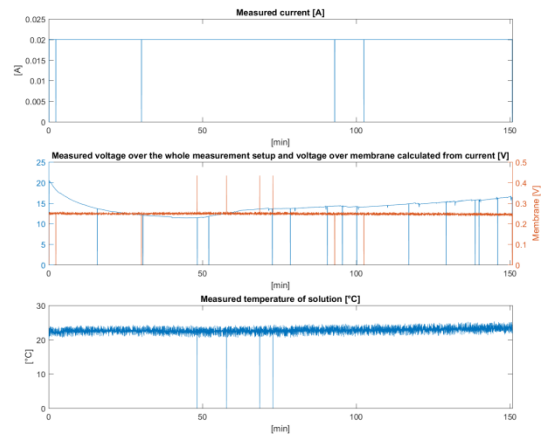
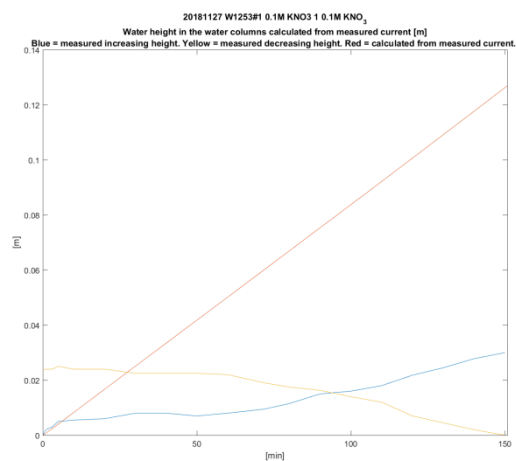
0.1mM



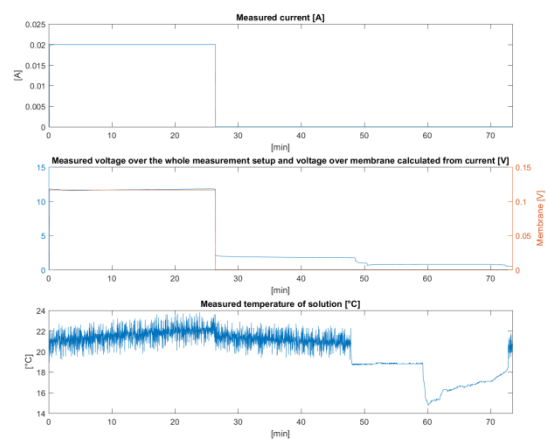
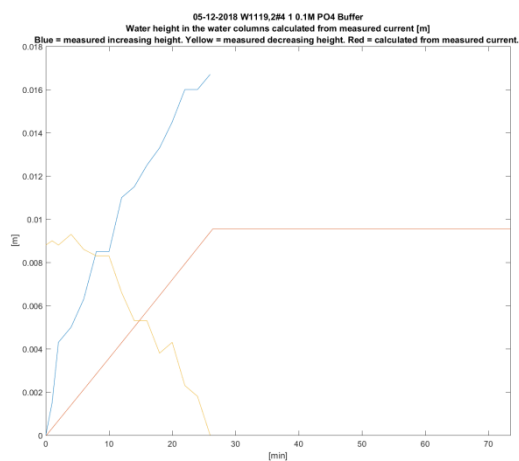
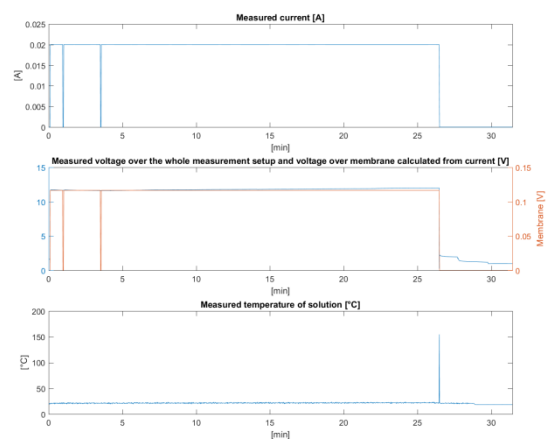
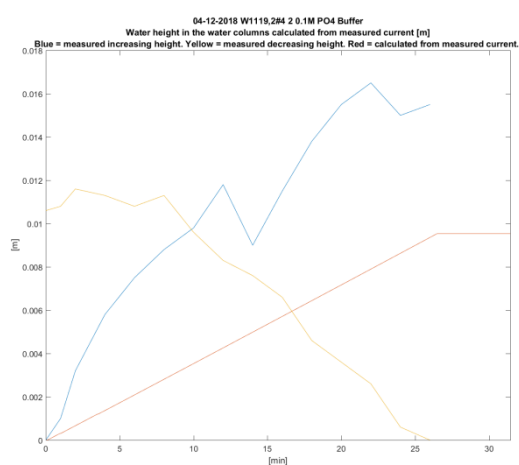
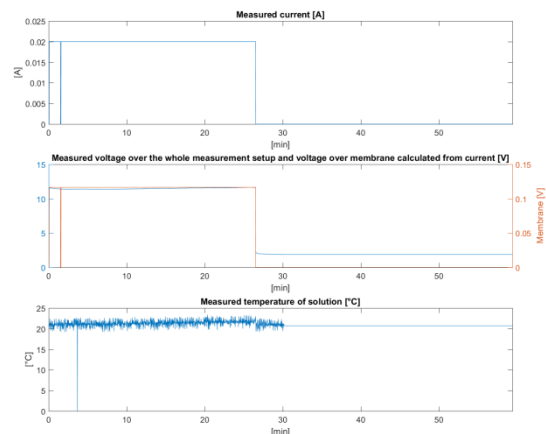
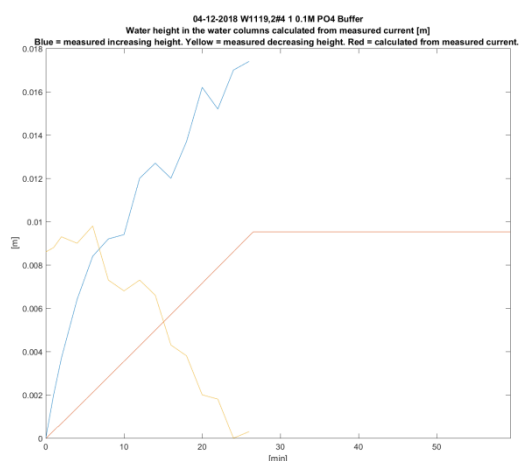
Measurement Results Batch 2 - Appendix I



Appendix I - Measurement Results Batch 2



0.2M K_2HPO_4 - KH_2PO_4 buffer



Appendix I - Measurement Results Batch 2

